Thesis for the degree Master of Pharmacy

INFLUENCE OF OSMOTIC STRESS ON LIPOSOME SIZE AND MORPHOLOGY

By

Helene Moen

May 2008

Supervisors:

Professor Martin Brandl

PhD student Stefan Hupfeld

Department of Pharmaceutics and Biopharmaceutics

Institute of Pharmacy

Faculty of Medicine

University of Tromsø

Acknowledgements

This master thesis was carried out at the Department of Pharmaceutics and Biopharmaceutics, Institute of Pharmacy at the University of Tromsø from September 2007 to May 2008.

First of all I would like to thank my two supervisors, Professor Martin Brandl and PhD student Stefan Hupfeld for giving me the opportunity to work with this project, but also for inspiration during my work.

Stefan , thank you for your valuable advice and useful input on the writing of this thesis. Thank you for all the help in the lab, for always being available and for all encouragement.

Martin, thank you for your constructive feedback and good advice in writing of this thesis.

Thanks to everyone in the department for their day-to-day support and conversation. Merete Skar deserves my thanks for always being helpful and giving me lots of technical advice in the lab. Rahul Haware, thank you so much for all the help with the viscosity measurements.

I wish also to express my gratitude to dr.scient Roy Lysaa for illustrating two of the figures in my thesis.

Thanks to all my friends for their support throughout these years and for motivating me to achieve my academic goals. A special thank to all the girls in the master student office, your optimistic spirit and support have been incredible.

Kent and Linn, thank you for everything you have done for me these last months.

Last but not least, I would like to thank my parents, Kirsten and Nils-Arnt, and my two sisters, Vibeke and Marie; I could not have done this without you. Thank you for always believing in me and encouraging me throughout these years. Vibeke deserves an extra appreciation for reading through the thesis and giving me helpful advice about the writing.

A lot of people deserve my sincere gratitude and thankfulness for giving me the motivation and feedback that made me able to do this. To all of you that are not mentioned by name; you are not forgotten!

Tromsø, May 2008

Helene Moen

CONTENTS

1 ABSTACT

Liposomes are currently being investigated as potential parenterally used drug carriers. The main factor that influences the in vivo behavior of such liposomes is their vesicle size. A detailed and reliable knowledge of vesicle size is therefore necessary in order to interpret results of physical and biological investigations in a correct manner.

It has earlier been discovered that it is feasible to determine the size distribution of vesicle dispersions in a reliable manner and it appears especially useful to employ the combination of SEC fractionation, PCS and the enzymatic PC quantitation. A drawback discovered was for certain liposome dispersions that in some of the dispersions SEC fractionation showed incomplete recovery of the vesicles. This indicated a demand for a different fractionation method which does not have the limitations that the SEC method described above has.

To this end flow field-flow fractionation was chosen. In a previous study the influence of some key factors such as ionic strength of the eluent as well as pore size of the semi-permeable membrane on liposome fractionation behavior has been evaluated. Neutral liposomes were found very dependent of the ionic strength when it comes to elution time.

In this study, the intention was to find out if the retention behavior and calculated geometric radius of liposomes obtained by flow field-flow fractionation in combination with multi-angle light scattering is affected by the osmotic pressure of the medium used for diluting the liposomes and/or running the AF4. In order to exclude ionic-strength effects the salt concentration was kept constant while the osmotic pressure was varied by using mono- and disaccharides.

In conclusion, this project has demonstrated that a change in osmotic pressure, with constant ionic strength, affects both elution time and calculated size of liposomes that were prepared by high pressure filter extrusion. But, osmotic stress was found to affect liposomes of different sizes in a different manner; liposomes that were smaller than the pore size of the filter used for extrusion were found to shrink in hyperosmotic medium but stay quite constant in size in hypo-osmotic medium. In contrast, liposomes that were larger than the pore size of the filter were found to shrink in hyperosmotic medium and swell in hypo-osmotic medium. A hypothesis is presented to explain this behavior.

2 ABBREVIATIONS

AF4	Asymmetrical flow field-flow fractionation
cP	Centipoise
E-80	Unsaturated egg phosphatidyl choline
g	Gram
HPLC	High performance liquid chromatography
kD	KiloDalton
kHz	Kilohertz
L	Liter
LAF	Laminar air flow
LN_2	Liquid nitrogen
LS	Light scattering
LUVs	Large unilamellar vesicles
MALS	Multi-angle light scattering
Min	Minutes
MLVs	Multi lamellar vesicles
mM	Millimolar
mPa·s	Milli pascal-second
Mw	Molecular weight
$NaNO_3$	Sodium nitrate
nm	Nanometer
No.	Number
P.I.	Polydispersity index
PC	Phosphatidylcholine
PCS	Photon correlation spectroscopy
QELS	Quasi-elastic light scattering
RI	Refractive index
rms	Root mean square
R_n	Number-average mean square radius
R_w	Weight-average mean square radius
R_z	z-average mean square radius

s	Second
SD	Standard deviation
SEC	Size exclusion chromatography
SUVs	Small unilamellar vesicles
$t_{1/2}$	Half-life
t_r	Retention time
µm	Micron/micrometer
µSec	Microseconds
UV	Ultraviolet
UV/VIS	Ultraviolet-visible
Vs.	Versus
w/w	Weight ratio

3 INTRODUCTION

3.1 Liposomes

3.1.1 Definitions and background

Liposomes are spherical vesicles which can be thought of as a hollow sphere whose size ranges from approximately 20 nanometers (nm) to some microns (μm). They are composed of a bilayer membrane which entraps an aqueous core. The membrane is composed of phospholipid molecules, the same type of molecules cell membranes are comprised of. Liposome membranes can be composed of naturally-derived phospholipids with mixed lipid chains and a variation of head groups or of pure synthetic lipids with defined acyl chains and head groups.

Liposomes do form spontaneously when phospholipids are mixed with aqueous medium, for review see (Liposomes: a practical approach Torchilin and Weissig 2003). Phosphatidyl choline (PC) molecules are not truly soluble in water, i.e. they self-assemble to liquid crystalline aggregates upon contact with aqueous media. Phospholipids are amphipathic, that is, part of their structure is hydrophilic and the other part is hydrophobic. Therefore, when added to water, the hydrophilic part of the phospholipid interacts with the water and the lipophilic part of the molecule avoids the water. In order to accomplish this, the phospholipids align themselves side-by-side with their lipophilic heads orienting themselves towards each other as shown in the middle figure below (Technical Summary - An Introduction to Lipid Nanoparticles Sciences 2008). This structure is known as a phospholipid bilayer of lamellar structure as shown to the right in figure 3.1.1.

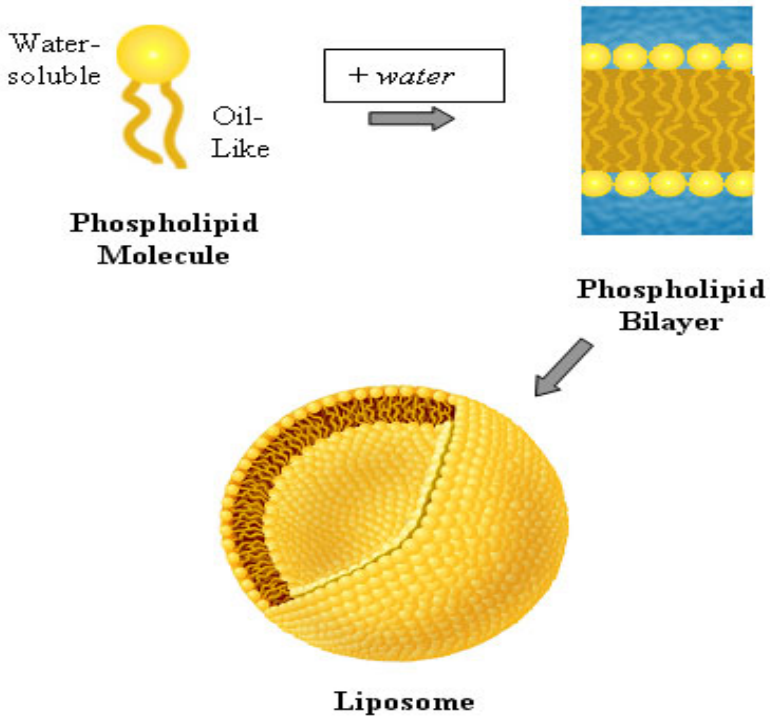

Figure 3.1.1: The formation of liposomes, from phospholipid molecules to a unilamellar vesicle. (Figure taken with permission from: http://www.encapsula.com/company.html)

The vesicles formed may consist of one or more lamellae. Small liposomes usually consist of only one bilayer but bigger liposomes can consist of multiple bilayers or several smaller liposomes can be formed inside the bigger liposome. The thickness of a bilayer is about 4 nm, reviewed in (Liposomes: from physics to applications Lasic 1993).

Materials can either be entrapped in the aqueous core or incorporated within the membrane for review see (Liposomes as drug carriers: a technological approach Brandl 2001). Lipophilic of amphiphilic drug are incorporated into the membrane and hydrophilic drugs are entrapped in the aqueous core for review see (Liposomal formulations of anticancer drugs: selectivity and effectiveness Massing and Fuxius 2000).

A multi lamellar liposome is shown in figure 3.1.2. We can see that there are many phospholipid bilayers with water in between the layers. The pink dots are water-soluble drugs which are entrapped in the core or in the aqueous space between the bilayers. The green rods are lipid-soluble drugs which are incorporated in the lipid membrane.

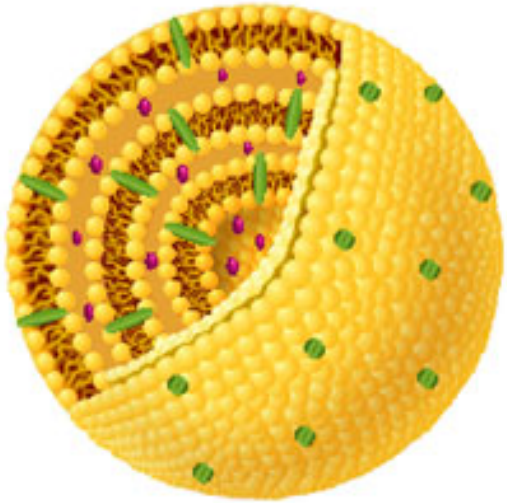

Figure 3.1.2: Drug encapsulation in liposomes, the water-soluble drugs (shown in pink) are entrapped in the aqueous compartments and the lipid-soluble drugs (shown in green) are entrapped within the membrane. (Figure taken with permission from: http://www.encapsula.com/company.html)

The choice of lipids for liposomal drug carriers depends on the desired stability of the liposome formulation, and the drug which should be incorporated into the liposomes. The most common phospholipid used in liposomal drug carriers is phosphatidyl choline. There exist two sorts of phospholipids, phosphodiglycerides and sphingolipids. PC belongs to the group of phosphodiglycerides. PC can be derived from natural sources as egg yolk and soyabeans or be made synthetically (Liposomes: a practical approach Torchilin and Weissig 2003).

PC is amphiphilic and is composed of a hydrophilic head group consisting of the quaternary ammonium moiety choline linked to the glycerol-backbone via a phosphor-ester and two lipophilic acyl chains. As the phosphate is negatively charged at physiological pH, PC is zwitterionic and liposomes made of it have no net charge. A schematic presentation of PC is shown in figure 3.1.3

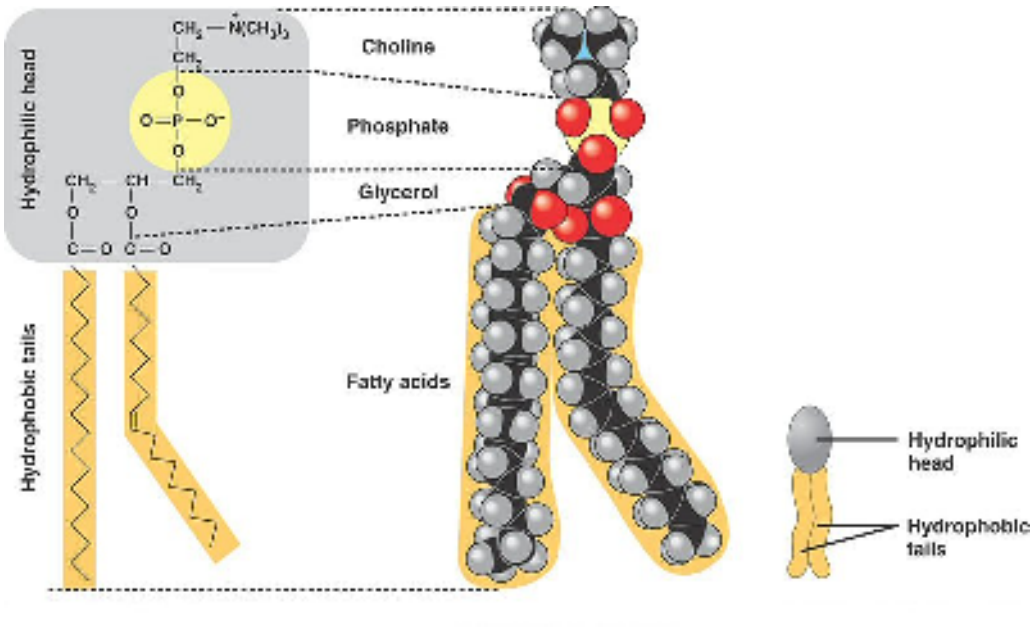

Figure 3.1.3: A schematic representation of PC (Figure taken with permission from: http://kvhs.nbed.nb.ca/gallant/biology/biology.html)

PC is hardly ever used alone in liposomal lipid formulations. Blends of PC with other lipids are used primarily to improve both in-vitro and in-vivo stability of the liposomes (Liposomes as drug carriers: a technological approach Brandl 2001). When drugs are incorporated into the liposome one usually wants to prevent leaking and loss of drug through the membrane.

A normal way to prevent leaking is adding cholesterol to the membrane, cholesterol will induce a tighter packing of the membrane and reduce the fluidity of the membrane, as shown in figure 3.1.4.

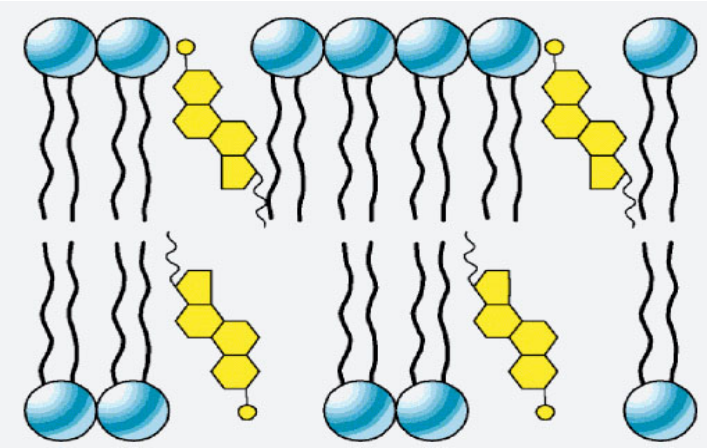

Figure 3.1.4: Phospholipid bilayer with cholesterol incorporated in the membrane. (Figure taken with permission from: http://www.uic.edu/classes/bios/bios100/lecturesf04am/lect08.htm

3.1.2 Classification of liposomes

Liposomes are often classified according to their size. Size and lamellarity of liposomes formed by spontaneous swelling depend on the type of lipid, composition of the medium and the mechanical stress exerted during swelling. Lipids with a net charge reduce both size and number of lamellae of the liposome.

Multi lamellar vesicles (MLVs) are vesicles covering a size range from 100-1000 nm and consist of five or more lamellae, for review see (Liposomes: a practical approach Torchilin and Weissig 2003).

Large unilamellar vesicles (LUVs) are vesicles in the same size range as MLVs, from 100-1000 nm, but they only have one lamella.

Small unilamellar vesicles (SUVs) are defined as the smallest phospholipid vesicles possible (approximately 20 nm) and up to 50 nm. The size depends on the ionic strength of the aqueous medium and the lipid composition in the membrane. They usually consist of one lamella.

3.1.3 Stability of liposomes

For phospholipids there are two major degradation reactions known which affect their chemical stability in aqueous dispersion, hydrolysis and oxidation (Liposomes as drug carriers: a technological approach Brandl 2001). Physical instability might affect the particle size of liposomes. Examples of this kind of instability are aggregation and fusion. Aggregation is the process where liposomes form aggregates. This is a reversible process which can be resolved by stirring. Fusion is the phenomenon where vesicles fuse together and make bigger liposomes. The process most often happens to very small liposomes with a diameter of approximately 20 nm. This is not a reversible process and therefore a much bigger problem.

3.1.4 Pharmaceutical use of liposomes

In the field of drug delivery, preparations based on submicron particles are emerging as an important tool for achieving either controlled or targeted delivery of the active compound. Examples of such drug carriers are polymeric and solid lipid nanoparticles as well as liposomes. The objective is to achieve selective localization of active drug in disease sites as tumors and inflammation sites. A potential field that is very interesting is cancer therapy. The systemic environment does not recognize the drug when it is incorporated into a liposome. It recognizes only the liposome and the intrinsic pharmacokinetics of the drug is masked by the pharmacokinetic behavior of the liposomal vesicle, hence it protects the drug from premature recognition, excretion and degradation in the blood stream. The liposomes are also able to accumulate in tumors because of the enhanced permeability and retention effect, EPR-effect, reviewed in (Liposomal formulations of anticancer drugs: selectivity and effectiveness Massing and Fuxius 2000). Blood vessels in tumors are leakier than normal blood vessels because of their fast growth. In addition, the cells in tumors are often not as closely packed as in healthy tissue.

Most of the cancer drugs on the marked now have dose-limiting toxicity problems and thus relatively low efficacy. The liposomal preparations may have the potential to change this with time. The physical properties of the liposomes, such as size and size distribution, play an important role in the work of developing successful drug formulations. Hence, there is a great demand on detailed and reliable information about this subject.

3.1.5 Challenges with liposome formulations

Intravenous injection is regarded as the most promising route of administration for liposomal drug delivery. The role of a liposomal drug carrier is to circulate in the blood pool and reach the desired organ or tissue. The pharmacokinetics and biodistribution of the carrier primarily depend on the size and surface characteristics of the liposome.

Upon entering the blood pool, liposomes should avoid to be taken up by macrophages. Big liposomes (diameter >200 nm) are quite rapidly taken up and disappear from the circulation. Liposomes with a diameter between 70 and 200 nm tend to circulate long enough in the blood stream to reach the desired organ. Smaller liposomes with a diameter under 70 nm show shorter circulation time due to extravasation through the capillary walls of the liver reviewed in (Liposomes as drug carriers: a technological approach Brandl 2001). The lipid composition and lamellarity is also important since it together with the physiochemical properties of the drug determines the retention of the active ingredient within the liposome reviewed in (Liposomal formulations of anticancer drugs: selectivity and effectiveness Massing and Fuxius 2000). Due to these facts, there is clearly a need to develop methods that are not only able to measure the size and the size distribution of liposome dispersions, but in a next step generates liposomes of defined size.

3.1.6 Size analysis of liposomes

The main factor that influences the in vivo behavior is the size of the liposomes. Because of that fact it is important to have methods for determining the size and size distributions in a reliable manner, and in a reproducible manner. Some of the techniques which have been used are various electron microscopic methods, photon correlation spectroscopy and methods based on fractionation of liposomes according to size such as size exclusion chromatography (SEC), ultracentrifugation and flow field-flow fractionation (AF4).

Preferable are methods which are able to give a qualitative and quantitative overview over the full size range, which unfortunately is difficult to achieve. Some of the methods mentioned above such as SEC and ultracentrifugation are rather time consuming, and when developing a method for routine size analysis of liposomes, use of time should be evaluated.

The method should be able to quantify the amount of large particles and eventually aggregates in comparison to the amount of SUVs (Size analysis of submicron particles and liposomes by size exclusion chromatography and photon correlation spectroscopy Ingebrigtsen 2001).

3.2 Influence of osmotic stress on liposome size

It is likely that liposomes diluted in a hypertonic medium will shrink and become smaller than they originally were. Liposomes, which exhibit similar permeability properties to biological membranes represents a convenient model system to study osmotic stress (Osmotic properties and water permeability of phospholipid liquid crystals Bangham 1967). A liposome can be seen as a cell with a semi-permeable membrane and an aqueous core. When a cell comes in contact with a hypertonic environment it is surrounded by a higher concentration of impermeable solute than exists inside of the cell. The difference in osmotic pressure inside and outside of the membrane causes a net movement of water out of the cell, causing it to shrink (Tonicity Wikipedia 2008). In the opposite case, a hypotonic environment causes a net movement of water in to the cell, causing it to swell. Both of these principles are shown in figure 3.2.1.

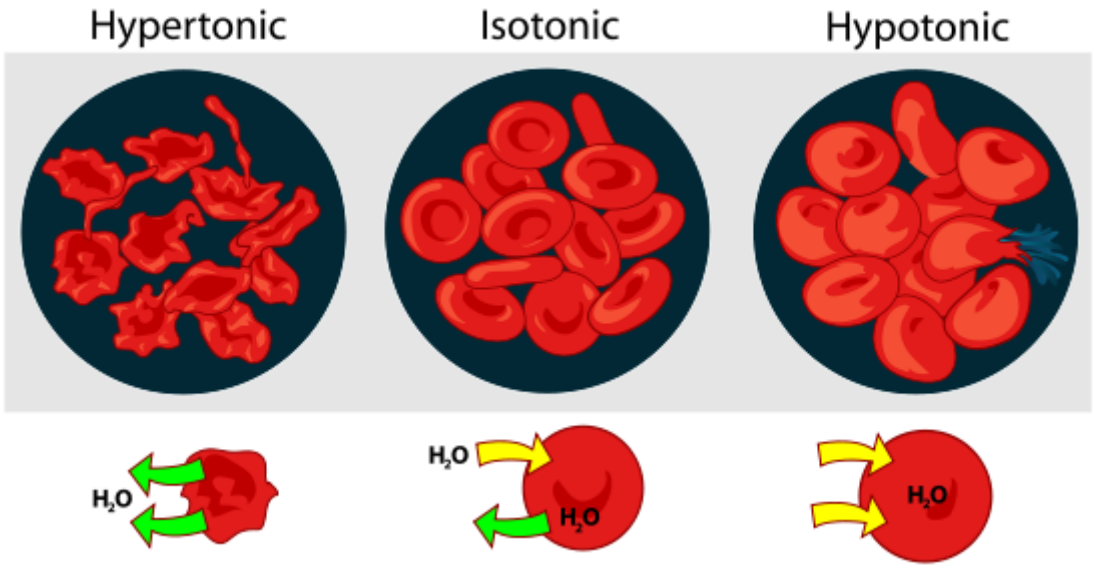

Figure 3.2.1: Effect of hypertonic and hypotonic solutions on blood cells. (Figure taken with permission from: http://en.wikipedia.org/wiki/Tonicity#Isotonicity)

3.3 Previous studies

Lars Ingebrigtsen and Christer Bakke Frantzen investigated in their master theses accomplished in December 2001 and May 2003 respectively, whether a combination of size exclusion chromatography with subsequent size analysis performed by photon correlation spectroscopy combined with a quantitative assay achieved a total qualitative as well as quantitative insight into the size distribution of liposome dispersions and thus was suited as a routine analysis method. Previous studies of the size distribution of liposomes gained qualitative results of various qualities, but none of them provided quantitative information. Ingebrigtsen checked how reliable results photon correlation spectroscopy (PCS) can give when it is used for routine particle analysis of latex beads of submicron sizes. He found out that PCS was able to resolve bimodal size distributions of the heterogeneous samples within certain limits, i.e. for certain ratios and for certain sizes. But it was obvious that PCS is inappropriate to resolve bimodal size distributions with a broader overlap or tri- or multimodal size distributions. In the second part of his study he employed SEC, PCS and a quantitative enzymatic PC assay. He found that it was feasible to determine the size distribution of vesicle dispersions in a reliable manner and it appears especially useful to employ the combination of SEC fractionation, PCS and the enzymatic PC quantitation. A drawback discovered was for certain liposome dispersions that in some of the dispersions SEC fractionation showed incomplete recovery of the vesicles. It can be explained in terms of aggregation of these rather small vesicles which subsequently got stuck on the SEC column. In addition, the described method is very time consuming.

This clearly indicated a demand for different fractionation method which does not have the limitations that the SEC method described above has.

Dominik Albert Ausbacher investigated in his diploma thesis accomplished in October 2007, if asymmetrical flow field-flow fractionation was convenient for fractionation of liposomes. He tried to evaluate the influence of some key factors such as ionic strength of the eluent as well as pore size of the semi-permeable membrane on liposome fractionation behavior. Neutral liposomes were found very dependent of the ionic strength when it comes to elution time. He saw a shift of the liposome peak to later retention times when an eluent with a higher

ionic strength was used, but he was not able to say whether the change in retention time of liposomes in higher ionic strength media was due to osmotic stress or zeta-potential.

Nevertheless, his master project can only be seen as a first step in paving on the way towards routine AF4-multi-angle light scattering (MALS) liposome analysis.

These previously executed master projects form the basis of this master project.

4 AIM

The purpose if this study was to investigate how a change in osmotic pressure, with constant ion strength, affects both elution time and calculated size of liposomes.

In more detail, our aim was to find out if the retention behavior and calculated geometric radius of liposomes obtained by flow field-flow fractionation in combination with multi-angle light scattering is affected by the osmotic pressure of the medium used for diluting the liposomes and/or running the AF4. In order to execute ionic-strength effects the salt concentration was kept constant while the osmotic pressure was varied by using mono- and disaccharides.

5 MATERIAL AND METHODS

5.1 Chemicals

Table 5.1.1: Lipid

Name of lipid	Batch numbers	Manufacturer
Unsaturated egg phosphatidyl choline Lipoid E-80	1031492-9/904, 1031492-11/902, 1031492-11/904	Lipoid GmbH, Ludwigshafen, Germany

Table 5.1.2: Latex bead

Name of latex bead	Mean diameter	Batch number	Manufacturer
Nanosphere ^{TM} size standards	102 nm ± 3 nm	28570	Duke Scientific Corporation, Freemont, CA, USA

Table 5.1.3: Chemicals

Chemical	Quality	Batch number	Manufacturer
Ethanol	96 %	N/A	Arcus Kjemi AS, Vestby, Norway
Glucose	For parenteral use	1A102/4	Norsk Medisinaldepot, Oslo, Norway
Liquid nitrogen	N/A	N/A	AGA AS, Trondheim, Norway
Purified Water	N/A	N/A	Prepared in-house by Millipore water purification system

Sodium chloride solution, 400 mOsm/kg	N/A	5484C41	Dr. Ing. Herbert Knauer GmbH, Berlin, Germany
Sodium nitrate	p.a.	A571737 519	Merck KGaA, Darmstadt, Germany
Sucrose	Ph Eur	K341881187 544 K33825286 524	Merck KGaA, Darmstadt, Germany VWR International Ltd, Poole, England

5.2 Equipment

Table 5.2.1: Equipment

Equipment	**Type**	**Manufacturer**
Filtration device, 142 mm diameter	SM 16275	Sartorius AG, Göttingen, Germany
Freezer (-80 °C)	Forma Laboratory Freezer, model 738	ThermoQuest/ Forma Scientific Division, Marietta, OH, USA
Glass tubes for PCS analysis	Borosilicate glass disposable culture tubes, 6 x 50 mm	VWR International AB, Karlskoga, Sweden
HPLC variable-wavelength-UV/VIS-detector	G1314A, 1100 series	Agilent Technologies Europe, Santa Rosa, CA, USA
LAF (laminar air flow) bench	Holten maxisafe 2000	Heto Holten A/S, Allerød, Denmark
MALS-detector	Dawn EOS	Wyatt Tech. Corp. Europe, Dernbach, Germany

Osmometer	Knauer Semi-Micro Osmometer, Type ML, No. A0299	Wissenschaftliche Gerätebau Dr. Ing. Herbert Knauer GmbH, Berlin, Germany
Photon Correlation Spectrometer- PCS	Submicron Particle Sizer Model 380	Nicomp Particle Sizing Systems, Santa Barbara, CA, USA
Prototype filter extruder	Continuous consisting of Lewa diaphragh pump type LDB 1 and Millipore 47 mm high pressure filter holder	Custom made, Lewa GmbH, Leonberg, Germany Millipore S.A. Molsheim, France
Pycnometer	Specific gravity bottle, 25 cm^3	Brand GMBH + CO KG, Wertheim, Germany
RI-detector	Optilab rEX	Wyatt, Tech. Corp. Europe. Dernbach, Germany
Stainless steel filtration vessel, 5 liter	SM 1753	Sartorius AG, Göttingen, Germany
Ultrasonic bath	Branson Ultrasonic Cleaner 1510E-MT	Branson Ultrasonic Corporation, Danbury, CT, USA
Viscometer	Capillary viscometer, capillary type 0c	Ubbelohde viscometers, Schott-Geräte, Hofheim, Germany
Water bath	Büchi Waterbath B-480	Büchi Labortechnik AG, Flawil, Switzerland
Water purification system	Millipore water purification system	Millipore S.A., Molsheim, France

Filters for: Filtration device, 142 mm	Nitrocellulose VCWP 0.1 µm filter, batch no: H5JN02152	Millipore Corporation, Billerica, MA, USA
Syringe filter	Acrodisc syringe filter, 0.2 µm filter, batch no: 21182	Pall Corporation, Ann Arbor, MI, USA
Liposome filter extruder	Millipore Isopore Membrane filters: 0.4 µm filter; batch no: R5SN28296 0.2 µm filter; batch no: R8MM92556 0.1 µm filter; batch no: R8NM25306	Millipore Ireland B.V., Cork, Ireland
Milli-Q water system; Millipak 20 Express	0.22 µm filter; batch no: MPGP02001	Millipore S.A., Molsheim, France
Milli-Q Synthesis Quantum EX Ultrapure organic	Cartridge; batch no: F5HN65923	Millipore S.A., Molsheim, France

5.3 Media and solutions

For all the solutions the composition is given per 1 liter:

Table 5.3.1: Media and solutions

Name of medium	Content	Application
10 mM sodium nitrate solution	Sodium nitrate 0.8499 g + Purified water ad 1000.0 ml	Hydration medium in MLV production and as diluting agent before PCS measurements Also used for diluting liposome dispersion 1:10 prior to investigation of size changes as a result of osmotic stress and as mobile phase in the AF4 experiments
20 mM sodium nitrate solution	Sodium nitrate 1.6998 g + Purified water ad 1000.0 ml	Osmolality measurements
50 mM sodium nitrate solution	Sodium nitrate 4.2495 g + Purified water ad 1000.0 ml	Osmolality measurements
10 mM sodium nitrate and 19.8 mM glucose solution	Sodium nitrate 0.8499 g + Glucose 3.5590 g + Purified water ad 1000.0 ml	Osmolality measurements
10 mM sodium nitrate and 16.6 mM sucrose solution	Sodium nitrate 0.8499 g + Sucrose 5.6940 g + Purified water ad 1000.0 ml	Osmolality measurements
10 mM sodium nitrate and 79 mM glucose solution	Sodium nitrate 0.8499 g + Glucose 14.2358 g + Purified water ad 1000.0 ml	Osmolality measurements
10 mM sodium nitrate and 66.4 mM sucrose solution	Sodium nitrate 0.8499 g + Sucrose 22.7780 g + Purified water ad 1000.0 ml	Osmolality measurements

10 mM sodium nitrate and 177.6 mM glucose solution	Sodium nitrate 0.8499 g + Glucose 32.0306 g + Purified water ad 1000.0 ml	Viscosity measurements. Also used for diluting liposome dispersion 1:10 prior to investigation of size changes as a result of osmotic stress and as diluting agent before PCS measurements
10 mM sodium nitrate and 149.3 mM sucrose solution	Sodium nitrate 0.8499 g + Sucrose 51.2490 g + Purified water ad 1000.0 ml	Hydration medium in MLV production and as diluting agent before PCS measurements Also used for diluting liposome dispersion 1:10 prior to investigation of size changes as a result of osmotic stress and as mobile phase in the AF4 experiments
100 mM sodium nitrate solution	Sodium nitrate 8.499 g + Purified water ad 1000.0 ml	Mobile phase in the AF4 experiments

All the different solutions were prepared according to the same procedure; the solid components were weighted in and transferred to a volumetric flask where they were dissolved with some water. The concentrated solution was then diluted by adding water up to the desired volume (1 liter) in a volumetric flask. All the solutions were filtered through a 0.1 μm nitrocellulose filter.

5.4 Preparative methods

5.4.1 Preparation of multilamellar vesicles (MLVs)

Theory:

MLVs form spontaneously when phospholipids are blended with excess aqueous medium (Diffusion of univalent ions across the lamellae of swollen phospholipids Bangham, Standish 1965).

Experiment:

MLVs were prepared according to the hand-shaken method:

Hand-shaken method:

10 % w/w E-80 (unsaturated egg phosphatidyl choline) in different aqueous media

1. E-80 5 g
2. Aqueous medium 45 g

E-80 and the aqueous medium were weighed in directly in a round bottom flask. The components were stirred using a magnetic stirrer until E-80 was finely dispersed, which takes approximately 45 minutes.

5.4.2 Reduction of lamellarity

Theory:

To increase the proportion of unilamellar vesicles in preparations it is a common practice to subject MLVs to freeze-thaw cycles prior to extrusion. (Osmotic properties of large unilamellar vesicles prepared by extrusion Mui, Cullis 1993). The freezing and thawing cycles cause the MLVs to rupture and re-assemble such as the aqueous layers between concentric lamellae increase in thickness; this probably reduces the number of closely associated bilayers. (Liposome technology Mui and Hope 2006)

Experiment:

In order to find out which freeze-thawing method would give the best result, four preliminary experiments were executed.

1. Freeze-thawing was performed before extrusion. The liposome dispersion was frozen in a -80°C freezer for 1 hour and then thawed on a 50°C water bath. The freeze-thaw cycle was repeated three times.

2. Freeze-thawing was performed before extrusion. The liposome dispersion was frozen in liquid nitrogen (LN_2) and then thawed on a 50°C water bath. The freeze-thaw cycle was repeated three times.

3. Freeze-thawing was performed between extrusion through 400 nm filer and 200 nm filter. The liposome dispersion was frozen for one hour in a -80°C freezer and thawed on a 50°C water bath. The freeze-thaw cycle was repeated three times.

4. Freeze-thawing was performed after extrusion. The liposome dispersion was frozen in a -80°C freezer for one hour and thawed on a 50°C water bath. The freeze-thaw cycle was repeated three times.

5.4.3 Reduction of liposome size

Theory:

MLVs have a broad particle size distribution and have multiple internal compartments. Due to this fact; unprocessed MLVs have limited use in medical research. In order to achieve liposomes with homogeneous size, filter extrusion was accomplished. The extrusion was performed on a custom made extruder, as shown in figure 5.4.1. Filter extrusion involves the process of forcing the liposome preparations through pores of membrane filters with defined pore sizes. The preferred filter type for reducing the size of liposomes is made of polycarbonate with straight-through, cylindrical pores. The pores have been formed by chemical etching along ion tracks. When the MLV preparation is squeezed through the filter pore under pressure a process of membrane rupture and resealing occurs, this process generates large to small unilamellar vesicles with a mean vesicle diameter usually slightly larger than the pore size of the polycarbonate membranes. After about 10 cycles through filters with 100-nm pores a homogeneous population of vesicles with a mean diameter of approximately 100 to 120 nm is obtained. (Liposome technology Mui and Hope 2006)

Experiment:

The MLV dispersion obtained by the hand-shaken method was extruded using filters with decreasing pore sizes of 400 nm, 200 nm and 100 nm. The transfer of liposomes through the filter was repeated 10 times, as recommended by (Liposome technology Mui and Hope 2006). The pump of the extruder was running at the same speed every time.

Figure 5.4.1: The custom made extruder

5.5 Analytical methods

5.5.1 Characterization of particle size by Photon Correlation Spectroscopy

Theory:

PCS is an analytical tool to determine the size distribution of submicron particles suspended in an aqueous medium. The technique has proven to be especially powerful in measuring particles with a diameter of approximately 20-200 nm. A laser light beam (typically 5 mW Helium and Neon laser) is focused on a glass tube containing a diluted suspension of particles. Each of the particles scatters light in all directions and the intensity of scattered light varies with the particles molecular weight, size and shape. The difference in refractive indices of the particle and the surrounding medium also play an important role (Windows based software, Dynamic light scattering theory User Manual 1997).

PCS measures the fluctuations in the scattered light intensity. Scattered light intensity fluctuates with time because many individual waves add coherently. This is the physical phenomenon known as interference. All the different waves interfere at a distant slit on the face of a photomultiplier detector, which measures the net scattering intensity at a 90 degrees scattering angle. The suspended particles move around randomly in the medium by Brownian motion. As a consequence of these motions, the phase of each of the scattered light waves that is arriving at the detector will fluctuate randomly in time due to the random positions of the particles (Size analysis of submicron particles and liposomes by size exclusion chromatography and photon correlation spectroscopy Ingebrigtsen 2001). The fluctuation of light intensity is dependent on the size of the particle. Small particles will move around faster and give rapid fluctuation of the light intensity.

The next step is to determine the diffusion coefficient, D, of the particles from the raw data. From D it is possible to calculate the particle diameter using the Stokes-Einstein equation.

Equation 1: $D = kT / 3\pi\eta d_s$

k = Boltzmann´s constant (1.38 X 10^{-16} erg K^{-1})

T = temperature (°K, = °C + 273)

η = shear viscosity of the solvent

d_s = Stokes particle diameter

From equation 1 we can see that the diffusion coefficient, D, of particles increases with increasing temperature, T. This is primarily due to the temperature dependent viscosity of the solvent, η.

Autocorrelation is the mathematical process of extracting quantitative information as the size of the particles and their size distribution in a sample from the fluctuation of the intensity of the scattered laser light (Size analysis of submicron particles and liposomes by size exclusion chromatography and photon correlation spectroscopy Ingebrigtsen 2001). The autocorrelation function is used to study the similarity between the value of I_s (light intensity) at a given time and the value of I_s at an earlier time, t-t´. Such comparisons are carried out for many values of (t) in order to get a statistical meaningful average value for C (t´).

The correlation function can be expressed:

Equation 2: $$C\ (t') = \Sigma\ Is\ (t) \times Is\ (t - t')$$

One can describe the autocorrelation function as an exponential function that gradually decreases as the value of (t´) increases. As expressed below in equation 3.

Equation 3: $$C\ (t') = A\ exp\ (-t'/\tau) + B$$

$A = \Sigma\ I_s^2\ (t)\ - \Sigma\ I_s\ (t)^2$

$B = \Sigma\ I_s(t)^2$

Variable τ is the characteristic decay time constant of the exponential function. The value of τ describes the duration of a major fluctuation in the scattered intensity I_s. Hence, the larger the particles, the slower fluctuations in I_s and the longer the decay constant τ. We are able to predict the diffusion coefficient of the particles from the decay constant τ.

Equation 4: $D = (1/2\,K2)\,(1/\tau)$

K = scattering wavevector (A constant which depends on the laser wavelength in the solvent and the angle between the laser beam and where the detector is placed.)

Fitting and interpretation of the results:

The PCS software fits the raw data, collected by the detector, using either the NICOMP model or the monomodal Gaussian model. NICOMP is used for bi- or multimodal size distribution and Gaussian is used for a unimodal size distribution. The Gaussian model states how good a fit is approaching a normal distribution.

The Gaussian analysis is restricted to simple, unimodal particle size distributions which are the case in this thesis, and NICOMP distribution analysis will consequently not be further explained.

Gaussian distribution:

The PCS software will indicate how well the measured results fit with the normal distribution or the Gaussian model. The quality of this fit is stated by the statistical value Chi squared. Any value close to or below one indicates an exceptionally good fit, but any value under three is regarded well enough. If the value of Chi squared is over three, the PCS software suggests that the Gaussian model is inappropriate, and the NICOMP model should be used instead.

The value for baselines adjust is indicating an adjustment needed to obtain a low value of Chi squared. The ideal value is zero. A higher baseline adjust value is indicative for large particles or aggregates in the sample.

Polydispersity index (P.I.) is stating how broad the distribution is around the mean particle size. A low P.I. value thus indicates a homogenous size distribution. A P.I. value close to zero is therefore most desirable. For highly polydisperse samples the P.I. approaches one (Windows based software, Dynamic light scattering theory User Manual 1997).

Experiment:

Measurements were carried out as described by (Determination of the size distribution of liposomes by SEC fractionation, and PCS analysis and enzymatic assay of lipid content Ingebrigtsen and Brandl 2002). In brief, the test tubes used for PCS measurements were sonicated for 10 minutes and then rinsed with the dilution medium. Samples were diluted using particle free medium, until the intensity was between 250 and 350 kilohertz (kHz). They were diluted with the same medium as used for producing the liposomes. It is very important that the intensity level is correct because the correlator´s input counter must not receive more photons than it can count in a single sample time otherwise the correlation function will be distorted (Particle size analysis in pharmaceutics and other industries: theory and practice Washington 1992). To avoid particle contamination the dilution medium was filtrated through a sterile filter with 0.2 µm pore size. All the preparative work was done in a laminar airflow bench to avoid particle contamination.

Before any measurement was carried out the instrument parameters were set according to the values listed in table 5.5.1. For statistical accuracy, a cycle of 5 minutes was run for each sample in order to calculate how long a sample need to be run to ensure count rates above 1000 K (1 million) in channel no. 1.

Table 5.5.1: PCS parameters

Parameter	Value
Channel width	Auto set
Temperature	Room temperature, usually 23-25 °C
Liquid viscosity	If the liquid only contained sodium nitrate, values of viscosity of water was used. The values were obtained from a table in the PCS manual. (E.g. if the temperature was 23 °C then the viscosity would be 0.9325 cP.) The viscosity values for the solutions that contained glucose or sucrose were measured with a capillary viscometer.
Liquid index of refraction	1.333 is the literature value of water, and the same value was used when the solution only contained water and sodium nitrate. Values for the solutions that contained sucrose and glucose were measured with the Optilab rEX refractive index detector
Intensity setpoint	300 ± 50 kHz
Laser wavelength	632.8 nm
Scattering angle	90 °

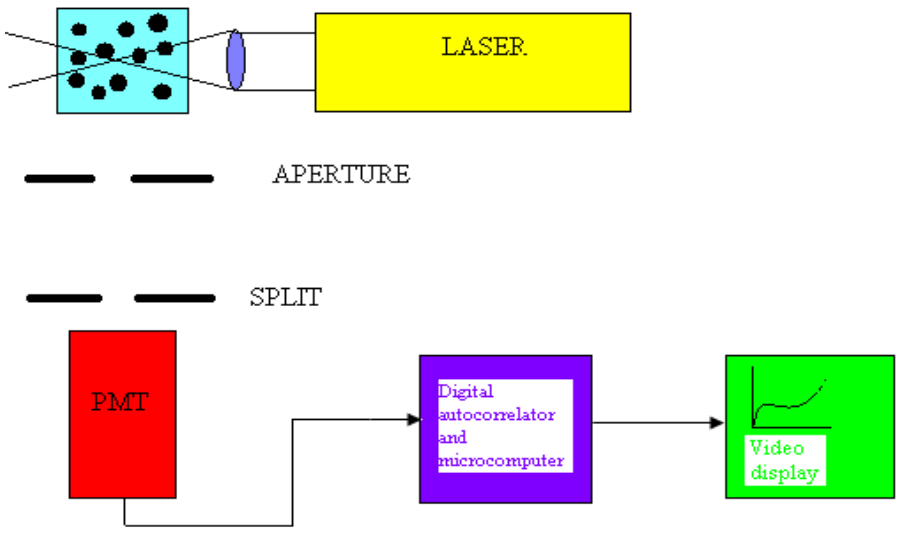

Figure 5.5.1: Block diagram of the PCS (NICOMP Model 380 submicron particle sizer)

5.5.2 Determination of osmolality in solutions

Theory:

Osmolality is a measure of the osmoles of solute, per kilogram of solvent. An osmole is the amount of substance that yields, in ideal solutions, that number of particles that would reduce the freezing point of the solvent by 1.86 °C. E.g., when one mole of non-ionic solute is added to one kilogram of water, the freezing point goes down 1.86 °C. When one mole ionic solute e.g., $NaNO_3$ is dissolved in a kilogram of water it will yield almost twice as many particles since $NaNO_3$ dissociates almost completely into one mole Na^+ and one mole NO_3^- ions (Refractive index 2008).

The osmotic strength of a solution can be measured by an osmometer. Currently available osmometers use the colligative properties of freezing point depression or vapour pressure depression.

The equation to determine the osmolality of a solution is shown in equation 5:

Equation 5: $$Osmolality = \Phi \times n \times molality$$

Φ = osmotic coefficient, which accounts for the degree of non-ideality of the solution. Φ is between 0 and 1, 1 means that 100 % dissociates.

n = number of particles into which the molecule can dissociate (e.g., 1 for sucrose, 2 for $NaNO_3$)

The unit of osmolality is Osm/kg (osmole per kilogram).

Experiment:

Calculations of the osmolalities were performed according to the calculation method described in appendix 1. Measurements were carried out by Knauer semi-micro osmometer to ensure that the calculations were correct. E.g., one solution with 20 mM $NaNO_3$ was compared to a solution with 10 mM $NaNO_3$ and an amount of glucose equivalent to 10 mM $NaNO_3$. Three parallels were measured for every solution. If the measured values were equal to each other, it would prove that the calculated amount of glucose was correct. The measurement was executed on an osmometer which measured the freezing point depression of the solutions. Figure 5.52 shows the osmometer used for these experiments.

Figure 5.5.2: Knauer semi-micron osmometer

5.5.3 Determination of viscosity in solutions

Theory:

Viscosity is a measure of the fluids resistance to flow. Viscosity can be measured by various types of viscometers. One of the most common and most accurate instruments for measuring kinematic viscosity of Newtonian fluid´s is the glass capillary viscometer. Dynamic viscosity coefficient is calculated from kinematic viscosity by multiplying the dynamic viscosity by the density of the Newtonian fluid (Viscosity Wikipedia 2008).

The equation to calculate dynamic viscosity from kinematic viscosity is shown in equation 6:

Equation 6: $\eta = \nu \times \rho$

η = dynamic viscosity

ν = kinematic viscosity

ρ = density

The unit of dynamic viscosity is mPa·s (pascal-second).

Experiment:

Measurements of viscosity were carried out because the knowledge of the accurate viscosity is crucial when PCS analysis is performed. Every solution that was used as dilution medium in PCS was measured, except those who only contained $NaNO_3$ because it was assumed that the viscosity would not change noticeably. The viscosity of both the solutions that contained sucrose and $NaNO_3$, or glucose and $NaNO_3$ were measured. The kinematic viscosity was measured using a glass capillary viscometer. To calculate the dynamic viscosity the density of the solution is needed. The density of the solutions was measured with a pycnometer. Four parallels for every solution were measured, and the average value was used in the PCS software.

5.5.4 Determination of refractive index in solutions

Theory:

Refractive index is the other parameter that needs to be determined to get reliable results from the PCS measurements, besides viscosity. The refractive index of a solution is a measure of how much the speed of light is reduced inside the medium or the bending of a ray of light when passing from one medium into another. The refractive index of vacuum is by definition 1, and the refractive index of water is 1.333.

A refractive index of 1.333 means that light travels at 1 / 1.333 = 0.75 times the speed in vacuum (Refractive index Wikipedia 2008).

The refractive index can be defined by equation 7:

Equation 7: $$n = \frac{c}{v_p}$$

n = the refractive index

c = phase velocity of a wave

v_p = phase velocity of the medium itself

Experiment:

The refractive indices were measures using the Optilab rEX on-line refractive index detector. All solutions used during this project were measured. For the measurements the respective solution was injected into the instrument with a syringe. It was necessary to set the Optilab rEX into purge mode, which means that both the glass cells in the instrument are flushed with medium and the absolute refractive index is measured. To prevent dilution of the medium that should be measured, the instrument was flushed until the value of refractive index did not change anymore.

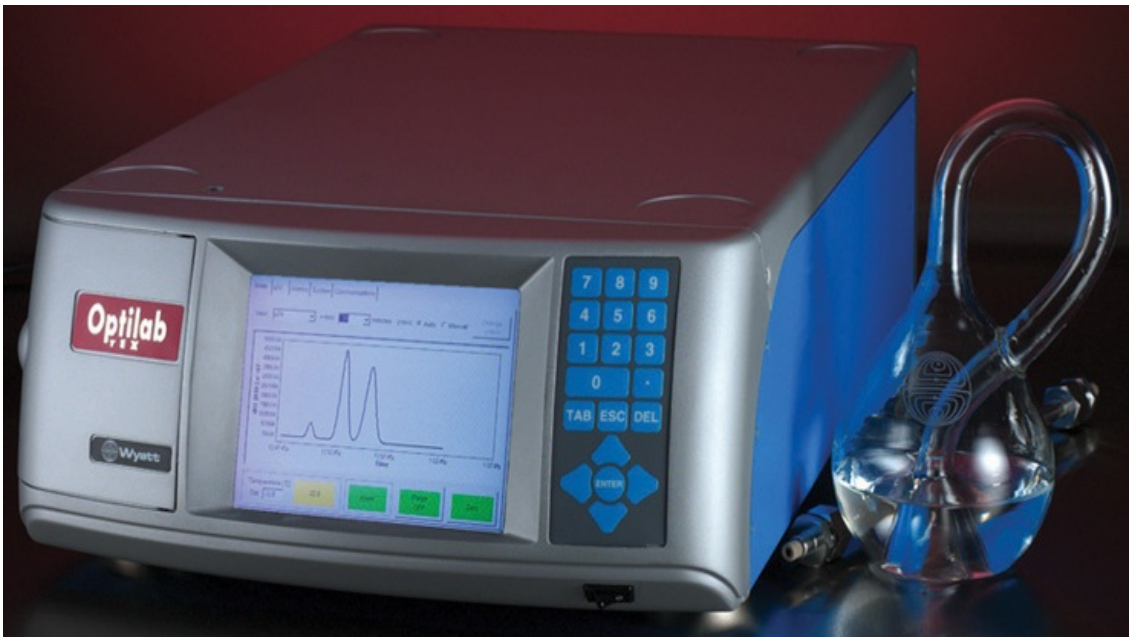

Figure 5.5.3: Picture of the Optilab rEX refractive index detector (Figure used with permission from: http://www.wyatt.com/solutions/hardware/Refractive_Index_Detector-OptilabrEx.cfm)

5.5.5 Characterization of liposomes, Flow Field-Flow Fractionation

Theory:

Asymmetrical flow field-flow fractionation is a one-phase chromatography technique which allows separation of heterogeneous samples and is able to perform fractionation ranging from the 1 nm up to 10 microns (Changes in Liposome Morphology Induced by Actin Polymerization in Submicrometer Liposomes Nickels 2003). The instrumental Set-Up of an AF4 system is comparable to a HPLC (high performance liquid chromatography) system. However, the fractionation of samples takes place in a separation channel instead of a separation column. Particles are separated by flow in aqueous media. This is done by the application of field force generated by the transverse movement of carrier liquid (cross flow) across the channel. AF4 is fractionating particles according to their size and determining size distribution of polydisperse particle samples from an observed retention profile (Size characterization of liposomes by flow field-flow fractionation and photon correlation spectroscopy Effect of ionic strength and pH of carrier solutions Moon, Park 1998).

The channel consists of a lower block which contains the cross flow outlet, the permeable frit, the membrane and the spacer. The spacer foil has a typical thickness of 100 to 500 µm. The thickness and the form of the spacer foil are defining the dimensions of the actual channel. The upper block contains the channel inlet, the injection port and the channel outlet as shown in figure 5.5.4.

The upper channel plate is impermeable, but the bottom channel plate, on the other hand, is permeable. An ultra filtration membrane with a typical size barrier of 10 kD, covers the bottom plate to prevent the sample from penetrating the channel (How Asymmetric Field Flow Fractionation (AFFF) Theory Works Technology 2008).

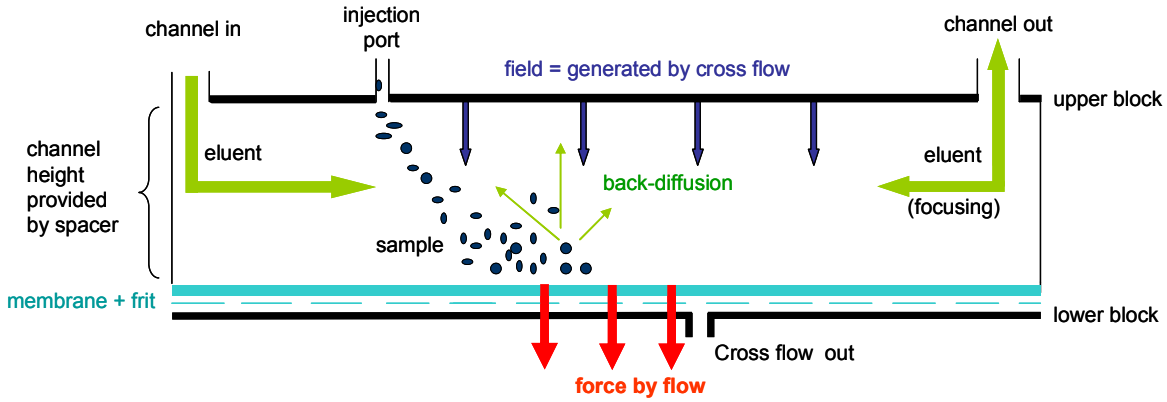

Figure 5.5.4: Channel setup, different flows and forces during A4F (Figure used with permission from Dominik Ausbacher (A4F/MALS-Analysis of Liposomes Influence of Key Factors on Fractionation Behavior and Evaluation of MALS Fit Routines Ausbacher 2007))

Upon injection into the AF4 channel particles are driven toward the bottom of the channel wall by the cross flow. After injection the sample is focused on a small band near the injection point by applying an inverse flow through the channel outlet.

Equilibrium positions are established away from the accumulation wall, due to the particles diffusive transport. The Brownian motion of the particles or vesicles leads them to be differentially distributed over the accumulation wall according to their size; large particles have a small diffusion coefficient and are therefore driven closer to the accumulation wall. The small particles will move around faster and float further from the accumulation wall hence they are displaced by the fast flow stream and are eluted earlier than the larger ones, as can be seen in figure 5.5.5 (A4F/MALS-Analysis of Liposomes Influence of Key Factors on Fractionation Behavior and Evaluation of MALS Fit Routines Ausbacher 2007).

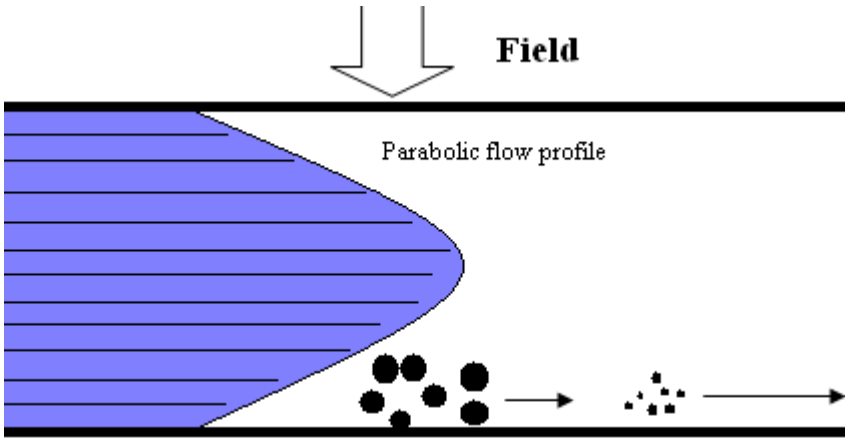

Figure 5.5.5: Side view of particle migration according to the size in the AF4 channel

The separation based on AF4 technology, is divided into four steps. These are injection, relaxation, focusing and elution. The first three steps injection, relaxation and focusing are quite simultaneous and are followed by the elution. In the first step, the channel flow is split and introduced both at the inlet and at the outlet of the channel (Asymmetric Flow Field-Flow Fractionation Analytics 2008). After focusing, the next step is the experiment is the so-called elution mode. In elution mode both the cross flow and channel flow active and fractionation can take place. In AF4 is retention time (t_r) of a particle given by equation 8.

Equation 8: $$t_r = \frac{w^2}{6D} \times \frac{V_x}{V}$$

V = channel flow

V_x = cross flow

w = channel thickness

D = diffusion coefficient

As we can see in equation 8, the retention time is directly proportional to the square of the channel thickness, and inversely proportional to the diffusion coefficient. The diffusion coefficient can be used for calculating the molecular dimensions in the form of the Stokes diameter (On-line coupling of flow field-flow fractionation and multi-angle laser light scattering Roessner and Kulicke 1994). The mathematical basis for this is provided by the Stokes-Einstein equation shown in equation 1. If we link equation 1 and equation 8 we get equation 9, which gives the dependence of the retention time on the material and experimental parameters.

Equation 9: $$t_r = \frac{\pi\eta w^2}{2kT} \times \frac{V_x}{V} \times d_s$$

Vesicle diameter can readily be calculated from experimental retention time (t_r) when the experimental parameters are known. A4F can give a direct measure of liposome size since separation is based on the difference in hydrodynamic radius of the particles (Size characterization of liposomes by flow field-flow fractionation and photon correlation spectroscopy Effect of ionic strength and pH of carrier solutions Moon, Park 1998). However a direct determination of hydrodynamic radius was not performed in this work because the applied method requires more complex mathematics for calculating the hydrodynamic radius which is not available at the time.

Theory:

Instead of determining the hydrodynamic radius from the retention time of particles in an AF4 run, the particles size is measured by MALS. In a MALS detector several photo diodes are arranged in a circle around a glass cell with a bore where the sample runs through. When light from a polarized laser light beam hits a sample molecule, LS (light scattering) will occur in all directions as demonstrated in figure 5.5.6. The resulting scattered light will then be detected by the photo diodes at the different angles from 10° to 160°. The wavelength of the laser light used to illuminate the solution containing the sample is 690 nm (Wyatt Technology Corporation User Manual 2007).

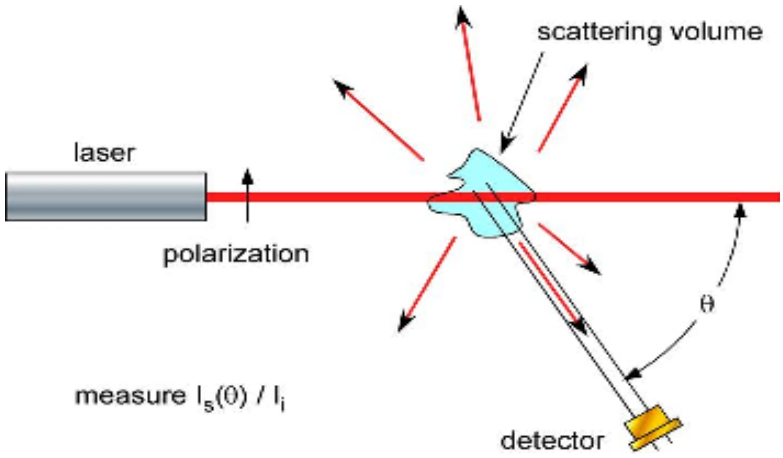

Figure 5.5.6: Laser light scattering. (Figure taken with permission from: Wyatt Technology (Introduction to Light Scattering, Light Scattering University Technology 2006))

One big advantage with light scattering experiments is that the solute can be measured in solution in a non-invasive manner. The symbol used to describe angle-dependent light scattering is R_θ, called the excess Rayleigh ratio. R_θ is defined in equation 10. The excess Rayleigh ratio is a ratio of the scattered light and incident light intensities that take into account different factors which are shown in equation 10. It is called the excess ratio because it is for scattered light in excess of scattered light from the solvent, for the solute or particle alone (Wyatt Technology Corporation User Manual 2007).

Equation 10:

$$R_\theta = \frac{(I_\theta - I_{\theta,solvent})r^2}{I_0 V}$$

I_θ = scattered intensity

$I_{\theta,\,solvent}$ = scattered intensity of the solvent

I_0 = intensity of the beam

V = volume of the scattering medium

r = distance between the scattering volume and the detector

If we know R_θ at a number of different angles it leads directly to the weight average molar mass and mean square size of the solute molecules. This makes R_θ the most important measured quantity in light scattering (Wyatt Technology Corporation User Manual 2007).

The intensity carries information about the molar mass, while the angular dependency carries information about the size of the macromolecule. It can hence give information about both the particle size and the molar mass of the particle. The calculations given from the MALS detector software are based on equation 11.

Equation 11: $$\frac{R_\theta}{Kc} = MP(\theta) - 2A_2cM^2P^2(\theta)$$

R_θ = excess Rayleigh ratio (cm^{-1})

K = optical constant ($=4\pi^2 n_0^2 (dn/dc)^2 \lambda_0^{-4} N_A^{-1}$), where n_0 is the refractive index of the solution, λ_0 is the radiation wavelength in vacuum expressed in nanometers, N_A is Avogadro´s number and dn/dc is the differential refractive index of the solvent-solute concentration

c = concentration

M = molar mass (g/mol)

P(θ) = theoretically-derived form factor

A_2 = second virial coefficient (mol mL/g^2)

Astra is the software which processes the MALS data. Astra calculates an rms (root mean square) radius moments for each peak. The different rms radius´s measured are number-average mean square radius (equation 12), z-average mean square radius (equation 13) and weight-average mean square radius (equation 14). All summaries are taken over one peak (Wyatt Technology Corporation User Manual 2007).

Equation 12: $$< r^2 >_n = \frac{\Sigma\left(\frac{c_i}{M_i}<r^2>_i\right)}{\Sigma \frac{c_i}{M_i}}$$

Equation 13: $$< r^2 >_z = \frac{\Sigma(c_i M_i <r_2>_i)}{\Sigma\ (c_i M_i)}$$

Equation 14: $$< r^2 >_w = \frac{\Sigma(c_i <r_2>_i)}{\Sigma c_i}$$

c_i = mass concentration

M_i = molar mass

$< r^2 >$ = mean square radius of the i^{th} slice

Experiment:

AF4 experiments were performed using the Eclipse 2 instrument system from Wyatt Technology Europe. The flow field-flow fractionation is coupled on-line with a Dawn EOS 18 angle light scattering, a single wavelength UV detector and an Optilab rEX differential refractive index detector (RI-detector). A 250-µm spacer was applied and a main flow of 1.0 ml/min. A cross flow gradient was applied; the cross flow was reduced from 1.0 to 0.15 ml/min. All the samples were diluted 1:10 with the mobile phase prior to the measurements. The injection volume was the same in every experiment, 10 µl.

The liposomes are assumed to be hollow spheres in which each of the lipid molecules acts as an isotropic scattering element. The angular dependence of the scattering is expressed by the so-called form factor or shape-factor, P(θ).

The form factor is assuming a shell thickness of 3.7 nm for phosphatidylcholine vesicles, as has been measured using X-ray diffraction (Characterization of vesicles by classical light scattering Van Zanten and Monbouquette 1991).

The form factor is the mathematical relationship describing the angular variation of the scattered intensity as a function of particle size, shape and structure. It is also called the particle scattering function (Introduction to Light Scattering, Light Scattering University Technology 2006). For processing the received data the ASTRA (version) 5.1.5 and Eclipse software from Wyatt Technology were used.

6 RESULTS AND DISCUSSION

6.1 Preliminary experiments

6.1.1 Osmolality measurements

In order to expose the liposomes to osmotic stress it was necessary to prepare solutions of distinct osmolalities. In addition to calculating the amount of solute that is needed for a solution with a given osmolality it was decided to measure the osmolality of different solutions to check the calculated values and to check that sodium nitrate dissociates completely. We calculated how much glucose or sucrose is needed to make a solution with the same osmolality as a solution with a known sodium nitrate concentration, as describes in appendix 1. The calculated amounts are given in table 6.1.1.

Table 6.1.1: Amount of sucrose, glucose and sodium nitrate needed to make solutions of various given osmolalities

Amount solid (given in gram per liter)	Concentration of the solution
3.5592 g glucose + 0.8499 g $NaNO_3$	Equivalent to 20 mM sodium nitrate
14.2363 g glucose + 0.8499 g $NaNO_3$	Equivalent to 50 mM sodium nitrate
0.5694 g sucrose + 0.8499 g $NaNO_3$	Equivalent to 20 mM sodium nitrate
2.2778 g sucrose + 0.8499 g $NaNO_3$	Equivalent to 50 mM sodium nitrate
0.8499 g $NaNO_3$	20 mM sodium nitrate
4.2495 g $NaNO_3$	50 mM sodium nitrate

We prepared two different solutions, one with 20 mM sodium nitrate and one with 50 mM sodium nitrate. Corresponding solutions that contained 10 mM sodium nitrate and an amount of glucose or sucrose (equivalent to either 10 mM sodium nitrate or 40 mM sodium nitrate) that made the osmolality equal to the corresponding sodium nitrate solution were also prepared. Both corresponding solutions contained the same amount of salt because we wanted to have the same ionic strength in all the solutions.

The freezing points of all the solutions were measured using an osmometer, against a sodium chloride calibration solution of known osmolality. The results, expressed in mOsm/kg, are summarized in table 6.1.2.

Table 6.1.2: Results from the osmolality measurements

Solution	**Measured value (average ± SD of three parallels)**
20 mM sodium nitrate	40.0 mOsm/kg ± 0 mOsm/kg
10 mM sodium nitrate and glucose equivalent to 10 mM sodium nitrate	42.0 mOsm/kg ± 0 mOsm/kg
10 mM sodium nitrate and sucrose equivalent of 10 mM sodium nitrate	39.0 mOsm/kg ± 1 mOsm/kg
50 mM sodium nitrate	95.3 mOsm/kg ± 0.58 mOsm/kg
10 mM sodium nitrate and glucose equivalent to 40 mM sodium nitrate	101.0 mOsm/kg ± 1 mOsm/kg
10 mM sodium nitrate and sucrose equivalent to 40 mM sodium nitrate	98.0 mOsm/kg ± 0 mOsm/kg

The results show that the measured osmolalities of the salt solutions and corresponding combined salt and sugar solutions were within 5 % variability. The calculated values of sugar needed to prepare a solution with a distinct osmolality were thus confirmed. It was decided that when other solutions with different osmolality were to be made, it would be adequate only to calculate the values and not measure every solution with the osmometer.

6.1.2 Viscosity measurements

It is also important to determine the exact viscosity of the various dispersion media used for PCS measurements. The reason why viscosity is so important can be described with the Stokes-Einstein equation expressed in equation 15:

Equation 15: $D = kT/6\pi\eta R$

From D (the diffusion coefficient) in the Stokes-Einstein equation it is easy to calculate the particle radius as described in section 5.5.1. η in equation 15 is liquid viscosity and it is affecting the size calculation.

If an incorrect viscosity value is entered in the PCS software the calculation will be wrong, resulting in an incorrect mean Stokes diameter.

Both media that contained sugar (glucose or sucrose) were measured. For the solution just containing sodium nitrate the viscosity was assumed to be the same as for water. In table 5.3.1 we can see that the solution with 10 mM sodium nitrate contained 0.8499 g/L or 0.8499 % sodium nitrate. The literature value for viscosity of an aqueous solution with 0.5 % sodium nitrate is 1.0016 cP (20°C), and for a solution with 1.0 % the viscosity is 1.0050 cP (20°C). If we compare those values to the viscosity of water 1.0020 cP (20°C) we can see that the amount of sodium nitrate in 10 mM sodium nitrate solution would not affect the viscosity markedly (CRC Handbook of Chemistry and Physics Lide 2008). The measurements were executed as described in section 5.5.3, with a glass capillary viscometer. The results are given in table 6.1.3. A calculation example is given in appendix 2.

Table 6.1.3: Results from the viscosity measurements

Solution	**Measured viscosity**
10 mM sodium nitrate and glucose equivalent to 90 mM sodium nitrate	1.001 cP (mPa·s)
10 mM sodium nitrate and sucrose equivalent to 90 mM sodium nitrate	0.9898 cP (mPa·s)

6.1.3 Refractive index measurements

The intensity of light scattered by a single, isolated particle depends on its molecular weight and overall size and shape, but also on the difference in refractive indices of the particle and the surrounding solvent. Therefore it is of great significance to know the exact refractive index of the dilution medium when PCS measurements are executed.

The refractive indices of media were measured with a RI (refractive index)-detector in the batch mode as described in section 5.5.4. The results are summarized in table 6.1.4.

Table 6.1.4: Results from refractive index measurements

Solution	Measured refractive index
10 mM sodium nitrate	1.333
10 mM sodium nitrate and glucose equivalent to 90 mM sodium nitrate	1.336
10 mM sodium nitrate and sucrose equivalent to 90 mM sodium nitrate	1.339

6.1.4 Influence of viscosity and refractive index on the accuracy of PCS size measurements of latex bead standards

Latex particles with a specified size of 102 ± 3 nm were used. Latex bead standards were diluted in all the different media used to dilute liposomes for PCS measurements. They were diluted in 10 mM sodium nitrate medium, in 10 mM sodium nitrate and glucose medium and in 10 mM sodium nitrate and sucrose medium. Firstly the viscosity and refractive index values of water were used in the PCS software. The PCS results are given in table 6.1.5.

Table 6.1.5: PCS mean diameters of latex beads calculated on the basis of viscosity and refractive index values of water. The number of valid parallels used for calculations of mean vesicle sizes and standard deviations are given in table 9.13-9.15 in appendix 3

Sample	**Mean vesicle size ± SD (from PCS measurements)**		
	Intensity weighting	Volume weighting	Number weighting
Latex bead standards diluted with 10 mM sodium nitrate	105.6 nm ± 0.21 nm	103.6 nm ± 1.52 nm	101.3 nm ± 1.97 nm
Latex bead standards diluted with 10 mM sodium nitrate and glucose equivalent to 90 mM sodium nitrate	113.5 nm ± 0.41 nm	110.7 nm ± 1.88 nm	107.6 nm ± 4.20 nm
Latex bead standards diluted with 10 mM sodium nitrate and sucrose equivalent to 90 mM sodium nitrate	117.9 nm ± 0.39 nm	116.6 nm ± 0.86 nm	115.1 nm ± 1.97 nm

From the table above it is possible to see that the viscosity and refractive index values play a significant role in the size measurements executed by PCS. As we can see the mean diameter is around 15 nm larger than the defined diameter when sucrose is used as medium with the viscosity and refractive index values of water.

In the next step the PCS results were recalculated size using the measured values for both refractive index and viscosity of the sugar solutions. The PCS results are given in table 6.1.6.

Table 6.1.6: PCS mean diameters of latex beads calculated on the basis of measured viscosity and refractive index values. The number of valid parallels used for calculations of mean vesicle sizes and standard deviations are given in table 9.16-9.17 in appendix 3

Sample	Mean vesicle size ± SD (from PCS measurements)		
	Intensity weighting	Volume weighting	Number weighting
Latex bead standards diluted with 10 mM sodium nitrate and glucose equivalent to 90 mM sodium nitrate	106.2 nm ± 0.40 nm	103.6 nm ± 1.74 nm	100.7 nm ± 3.86 nm
Latex bead standards diluted with 10 mM sodium nitrate and sucrose equivalent to 90 mM sodium nitrate	104.6 nm ± 0.34 nm	103.8 nm ± 0.64 nm	102.8 nm ± 1.52 nm

As we can see in table 6.1.6 the measured viscosity and refractive indices yield diameters closer to the value specified by the manufacturer. The mean diameter of the latex particles is smaller as compared to the data based on the viscosity and refractive index value of water, and is close to 102±3 nm as specified by the producer.

6.1.5 Freeze-thaw experiments

Liposomes were prepared by the hand-shaken method according to section 5.4.1, with subsequent extrusion of the raw MLV dispersion through polycarbonate filters. Extrusions were carried out following the method described in section 5.4.3, continuous filter extrusion. It is a common practice to increase the proportion of unilamellar vesicles in preparations by subjecting MLVs to freeze-thaw cycles prior to extrusion (Liposome technology Mui and Hope 2006). Experiments were executed to investigate how different freezing methods affected the size distributions of liposomes.

-80°C freezer and liquid nitrogen were used for freezing the liposome dispersions. In addition we investigated whether it would make a difference if the freeze-thawing cycles were done before, after or during the extrusion process. All the different liposome preparations were thawed on a 50°C water bath for approximately 20 minutes, until the liposome dispersion was completely thawed. In total, four preliminary freeze-thaw experiments were executed as described in section 5.4.2. The results from the PCS measurements are given in table 6.1.7.

Table 6.1.7: PCS mean diameter ± standard deviation and distribution width ± standard deviation from freeze-thawing experiments. The number of valid parallels used for calculations of mean vesicle sizes, distribution widths and standard deviations are given in table 9.18-9.23 in appendix 3

Experiment description	**Mean vesicle size ± standard deviation**		
	Intensity weighting	Volume weighting	Number weighting
1. Liposome dispersion frozen in -80°C freezer before extrusion	116.6 nm ± 0.35 nm	116.5 nm ± 0.40 nm	89.9 nm ± 2.81 nm
2. Liposome dispersion frozen in LN_2 before extrusion	112.4 nm ± 0.38 nm	111.7 nm ± 0.45 nm	86.1 nm ± 2.17 nm
3. Liposome dispersion frozen in -80°C freezer during extrusion	114.5 nm ± 0.25 nm	114.1 nm ± 0.28 nm	91.3 nm ± 2.70 nm
4. Liposome dispersion frozen in -80°C freezer after extrusion	Not possible, the liposomes were broken and formed much bigger aggregates. It was not possible to measure the liposomes by PCS.		
Experiment description	**Distribution width ± standard deviation**		
	Intensity weighting	Volume weighting	Number weighting
1. Liposome dispersion frozen in -80°C freezer before extrusion	32.1 nm ± 1.81 nm	32.1 nm ± 1.83 nm	24.7 nm ± 0.62 nm
2. Liposome dispersion frozen in LN_2 before extrusion	31.3 nm ± 1.17 nm	31.1 nm ± 1.17 nm	23.9 nm ± 0.38 nm
3. Liposome dispersion frozen in -80°C freezer during extrusion	29.5 nm ± 1.62 nm	29.4 nm ± 1.62 nm	23.5 nm ± 0.67 nm

As the results in table 6.1.7 show, there is no major difference in the measured mean sizes for the first three preparation methods. It seems that it does not make a big difference whether the freeze-thawing cycles are done before extrusion or during extrusion. It might help to look at the distribution width (expressed as standard deviation), because ideally the liposomes should be more homogenous in size after freeze-thawing cycles and then the standard deviation would decrease. There is a minor difference, but it is too small to say whether one method should be preferred above another.

It was decided to perform a two sample t-test to see if there was a significant difference between the different freeze-thawing methods. All the t-tests were executed with a significance level of 0.05. It was discovered that there was a significant difference between the liposome dispersion frozen in a -80° freezer before extrusion and the liposome dispersion frozen in a -80° freezer during extrusion. When the other liposomes dispersions were compared it was not discovered a statistical significant difference.

There is not a large size difference from the liposomes frozen in liquid nitrogen to the liposomes frozen in -80°C freezer. Again only small differences could be seen when looking at the standard deviations of the different methods. The third setup/experiment was rather impractical because the extrusion process had to be stopped. This doubled the loss of dispersion and the extruder had to be cleaned twice. For being the most time saving method the first procedure was chosen for further preparations.

All liposomes show a slightly larger mean diameter than the pore size of the filter used for the extrusions. This can be explained by the flexibility of the liposomal membranes. Lipoid E-80 forms very flexible liposomes that are assumed to alter their shapes while squeezing through the filter pores (Liposome technology Gregoriadis 2006). Liposomes that are substantially bigger then 100 nm will either break and form smaller liposomes that are able to pass through the polycarbonate filter, or they can alter their shape and hence pass through the filter even though the diameter is bigger than 100 nm.

6.2 Influence of osmotic stress on liposome size, measured by PCS

All the liposome dispersions made throughout this project were prepared as the liposomes in experiment 1 in section 5.4.2. Every liposome dispersion was made as a 10 % lipid dispersion, produced by the hand-shaken method, described in section 5.4.1 with subsequent filter extrusion, as described in section 5.4.3. The dispersion media varied between sodium nitrate solution, sodium nitrate and glucose solution or sodium nitrate and sucrose solution.

We could have used more sodium nitrate to adjust the osmolality, but it would also influence the ionic strength and thus potentially the retention behavior in the flow field-flow fractionation experiments (A4F/MALS-Analysis of Liposomes Influence of Key Factors on Fractionation Behavior and Evaluation of MALS Fit Routines Ausbacher 2007).

6.2.1 Hypertonic osmotic stress experiment with 10 mM $NaNO_3$ and glucose equivalent to 90 mM $NaNO_3$ as dilution medium

The first experiment was executed with liposomes prepared in 10 mM sodium nitrate medium. The liposome dispersion was freeze-thawed as described in section 6.1.5 before extrusion, and the mean diameter was measured by PCS right after preparation. The liposome dispersion was diluted 1:10 with 10 mM sodium nitrate and glucose equivalent to 90 mM sodium nitrate (a hyperosmolal medium). The liposome size was measured by PCS 1 hour, 24 hours and 48 hours after dilution, to see if the osmotic stress affected their size. The results from the PCS measurements are given in table 6.2.1.

Table 6.2.1: The liposomes mean diameters during osmotic stress experiments (hyperosmolal dilution) with glucose. Valid parallels used for calculations of mean vesicle sizes and standard deviations are given in table 9.1-9.4 in appendix 3

Experiment description	**Mean vesicle size ± SD (from PCS measurements)**		
	Intensity weighting	Volume weighting	Number weighting
Liposome dispersion prepared with 10 mM sodium nitrate	119.7 nm ± 0.73 nm	120.4 nm ± 0.91 nm	86.8 nm ± 1.77 nm
Liposome dispersion 1 hour after dilution with 10 mM sodium nitrate and glucose equivalent to 90 mM sodium nitrate	110. 8 nm ± 0.93 nm	93.5 nm ± 2.02 nm	76.4 nm ± 3.11 nm
Liposome dispersion 24 hours after dilution with 10 mM sodium nitrate and glucose equivalent to 90 mM sodium nitrate	113.9 nm ± 0.44 nm	96.3 nm ± 2.36 nm	78.8 nm ± 4.32 nm
Liposome dispersion 48 hours after dilution with 10 mM sodium nitrate and glucose equivalent to 90 mM sodium nitrate	113.8 nm ± 0.35 nm	95.7 nm ± 0.96 nm	77.7 nm ± 1.60 nm

Obviously the mean sizes after dilution with hyperosmotic medium changed. The mean diameter has reduced by almost 6 nm with intensity weighting, almost 27 nm with volume weighting and over 10 nm with number weighting. Intensity weighting reflects the relative intensity of scattered light vs. diameter for a sample run. Volume weighting reflects the relative particle diameter vs. diameter; the value of the volume-weighted particle size distribution assumes that the particles are spheres of uniform density. Volume weighting and mass weighting are equal terms. Number weighting displays the relative number of particles in a sample run vs. diameter, and they are also calculated assuming that the particles are spheres.

The value of the mean diameter can vary significantly with the choice of weighting, depending on the width of the gaussian-like distribution (Windows based software, Dynamic light scattering theory User Manual 1997). One big particle will hence affect the mean size distribution in volume weighting more than number weighting. This may explain why the measured size difference is so deviating when looking at the different weightings.

But, irrespective of weighting a clear change of size can be seen when the liposomes were diluted with the hyperosmolal solution. As we could expect it does look like the liposomes have shrunk. When the osmotic pressure inside the liposomes is smaller than the osmotic pressure outside, water will diffuse out of the liposomes, in order to equal the concentration inside and outside the liposomes. The biggest mean size difference can be seen 1 hour after dilution. The mean size does not change much from 1 hour to 24 hours, there is a small difference and it could well be that the glucose starts to penetrate the membrane and hence reverse the shrinking to some extent.

It was reported that glucose is slowly membrane permeable, half-life ($t_{1/2}$) = 1 hour, at 45°C. According to (Osmotic properties of large unilamellar vesicles prepared by extrusion Mui, Cullis 1993) glucose will penetrate the liposome membrane. . (Osmotic properties of large unilamellar vesicles prepared by extrusion Mui, Cullis 1993) used another liposome membrane, their membrane contained cholesterol which will make the membrane stiffer and less permeable. Since Lipoid E-80 forms a less stiff membrane one could assume that glucose will penetrate the membrane even faster. Since we did not know if that could occur in our experiment it was decided to perform a similar experiment with sucrose instead of glucose. If glucose to some extent penetrates the membrane the osmotic stress would not be as large as it was supposed to be. Sucrose is a bigger molecule (almost twice as big as glucose) and should thus penetrate the liposome membrane to an even lower extent than glucose. The molecular weight (Mw) of glucose is 180.16 g/mol while the sucrose has an Mw of 342.30 g/mol. Since we were not sure how fast glucose was able to penetrate through our liposome membrane it was decided to also perform the next experiment with sucrose.

6.2.2 Hypertonic osmotic stress experiment with 10 mM $NaNO_3$ and sucrose equivalent to 90 mM $NaNO_3$ as dilution medium

Liposomes again were prepared according to the hand-shaken method as described before, with 10 mM sodium nitrate as dispersion medium. The size was measured by PCS right after preparation, and the liposome dispersion was diluted 1:10 with 10 mM sodium nitrate and sucrose equivalent to 90 mM sodium nitrate (a hyperosmolal medium). It is the same experiment as the one described in section 6.2.1, the only difference is that glucose is replaced by sucrose. The liposome size was measured by PCS 1 hour, 24 hours and 48 hours after dilution. This was done to see if a size difference from the original undiluted sample could be detected, and how fast it happened. Results from the PCS measurements are given in table 6.2.2.

Table 6.2.2: Mean diameters during osmotic stress experiment (hyperosmolal dilution) with sucrose. Valid parallels used for calculations of mean vesicle sizes ± SD are given in table 9.5-9.8 in appendix 3

Experiment description	**Mean vesicle size ± SD (from PCS measurements)**		
	Intensity weighting	Volume weighting	Number weighting
Liposome dispersion prepared with 10 mM sodium nitrate	118.3 nm ± 0.61 nm	118.6 nm ± 0.67 nm	90.5 nm ± 3.34 nm
Liposome dispersion 1 hour after dilution with 10 mM sodium nitrate and sucrose equivalent to 90 mM sodium nitrate	114.3 nm ± 0.29 nm	93.7 nm ± 1.71 nm	73.8 nm ± 2.73 nm
Liposome dispersion 24 hours after dilution with 10 mM sodium nitrate and sucrose equivalent to 90 mM sodium nitrate	116.5 nm ± 0.46 nm	97.0 nm ± 3.04 nm	77.8 nm ± 4.97 nm
Liposome dispersion 48 hours after dilution with 10 mM sodium nitrate and sucrose equivalent to 90 mM sodium nitrate	116.6 nm ± 0.29 nm	95.1 nm ± 2.10 nm	74.4 nm ± 3.54 nm

Again a difference in the sizes before and after dilution with the sucrose medium is seen. The size difference in this experiment is almost 17 nm (number weighting) and almost 25 nm (volume weighting). If we compare these results with the results when glucose was used, a somewhat bigger size difference can be seen here.

6.2.3 Hypotonic osmotic stress experiment with 10 mM $NaNO_3$ as dilution medium

After it could be seen that is was possible to discover a size difference when liposomes were diluted with a hyperosmolal solution, the liposome dispersion was prepared with 10 mM sodium nitrate and sucrose equivalent to 90 mM sodium nitrate. The exact viscosity and refractive index of the sucrose medium was already determined, so these values were used when the size was measured by PCS. The liposomes were then diluted with 10 mM sodium nitrate (hypoosmolal medium). And the sizes were measured by PCS after one hour, 24 hours and 48 hours. The results from the PCS measurements are given in table 6.3.2.

Table 6.2.3: Liposome sizes during osmotic stress experiment (hypoosmolal dilution) with sucrose. Valid parallels used for calculations of mean vesicle sizes ± SD are given in table 9.9-9.12 in appendix 3

Experiment description	**Mean vesicle size ± SD (from PCS measurements)**		
	Intensity weighting	Volume weighting	Number weighting
Liposome dispersion prepared with 10 mM $NaNO_3$ and sucrose equivalent to 90 mM $NaNO_3$	121.6 nm ± 0.36 nm	103.8 nm ± 2.20 nm	85.4 nm ± 3.86 nm
Liposome dispersion 1 hour after dilution with 10 mM $NaNO_3$	118.4 nm ± 0.36 nm	118.5 nm ± 0.40 nm	96.1 nm ± 4.49 nm
Liposome dispersion 24 hours after dilution with 10 mM $NaNO_3$	118.3 nm ± 0.26 nm	118.4 nm ± 0.25 nm	94.1 nm ± 2.34 nm
Liposome dispersion 48 hours after dilution with 10 mM $NaNO_3$	118.4 nm ± 0.35 nm	118.5 nm ± 0.37 nm	95.1 nm ± 2.28 nm

From the table above we can see that the mean size of the liposomes increases after they are diluted in a hypoosmolal medium at least when looking at volume weighting and number weighting. The intensity weighting shows only little change and it looks like the liposomes have shrunk because the mean diameter is smaller after the dilution.

But the change in diameter is only 3.2 nm and it is not considered as a change due to the osmotic stress the liposomes have been exposed to. When we look at the size changes with volume weighting we can see a much bigger effect, the mean diameter increases with almost 15 nm. As one could predict, it seems that the liposomes have swollen when they were diluted with the hypoosmolal medium. The concentration is bigger inside, than outside of the liposome and as a consequence water will diffuse from the surrounding liquid into the liposome.

6.3 Influence of osmotic stress on liposome size, measured by AF4

The liposomes used for these following experiments were prepared in the same manner as those described in section 6.2. Again was chosen to adjust different osmotic pressures by adding sucrose. After the previous experiments with both 10 mM sodium nitrate and glucose solution and 10 mM sodium nitrate and sucrose solution as dilution agent it was decided to only use the sucrose solution in the following experiments, because glucose might penetrate the membrane as discussed earlier is section 6.2.1. Increasing the sodium nitrate concentration is at the same time influencing the ionic strength which however could influence retention time to an unknown degree (A4F/MALS-Analysis of Liposomes Influence of Key Factors on Fractionation Behavior and Evaluation of MALS Fit Routines Ausbacher 2007).

Two different liposome batches were prepared, one with 10 mM sodium nitrate and one with 10 mM sodium nitrate and sucrose equivalent to 90 mM sodium nitrate as dispersion medium. Both of the two batches were then diluted 1:10 with either the same medium as the one used for preparing the liposome or the other medium giving four different experiment, as shown in table 6.3.1. Every sample was analyzed by AF4 one hour after dilution. We had already learned, from the PCS measurements, that the change of particle size by osmotic pressure occurs within the first hour. The mobile phase in the AF4 experiments was always the same medium as the one used as dilution medium.

Table 6.3.1: The four different liposome preparations used for analysis by the flow field-flow fractionation

Liposome sample	Dilution medium and mobile phase
100 nm liposomes prepared in 10 mM sodium nitrate	10 mM sodium nitrate
100 nm liposomes prepared in 10 mm sodium nitrate	10 mM sodium nitrate and sucrose equivalent to 90 mM sodium nitrate
100 nm liposomes prepared in 10 mM sodium nitrate and sucrose equivalent to 90 mM sodium nitrate	10 mM sodium nitrate
100 nm liposomes prepared in 10 mM sodium nitrate and sucrose equivalent to 90 mM sodium nitrate	10 mM sodium nitrate and sucrose equivalent to 90 mM sodium nitrate

It was decided to compare the liposome samples prepared in the same medium, because they were from the same batch and hence we knew that they had the same size before dilution and that they generally had the same physical properties. We could not know if the liposomes made in 10 mM sodium nitrate and the liposomes made in 10 mM sodium nitrate and sucrose equivalent to 90 mM sodium nitrate had the same size after preparation. The extrusion of the two different batches was performed in the same manner, but it is unknown how parameters like different viscosity of the dispersion medium were influencing the size distribution and the properties of the liposomes.

If we look at table 6.2.2, we can see the mean size distribution of the liposomes prepared in 10 mM sodium nitrate and we can compare them to table 6.2.3 where we can see that the mean size distribution of the liposomes prepared in 10 mM sodium nitrate and sucrose equivalent to 90 mM sodium nitrate. The liposomes prepared in 10 mM sodium nitrate have an intensity weighted mean diameter of 118.3 nm, a volume weighted mean diameter of 118.6 nm and a number weighted mean diameter of 90.5 nm. The liposomes prepared in 10 mM sodium nitrate and sucrose equivalent to 90 mM sodium nitrate have an intensity weighted mean diameter of 121.6 nm, a volume weighted mean diameter of 103.8 nm and a number weighted mean diameter of 85.4 nm. We can see that the mean diameter of the liposomes is not the equal when the liposomes are prepared in the two different media.

And it is unknown if the liposomes prepared in different media would react differently when they are diluted in a hypo-/hyperosmolal solution.

6.3.1 Hyperosmotic osmotic stress experiment with 10 mM $NaNO_3$ and sucrose equivalent to 90 mM $NaNO_3$ as dilution medium

First we looked at the two samples prepared in 10 mM sodium nitrate, diluted in either 10 mM sodium nitrate or 10 mM sodium nitrate and sucrose equivalent to 90 mM sodium nitrate. (The first two experiments listed in table 6.3.1.)

Each of the samples was run in five parallels and both; the UV/VIS-absorbance and the Rayleigh ratio were recorded over time. UV/VIS-detection is common in flow field-flow fractionation. The first plot, shown in figure 6.3.1 presents the absorbance vs. time.

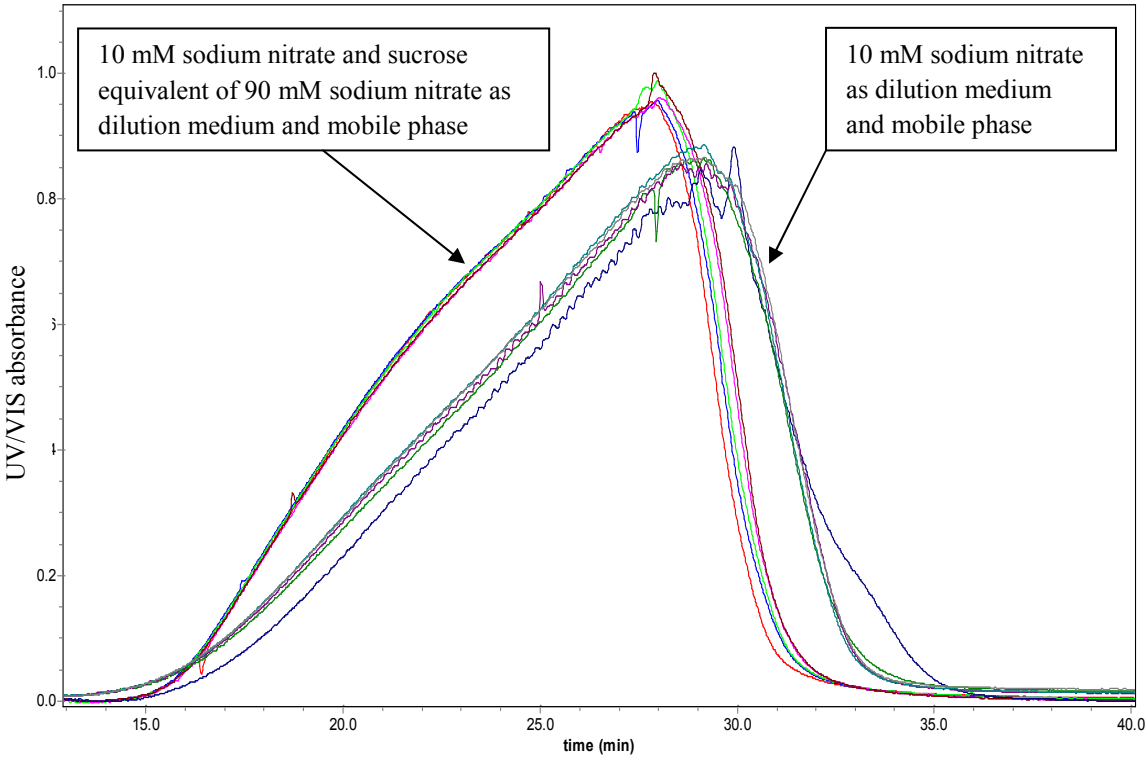

Figure 6.3.1: UV/VIS absorbance vs. time for the two liposomes samples prepared in 10 mM sodium nitrate, diluted in either 10 mM sodium nitrate or 10 mM sodium nitrate and sucrose equivalent to 90 mM sodium nitrate (five parallels each)

The Rayleigh ratio is a quantity used to characterize the scattered intensity as a function of scattering angle and is defined in section 5.5.5. Figure 6.3.2 show a plot of Rayleigh ratio vs. time.

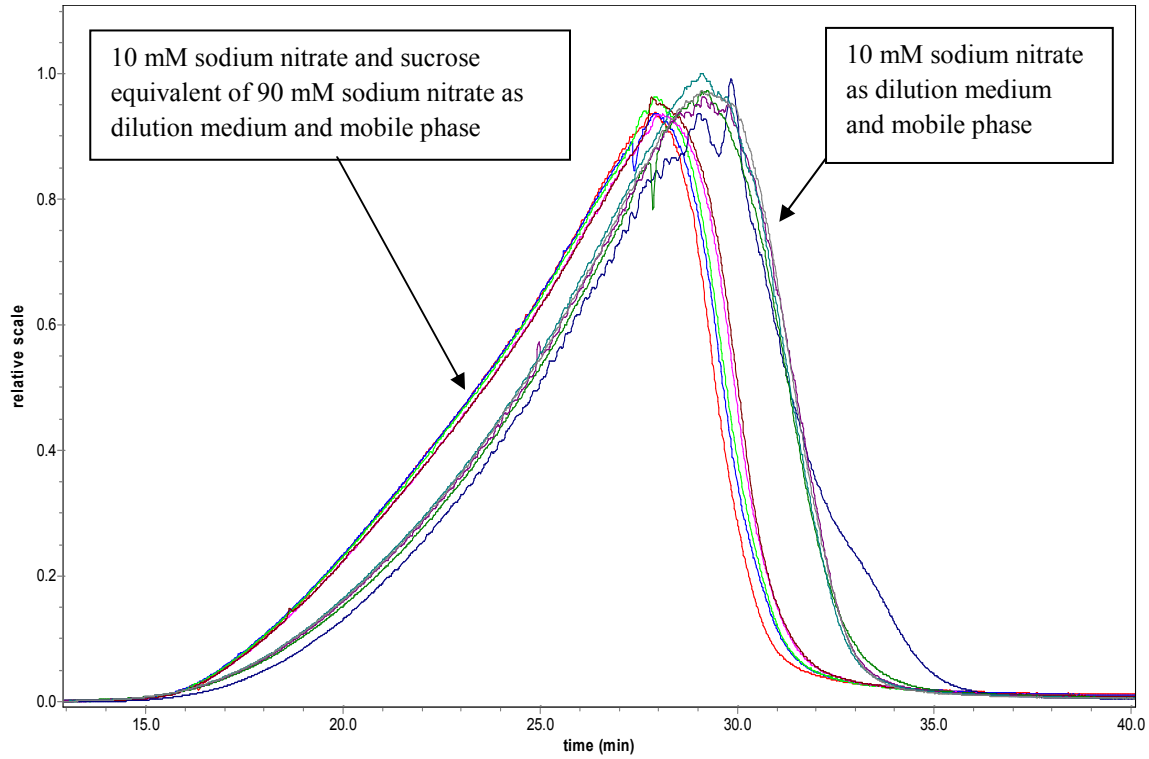

Figure 6.3.2: Plot of Rayleigh ratio vs. time for the two liposome samples prepared in 10 mM sodium nitrate, diluted in either 10 mM sodium nitrate or 10 mM sodium nitrate and sucrose equivalent to 90 mM sodium nitrate (five parallels each)

As we can see are the two plots very similar. The parallels for the same sample are very close to each other, whereas the two samples behave markedly different: The curves of the liposome dispersion diluted in 10 mM sodium nitrate and sucrose equivalent to 90 mM sodium nitrate appear shifted left in both plots. This indicates that the liposomes prepared in 10 mM sodium nitrate solution and diluted in 10 mM sodium nitrate and sucrose equivalent to 90 mM sodium nitrate (hypertonic) solution elutes before the liposomes prepared and diluted in 10 mM sodium nitrate solution. According to the AF4 theory; smaller particles will elute earlier from the channel as described in section 5.5.5.

When we are comparing these two samples we can see that the sample diluted in the hypertonic medium elutes before the sample diluted in the isotonic medium. We can assume thus that the liposomes have become smaller when they were blended with the hypertonic medium since they eluted earlier.

Next, from the angular dependence of the light scattering signal the geometric radii were calculated for all slices over the whole elution. Figure 6.3.3 shows the resulting size, geometric radius vs. elution type. Since we used a sphere model for the sample is the radius presented as geometric radius (Wyatt Technology Corporation User Manual 2007). Figure 6.3.3 shows the same samples as figure 6.3.1 and 6.3.2. We can see in figure 6.3.3 that both the samples show very similar sizes over time. The geometric radii reach from approximately 25 nm to 70 nm for both, the liposome sample diluted in 10 mM sodium nitrate and the liposome samples diluted in 10 mM sodium nitrate and sucrose equivalent of 90 mM sodium nitrate.

The lower part of figure 6.3.3 shows the same plot as the one above, but here the area between 20 and 25 min is enlarged to show the difference between the two samples clearer. Here it is possible to see that there is a slight shift to smaller sizes for a given elution time for the liposomes in hypertonic medium.

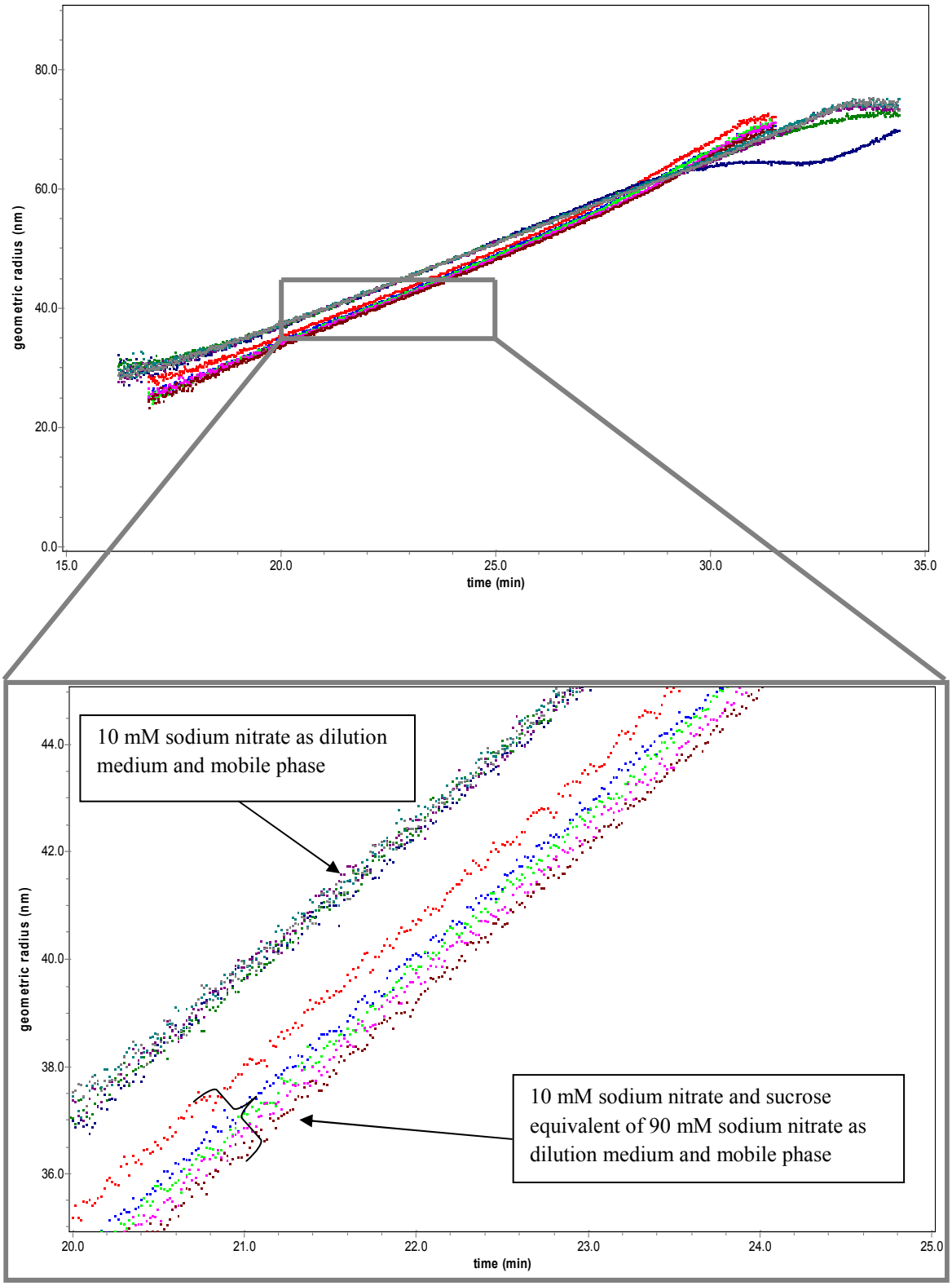

Figure 6.3.3: Geometric radius of the two liposome samples prepared in 10 mM sodium nitrate, diluted in either 10 mM sodium nitrate or 10 mM sodium nitrate and sucrose equivalent to 90 mM sodium nitrate (five parallels of each). The lower picture shows an enlarged section of the upper plot

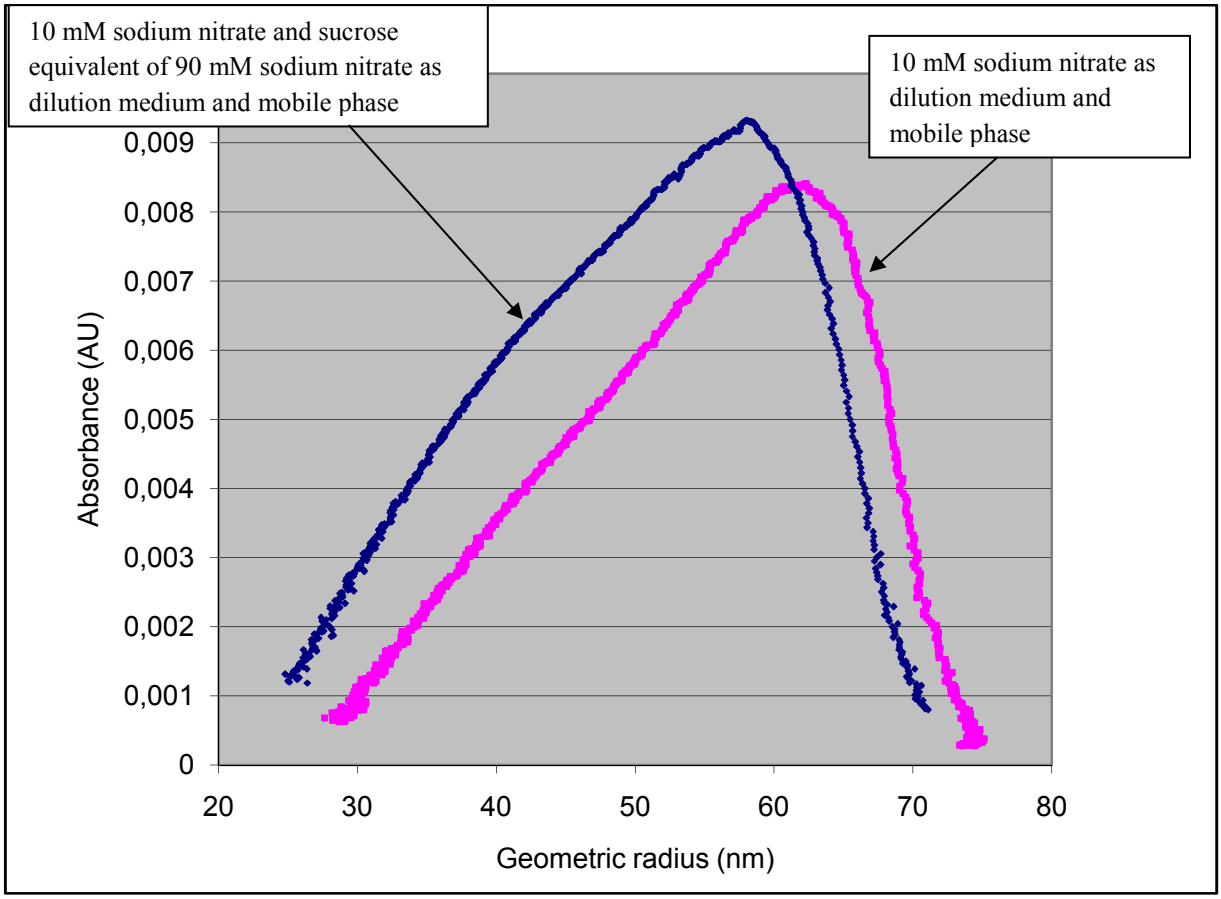

Figure 6.3.4: Parametric plot of the two liposome samples prepared in 10 mM sodium nitrate, diluted in either 10 mM sodium nitrate or 10 mM sodium nitrate and sucrose equivalent to 90 mM sodium nitrate

Finally a plot was constructed where the measured UV absorbance was plotted over the calculated geometric radii, a parametric plot. A parametric plot is a plot that generates a new data set for two different types of x-y data that share the same x-axis (Wyatt Technology Corporation User Manual 2007). For example, we can make a plot of absorbance vs. geometric radius, as shown in figure 6.3.4. In figure 6.3.4 only one parallel of each sample is shown. This is done because it gives a more perspicuous plot. The five parallels of each sample are shown in appendix 3; figure 9.5 and figure 9.6. The size distributions obtained this way are clearly different from each other. The size distribution of the liposomes in the hypertonic medium appears shifted towards smaller sizes as compared to liposomes in isotonic medium. This confirms that the shift in elution time seen before in figure 6.3.1 and figure 6.3.2 is due to a difference in the liposome size after the sample has been diluted in a hypertonic medium.

In the parametric plot we can see that all the liposomes from the lower end of the distribution (approximately 30 nm radius) to the upper end of the distribution (approximately 75 nm radius) have been equally affected by the osmotic stress they have been exposed to. The parallel shift of the whole curve to the left in figure 6.3.4 indicates that all the different sized liposomes are the sample is almost equally affected by the osmotic stress.

Table 6.3.2: Mean radii and standard deviation of the liposome samples prepared in 10 mM sodium nitrate, diluted in either 10 mM sodium nitrate and sucrose equivalent to 90 mM sodium nitrate or 10 mM sodium nitrate, from table 9.26 in appendix 3

Sample	**$R_n \pm SD$**	**$R_w \pm SD$**	**$R_z \pm SD$**
Liposomes prepared in 10 mM sodium nitrate, diluted in 10 mM sodium nitrate and sucrose equivalent to 90 mM sodium nitrate	46.8 nm ± 0.49 nm	51.8 nm ± 0.26 nm	55.5 nm ± 0.23 nm
Liposomes prepared in 10 mM sodium nitrate, diluted in 10 mM sodium nitrate	53.1 nm ± 0.35 nm	57.0 nm ± 0.08 nm	59.8 nm ± 0.32 nm

Table 6.3.2 shows the mean radius of two liposome samples prepared in 10 mM sodium nitrate as calculated from AF4 analysis. The liposomes diluted in the hypertonic medium are in mean smaller than the liposomes diluted in the isotonic medium. This corresponds with the result as we have seen from the plots in figure 6.3.1- figure 6.3.4. Here we can see that the number-average mean square radius decrease after hypertonic dilution by 6.3 nm, the weight-average mean square radius decrease by 5.2 nm and the z-average mean square radius decrease by 4.3 nm.

Table 6.2.2 shows the mean diameter, measured by PCS, of the same two liposome samples as the liposome samples in table 6.3.2.

The same hyperosmolal experiment are performed in both cases, the only difference is that the liposome sizes are measured with two different techniques. As we can see from the results, the same principles are constituted; the liposome shrink and the size decrease when it is diluted in a hypertonic medium.

6.3.2 Hypotonic osmotic stress experiment with 10 mM $NaNO_3$ as dilution medium

Secondly we looked at the liposome samples that were prepared in 10 mM sodium nitrate and sucrose equivalent to 90 mM sodium nitrate, diluted in either the same medium or in 10 mM sodium nitrate (hypotonic solution), the last two experiments in table 6.3.1. Here we would expect that the liposomes diluted in the hypoosmolal medium would expand and become larger. In figure 6.3.1 and 6.3.2 we saw that the liposomes shrunk when they were diluted in the hyperosmolal medium. This is the exact opposite experiment where the liposomes have a greater concentration inside than outside. If they became larger as we predicted they would elute last.

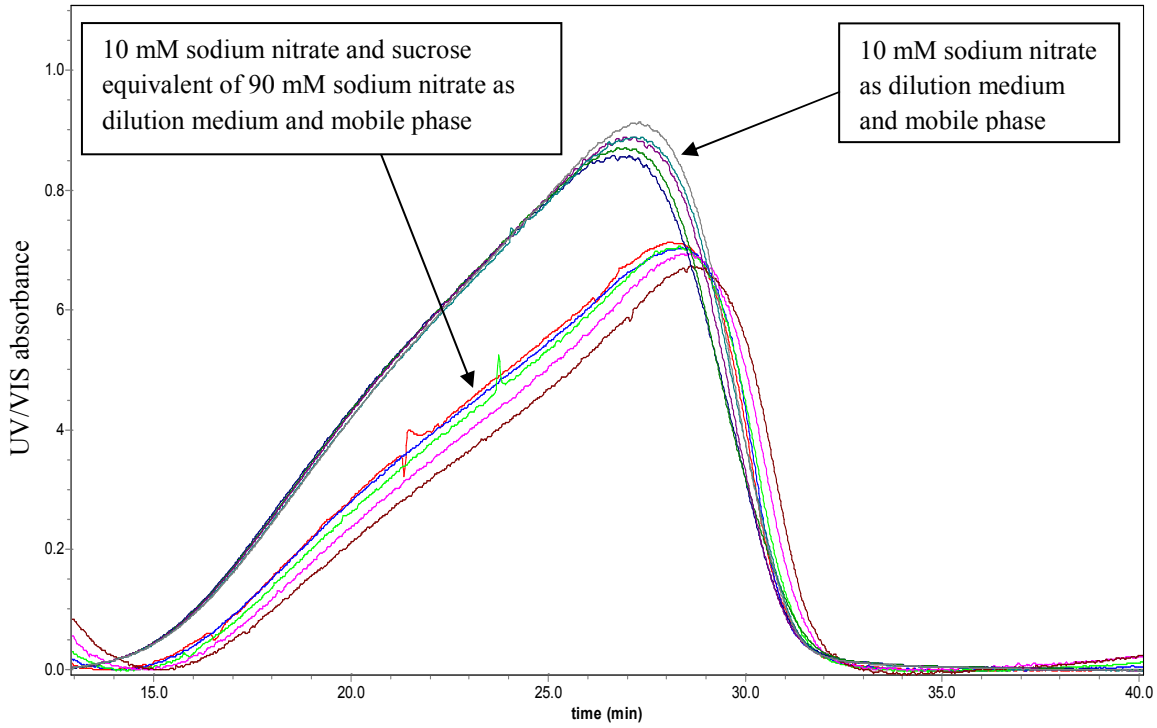

Figure 6.3.5: UV/VIS plot of absorbance vs. time for the two liposomes samples prepared in 10 mM sodium nitrate and sucrose equivalent to 90 mM sodium nitrate, diluted in either 10 mM sodium nitrate or 10 mM sodium nitrate and sucrose equivalent to 90 mM sodium nitrate (five parallels each)

Both the plots in figure 6.3.5 and figure 6.3.6 shows the same liposome samples which were prepared in 10 mM sodium nitrate and sucrose equivalent to 90 mM sodium nitrate. In figure 6.3.5 the absorbance is plotted against elution time. It looks like both the liposome samples elute roughly at the same time.

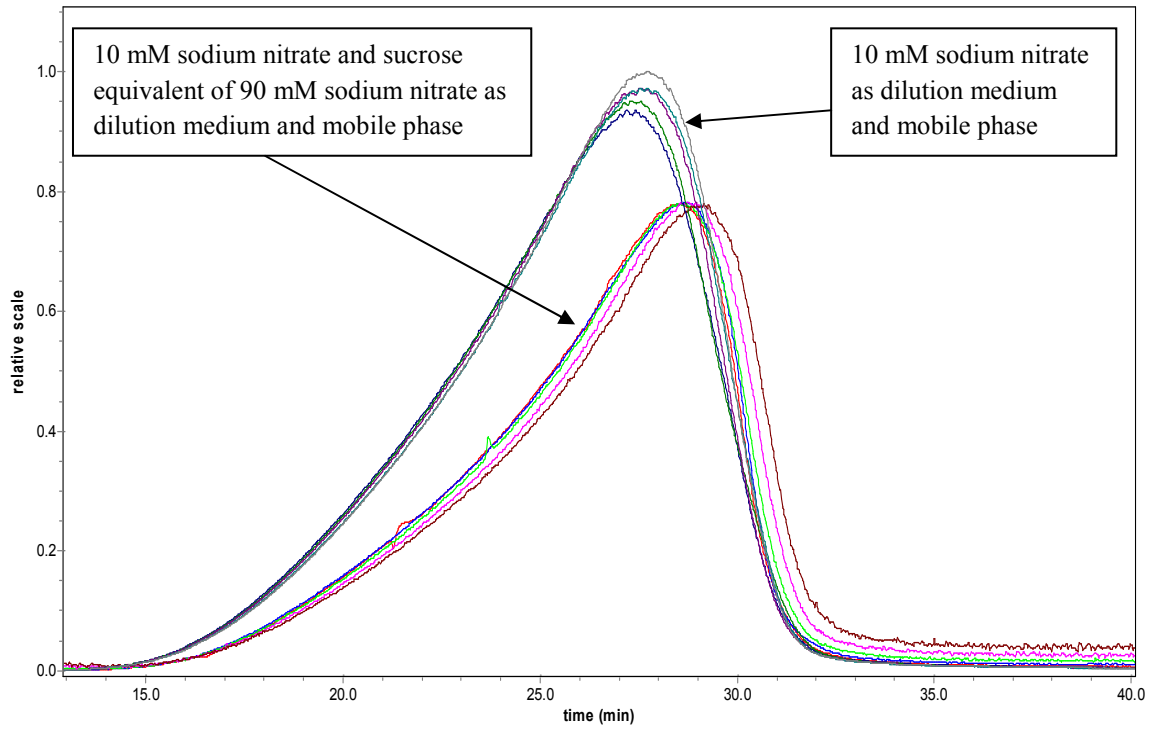

Figure 6.3.6: Plot of Rayleigh ratio vs. time for the two liposome samples prepared in 10 mM sodium nitrate and sucrose equivalent to 90 mM sodium nitrate, diluted in either 10 mM sodium nitrate or 10 mM sodium nitrate and sucrose equivalent to 90 mM sodium nitrate (five parallels each)

In figure 6.3.6 Rayleigh ratio is plotted against elution time. As in figure 6.3.5 both of the liposome samples elute at almost the same time. We can see it is no major difference in the two graphs.

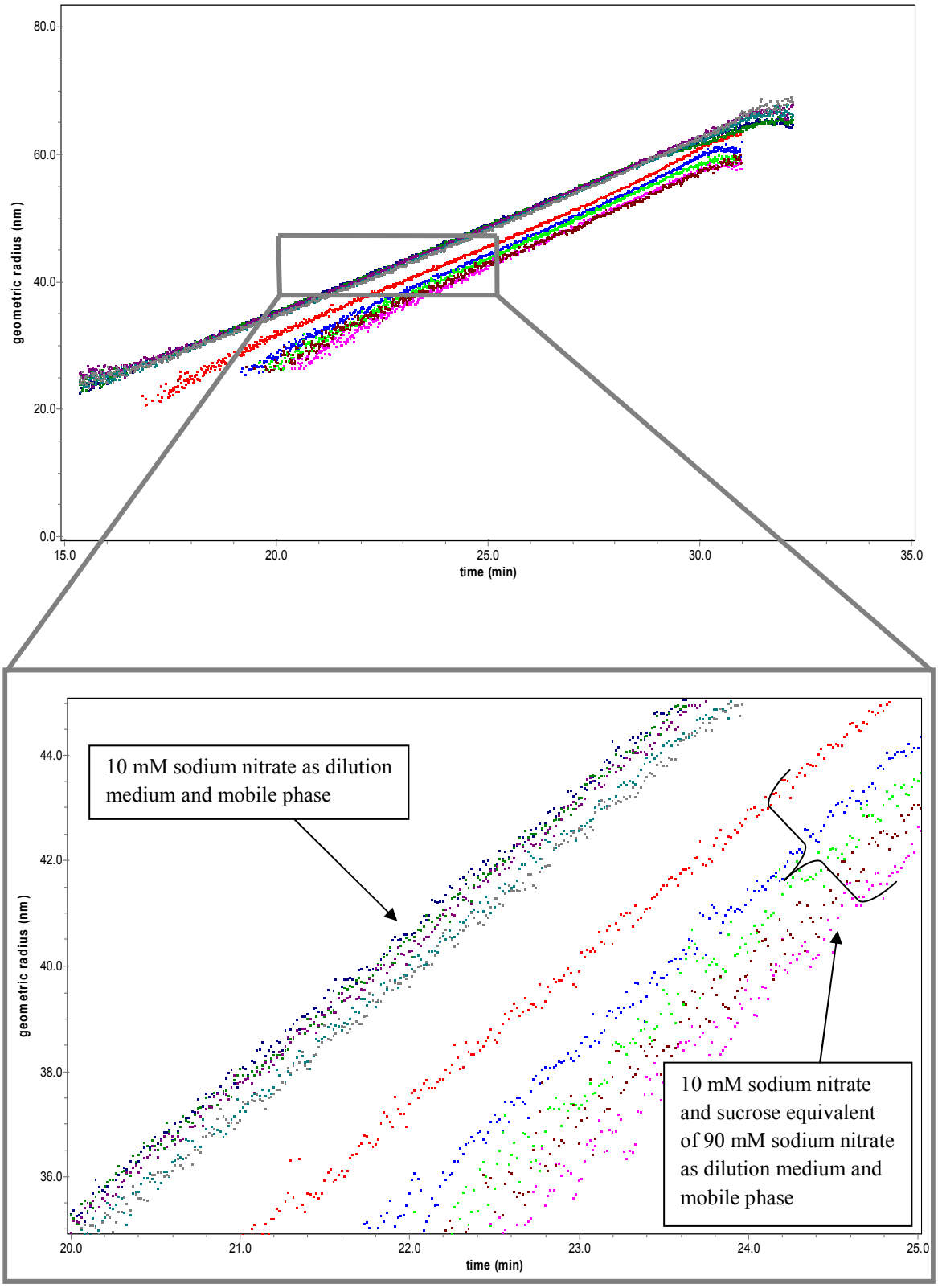

Figure 6.3.7: Geometric radius of the two liposome samples prepared in 10 mM sodium nitrate and sucrose equivalent to 90 mM sodium nitrate, diluted in either 10 mM sodium nitrate or 10 mM sodium nitrate and sucrose equivalent of 90 mM sodium nitrate (five parallels of each). The lower picture shows an enlarged section of the upper plot

Figure 6.3.7 shows a plot of sizes over time of the samples prepared in 10 mM sodium nitrate and sucrose equivalent to 90 mM sodium nitrate. It shows the same two samples as figure 6.3.5 and 6.3.6. When we compare these two samples it is possible to see a clear difference in sizes. The liposomes that were diluted in a hypotonic medium appear to have become larger. Furthermore the size-over-time lines are not fully parallel. When the concentration is higher inside of the liposomes than outside of the liposome, water will diffuse through the membrane into the core of the liposomes to equal the osmotic pressure. As a consequence the liposome will swell and become bigger. The geometric radius of the liposomes diluted in the hypotonic medium ranges from approximately 20 nm to 65 nm. The liposomes diluted in the isotonic medium ranges from approximately 20 nm to a little less than 60 nm. The lower part of figure 6.3.7 shows the same plot as the upper plot, but here the area between 20 and 25 min is enlarged to show the difference between the two samples clearer.

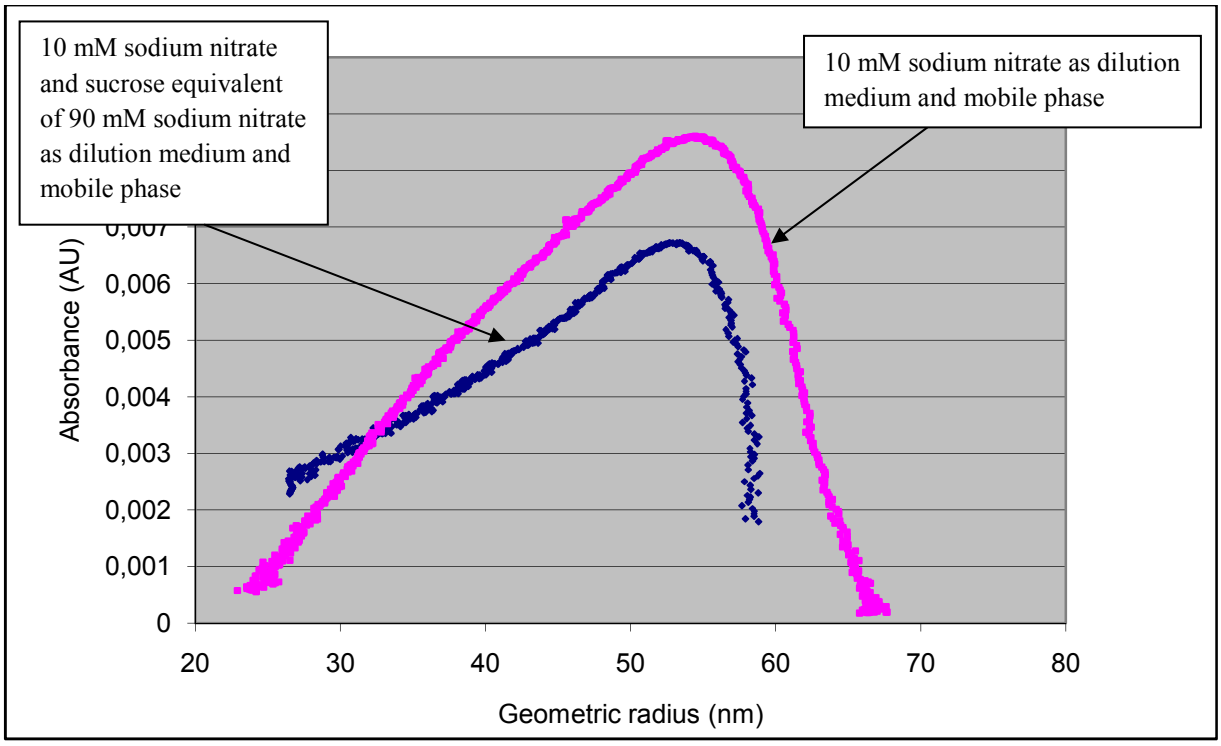

Figure 6.3.8: Parametric plot of the two liposome samples prepared in 10 mM sodium nitrate and sucrose equivalent to 90 mM sodium nitrate, diluted in either 10 mM sodium nitrate or 10 mM sodium nitrate and sucrose equivalent to 90 mM sodium nitrate

As we have seen before there is a difference in the liposome size after the sample has been diluted in a hypotonic medium. In the parametric plot in figure 6.3.8 we can see that not all the liposomes have been affected to the same extend when they are diluted in the hypotonic medium. Only one parallel of each sample is shown in figure 6.3.8, but all the five parallels are shown in appendix 3; figure 9.7 and figure 9.8. The outer curve in figure 6.3.8 shows the liposomes that have been diluted in the hypoosmolal medium; inner curve is the liposomes diluted in the isotonic medium. On the right side of the curve we can see that the liposomes that have been diluted in the hypoosmolal solution have become bigger. This is the same information we received from the geometric radius plots. And it is agreeing with the theory.

There will always be some liposomes that are smaller then the rest when they are prepared by extrusion, these liposomes is shown on the left side of the curve. On that side it is not possible to see a size difference between the two liposome samples. This information is also shown in figure 6.3.8, where the liposomes diluted in the hypotonic solution has almost the same minimum diameter as the liposomes diluted in the isotonic solution.

We could see from the plot that both of the liposome samples had geometric radius reaching from approximately 20 nm. The difference between the two samples was in the maximum size; there we could clearly see that the liposomes diluted in the hypotonic medium were bigger than the liposomes diluted in the isotonic medium. The two curves are crossing when the geometric radius is approximately 25 nm.

A conceivable explanation can be that the smaller liposomes have a different shape than the bigger liposomes and hence can change less in size. The liposomes that are smaller then 100 nm will pass through the filter without problem, and they will maintain their original conformation. But the liposomes that are larger than 100 nm need to either break and form smaller spheres or change their conformation when they are squeezing through the pores on the filter. In figure 6.3.9 and figure 6.3.10 the phenomenon is illustrated which we think might explain the size difference we saw in the parametric plot.

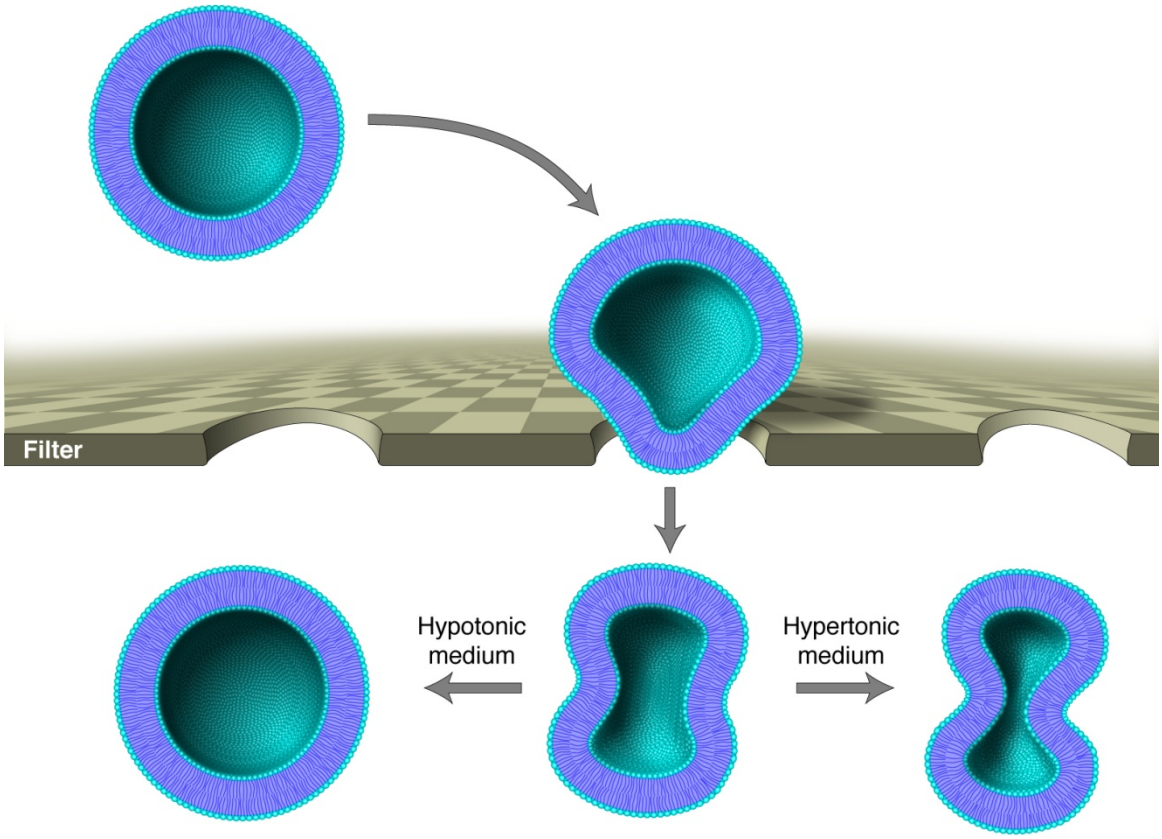

Figure 6.3.9: A liposome bigger than 100 nm squeezing itself through a 100 nm filter by altering its conformation, then it is diluted in either hypo- or hypertonic medium

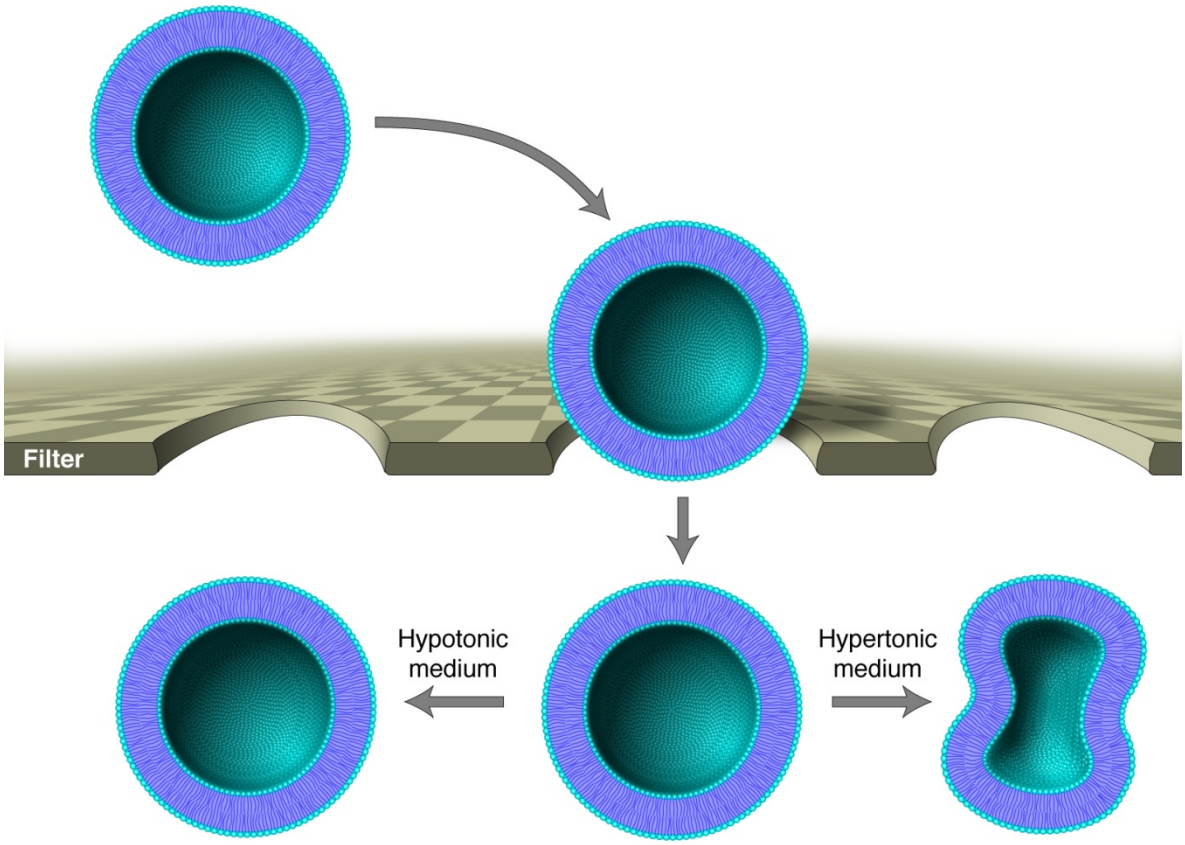

Figure 6.3.10: A liposome smaller than 100 nm passing through a 100 nm filter, then it is diluted in either hypo- or hypertonic medium

Table 6.3.3: Mean radius of the liposome samples prepared in 10 mM sodium nitrate and sucrose equivalent to 90 mM sodium nitrate, diluted in either 10 mM sodium nitrate and sucrose equivalent to 90 mM sodium nitrate or 10 mM sodium nitrate, from table 9.26 in appendix 3

Sample	**R_n**	**R_w**	**R_z**
Liposomes prepared in 10 mM sodium nitrate and sucrose equivalent of 90 mM sodium nitrate, diluted in 10 mM sodium nitrate and sucrose equivalent to 90 mM sodium nitrate	44.1 nm ± 0.15 nm	48.1 nm ± 0.47 nm	50.9 nm ± 0.70 nm
Liposomes prepared in 10 mM sodium nitrate and sucrose equivalent to 90 mM sodium nitrate, diluted in 10 mM sodium nitrate	45.8 nm ± 0.09 nm	50.1 nm ± 0.10 nm	53.1 nm ± 0.18 nm

Table 6.3.3 shows the mean radius of the liposomes prepared in 10 mM sodium nitrate and sucrose equivalent to 90 mM sodium nitrate. The liposomes diluted in 10 mM sodium nitrate (hypotonic medium) are slightly bigger than the liposomes diluted in the isotonic medium. The number-average mean square radius increase with 1.7 nm, the weight-average mean square radius increase with 2 nm and the z-average mean square diameter increase with 2.2 nm.

Table 6.2.3 shows the mean diameter of the same liposomes as the liposomes shown in table 6.3.3; the only difference is that the sizes are measured with different techniques. First was the liposomes measured by PCS and then by AF4. Both methods show the same principle, the liposome swell and the size increase after the liposome has been diluted in the hypoosmolal medium.

7 CONCLUSION

In conclusion, this project has demonstrated that a change in osmotic pressure, with constant ionic strength, affects both elution time and calculated size of liposomes. But, osmotic stress was found to affect liposomes of different sizes in a different manner; liposomes that were smaller than the pore size of the filter used for extrusion were found to shrink in hyperosmotic medium but stay quite constant in size in hypo-osmotic medium. In contrast, liposomes that were larger than the pore size of the filter were found to shrink in hyperosmotic medium and swell in hypo-osmotic medium. A hypothesis is presented to explain this behavior.

It was found that the retention behavior and calculated geometric radius of liposomes obtained by flow field-flow fractionation in combination with multi-angle light scattering is affected by the osmotic pressure of the medium used for diluting the liposomes and/or running the AF4.

Ideally, thus aqueous media with the same osmotic pressure as the liposome dispersion should be used as dilution medium/mobile phase when liposomes are fractionated by AF4. This gives some limitations with the AF4 method. Sugar should be added to adjust the osmotic pressure of the mobile phase to avoid osmotic stress artifacts and to avoid changes in ionic strength, which could alter the elution behavior.

8 REFERENCES

Asymmetric Flow Field-Flow Fractionation. 2008 [updated 2008]; Available from: http://www.postnova.com/content/english/theory/theory_fff.htm.

Ausbacher DA. A4F/MALS-Analysis of Liposomes Influence of Key Factors on Fractionation Behavior and Evaluation of MALS Fit Routines. 2007.

Bangham AD. Osmotic properties and water permeability of phospholipid liquid crystals. Chemistry and physics of lipids. 1967;1:225.

Bangham AD, Standish MM, Watkins JC. Diffusion of univalent ions across the lamellae of swollen phospholipids. Journal of molecular biology. 1965;13(1):238-52.

Brandl M. Liposomes as drug carriers: a technological approach. Biotechnol Annu Rev. 2001;7:59-85.

Gregoriadis G. Liposome technology. 3rd ed. New York: Informa Healthcare; 2006.

How Asymmetric Field Flow Fractionation (AFFF) Theory Works. 2008 [updated 2008]; Available from: http://www.wyatt.com/theory/fieldflowfractionation/.

Ingebrigtsen L. Size analysis of submicron particles and liposomes by size exclusion chromatography and photon correlation spectroscopy. Tromsø: University of Tromsø, Institute of Pharmacy; 2001.

Ingebrigtsen L, Brandl M. Determination of the size distribution of liposomes by SEC fractionation, and PCS analysis and enzymatic assay of lipid content. AAPS PharmSciTech. 2002;3(2).

Lasic D. Liposomes: from physics to applications. Amsterdam: Elsevier; 1993.

Lide DR. CRC Handbook of Chemistry and Physics. Taylor and Francis Group, LLC; 2008. Available from: http://www.hbcpnetbase.com/.

Massing U, Fuxius S. Liposomal formulations of anticancer drugs: selectivity and effectiveness. Drug resistance updates. 2000;3(3):171-7.

Moon MH, Park I, Kim Y. Size characterization of liposomes by flow field-flow fractionation and photon correlation spectroscopy Effect of ionic strength and pH of carrier solutions. Journal of chromatography. 1998;813(1):91.

Mui BL, Cullis PR, Evans EA, Madden TD. Osmotic properties of large unilamellar vesicles prepared by extrusion. Biophysical Journal. 1993;64(2):443-53.

Mui BL, Hope MJ. Liposome technology. In: Gregoriadis G, editor. 3rd ed. New York: Informa Healthcare; 2006. p. 324.

Nickels JCH. Changes in Liposome Morphology Induced by Actin Polymerization in Submicrometer Liposomes. Langmuir. 2003;19(25):10581.

Refractive index. 2008 [updated 2008]; Available from: http://en.wikipedia.org/wiki/Refractive_index.

Roessner D, Kulicke W-M. On-line coupling of flow field-flow fractionation and multi-angle laser light scattering. Journal of chromatography. 1994;687(2):249.

Technical Summary - An Introduction to Lipid Nanoparticles. 2008 [updated 2008]; Available from: http://www.encapsula.com/company.html.

Tonicity. 2008 [updated 2008]; Available from: http://en.wikipedia.org/wiki/Tonicity#Isotonicity.

Torchilin VP, Weissig V, editors. Liposomes: a practical approach. 2nd ed. Oxford: Oxford University Press; 2003.

User Manual ASTRA V User´s Guide. Wyatt Technology Corporation. 2007. 300 p.

User Manual Nicomp Model 380. Windows based software, Dynamic light scattering theory. 1997.

Van Zanten JH, Monbouquette HG. Characterization of vesicles by classical light scattering. Journal of colloid and interface science. 1991;146(2):330.

Viscosity. 2008 [updated 2008]; Available from: http://en.wikipedia.org/wiki/Viscosity.

Washington C. Particle size analysis in pharmaceutics and other industries: theory and practice. New York: Ellis Horwood; 1992.

Wyatt Technology Introduction to Light Scattering, Light Scattering University. 2006.

9 APPENDICES

Appendix 1

Calculation of osmolality in solutions

Example:

E-value $NaNO_3$ = 0.67

E-value glucose = 0.16

If we should make a solution with 10 mM $NaNO_3$ and glucose equivalent to 90 mM $NaNO_3$

Amount $NaNO_3$ in a 100 mM solution: 84.99 g/mol × 0.1 mol/l = 8.499 g/l

Amount after correction with the E-value ($NaNO_3$): 8.499 g × 0.67 = 5.694 g

Amount $NaNO_3$ in 10 mM solution: 84.99 g/mol × 0.01 mol/l = 0.8499 g/l

Amount after correction with the E-value ($NaNO_3$): 0.8499 g × 0.67 = 0.569 g

The amount needed from glucose: 5.694 g – 0.569 g = 5.125 g

Amount glucose needed (when corrected with the E-value of glucose): 0.16 × X = 5.125 g → 32.031 g

Appendix 2

Calculation of dynamic viscosity of solutions

Kinematic viscosity (u):

$$u = K \times (t - \vartheta)$$

ϑ = Hagenbach correction for average flow time (s) (from manual)

K = constant (mm^2/s^2) (from manual)

t = time (seconds)

Example:

u = 0.003 mm^2/s^2 × (331.39 s – 0.61 s)

u = 0.9923 mm^2/s

Dynamic viscosity (η):

$$\eta = u \times \rho$$

ρ = density

Example:

η = 0.9923 mm^2/s × 1.0092 g/cm^3

η = 1.0014 mPa × s

Appendix 3

PCS results

All the results marked red in appendix 3 are excluded from the summary because they did not fulfill the requirements that chi squared should be < 3, and baseline adjust should be ≤ 0.05 %.

All results are from Gaussian distributions.

Table 9.1: PCS measurements of 100 nm liposomes, prepared with 10 mM $NaNO_3$

Intensity weighting	Volume weighting	Number weighting	Channel width	Chi squared	Baseline adjust
119.0 nm	119.6 nm	84.6 nm	13.0 µSec	0.50	0.00 %
119.2 nm	119.6 nm	90.7 nm	13.0 µSec	0.35	**0.08 %**
119.2 nm	119.7 nm	87.2 nm	13.0 µSec	0.33	0.00 %
120.1 nm	120.8 nm	86.8 nm	13.0 µSec	0.33	0.00 %
120.6 nm	121.6 nm	85.8 nm	13.0 µSec	0.47	0.00 %
121.0 nm	122.0 nm	85.4 nm	13.0 µSec	0.99	0.00 %
119.2 nm	119.8 nm	86.0 nm	13.0 µSec	0.54	0.00 %
119.1 nm	119.5 nm	88.2 nm	13.0 µSec	0.22	0.03 %
119.3 nm	120.0 nm	86.5 nm	13.0 µSec	0.32	0.00 %
119.9 nm	120.4 nm	90.6 nm	13.0 µSec	1.92	0.00 %

Table 9.2: PCS measurements of 100 nm liposomes prepared with 10 mM $NaNO_3$, 1 hour after dilution with 10 mM $NaNO_3$ and glucose equivalent of 90 mM $NaNO_3$

Intensity weighting	Volume weighting,	Number weighting	Channel width	Chi squared	Baseline adjust
109.7 nm	91.8 nm	74.3 nm	13.0 µSec	2.80	0.00 %
110.0 nm	92.8 nm	75.8 nm	13.0 µSec	2.51	0.00 %
109.7 nm	91.4 nm	73.7 nm	13.0 µSec	0.44	0.00 %
110.4 nm	92.7 nm	75.3 nm	13.0 µSec	1.71	0.00 %
110.6 nm	94.4 nm	78.3 nm	13.0 µSec	0.59	0.00 %
111.0 nm	94.6 nm	78.3 nm	13.0 µSec	1.15	0.00 %
111.0 nm	91.5 nm	72.7 nm	13.0 µSec	0.68	0.00 %
111.8 nm	93.4 nm	75.4 nm	13.0 µSec	0.94	0.00 %
111.7 nm	94.0 nm	76.6 nm	13.0 µSec	1.23	0.00 %
112.4 nm	98.2 nm	83.6 nm	13.0 µSec	2.52	0.00 %

Table 9.3: PCS measurements of 100 nm liposomes, prepared with 10 mM $NaNO_3$, 24 hours after dilution with 10 mM $NaNO_3$ and glucose equivalent of 90 mM $NaNO_3$

Intensity weighting	Volume weighting	Number weighting	Channel width	Chi squared	Baseline adjust
113.4 nm	100.5 nm	87.1 nm	15.0 µSec	1.03	0.05 %
113.3 nm	93.8 nm	74.8 nm	15.0 µSec	2.80	0.00 %
114.6 nm	99.0 nm	83.0 nm	15.0 µSec	**6.32**	0.00 %
113.9 nm	97.5 nm	81.0 nm	15.0 µSec	1.23	0.00 %
113.5 nm	94.1 nm	75.3 nm	15.0 µSec	0.38	0.00 %
114.5 nm	97.6 nm	80.4 nm	15.0 µSec	1.82	0.00 %
113.9 nm	98.7 nm	83.1 nm	15.0 µSec	0.62	0.02 %
114.3 nm	95.0 nm	76.1 nm	15.0 µSec	0.53	0.00 %
113.8 nm	94.7 nm	76.0 nm	15.0 µSec	0.44	0.01 %
114.4 nm	94.7 nm	75.5 nm	15.0 µSec	1.10	0.00 %

Table 9.4: PCS measurements of 100 nm liposomes, prepared with 10 mM $NaNO_3$, 48 hours after dilution with 10 mM $NaNO_3$ and glucose equivalent of 90 mM $NaNO_3$

Intensity weighting	Volume weighting	Number weighting	Channel width	Chi squared	Baseline adjust
113.2 nm	94.8 nm	76.8 nm	14.0 µSec	0.37	0.00 %
113.6 nm	95.1 nm	76.9 nm	14.0 µSec	1.08	0.00 %
113.9 nm	96.4 nm	78.9 nm	14.0 µSec	0.87	0.00 %
113.7 nm	94.8 nm	76.2 nm	14.0 µSec	0.91	0.00 %
113.6 nm	96.8 nm	79.8 nm	14.0 µSec	0.37	0.00 %
113.8 nm	96.2 nm	78.7 nm	14.0 µSec	1.35	0.00 %
113.9 nm	94.2 nm	75.0 nm	14.0 µSec	0.92	0.00 %
114.3 nm	98.0 nm	81.4 nm	14.0 µSec	**3.32**	0.00%
114.3 nm	95.9 nm	77.7 nm	14.0 µSec	1.76	0.00 %
114.3 nm	96.8 nm	79.3 nm	14.0 µSec	0.96	0.00 %

Table 9.5: PCS measurements of 100 nm liposomes, prepared with 10 mM $NaNO_3$

Intensity weighting	Volume weighting	Number weighting	Channel width	Chi squared	Baseline adjust
118.9 nm	119.4 nm	86.4 nm	14.0 µSec	0.69	0.00 %
118.3 nm	118.5 nm	93.9 nm	14.0 µSec	2.20	0.00 %
118.1 nm	118.3 nm	91.2 nm	14.0 µSec	0.32	**0.08 %**
118.4 nm	118.7 nm	90.8 nm	14.0 µSec	0.90	0.00 %
118.7 nm	119.1 nm	89.7 nm	14.0 µSec	1.06	0.00 %
117.6 nm	117.8 nm	88.6 nm	14.0 µSec	0.28	0.03 %
117.2 nm	117.4 nm	86.4 nm	14.0 µSec	0.36	0.03 %
118.7 nm	118.9 nm	92.6 nm	14.0 µSec	1.15	0.00 %
119.2 nm	119.3 nm	98.2 nm	14.0 µSec	**3.98**	0.00 %
118.8 nm	118.9 nm	95.4 nm	14.0 µSec	1.06	0.00 %

Table 9.6: PCS measurements of 100 nm liposomes, prepared with 10 mM $NaNO_3$, 1 hour after dilution with 10 mM $NaNO_3$ and sucrose equivalent of 90 mM $NaNO_3$

Intensity weighting	Volume weighting	Number weighting	Channel width	Chi squared	Baseline adjust
114.6 nm	95.5 nm	76.6 nm	14.0 µSec	1.69	0.00 %
113.7 nm	90.2 nm	68.3 nm	14.0 µSec	0.59	0.00 %
114.3 nm	94.2 nm	74.6 nm	14.0 µSec	1.04	0.00 %
114.4 nm	95.5 nm	76.9 nm	14.0 µSec	1.27	0.00 %
114.4 nm	94.2 nm	74.5 nm	14.0 µSec	1.26	0.00 %
115.0 nm	97.6 nm	80.0 nm	14.0 µSec	**4.32**	0.00 %
114.6 nm	94.5 nm	74.9 nm	14.0 µSec	1.63	0.00 %
114.2 nm	93.6 nm	73.6 nm	14.0 µSec	0.48	0.00 %
114.0 nm	93.7 nm	74.0 nm	14.0 µSec	0.69	0.00 %
114.1 nm	91.8 nm	70.7 nm	14.0 µSec	0.38	0.00 %

Table 9.7: PCS measurements of 100 nm liposomes, prepared with 10 mM $NaNO_3$, 24 hours after dilution with 10 mM $NaNO_3$ and sucrose equivalent of 90 mM $NaNO_3$

Intensity weighting	Volume weighting	Number weighting	Channel width	Chi squared	Baseline adjust
116.1 nm	93.7 nm	72.3 nm	15.0 µSec	0.35	0.00 %
116.6 nm	97.3 nm	78.2 nm	15.0 µSec	2.63	0.00 %
115.6 nm	91.9 nm	69.7 nm	15.0 µSec	0.30	0.01 %
117.0 nm	100.9 nm	84.2 nm	15.0 µSec	2.34	0.00 %
116.4 nm	95.6 nm	75.4 nm	15.0 µSec	0.54	0.00 %
117.2 nm	101.9 nm	85.9 nm	15.0 µSec	2.05	0.00 %
116.3 nm	96.4 nm	76.9 nm	15.0 µSec	1.13	0.00 %
116.7 nm	96.8 nm	77.1 nm	15.0 µSec	1.79	0.00 %
116.7 nm	99.1 nm	81.3 nm	15.0 µSec	1.59	0.00 %
116.2 nm	96.5 nm	77.2 nm	15.0 µSec	1.32	0.00 %

Table 9.8: PCS measurements of 100 nm liposomes, prepared with 10 mM $NaNO_3$, 48 hours after dilution with 10 mM $NaNO_3$ and sucrose equivalent of 90 mM $NaNO_3$

Intensity weighting	Volume weighting	Number weighting	Channel width	Chi squared	Baseline adjust
117.0 nm	98.2 nm	79.4 nm	14.0 µSec	1.46	0.00 %
116.7 nm	93.9 nm	72.0 nm	14.0 µSec	0.41	0.00 %
117.1 nm	99.8 nm	82.1 nm	14.0 µSec	**4.91**	0.00 %
117.2 nm	98.7 nm	80.1 nm	14.0 µSec	**3.14**	0.00 %
116.8 nm	96.1 nm	75.8 nm	14.0 µSec	1.95	0.00 %
117.6 nm	99.9 nm	82.0 nm	14,0 µSec	**4.65**	0.00 %
116.2 nm	93.1 nm	71.1 nm	14.0 µSec	0.30	0.00 %
116.4 nm	97.2 nm	78.1 nm	14.0 µSec	1.34	0.00 %
116.5 nm	92.7 nm	70.2 nm	14.0 µSec	0.33	0.00 %
116.3 nm	94.7 nm	73.9 nm	14.0 µSec	0.39	0.00 %

Table 9.9: PCS measurements of 100 nm liposomes, prepared with 10 mM $NaNO_3$ and sucrose equivalent of 90 mM $NaNO_3$

Intensity weighting	Volume weighting	Number weighting	Channel width	Chi squared	Baseline adjust
121.5 nm	104.6 nm	87.0 nm	15.0 µSec	0.51	0.03 %
120.9 nm	101.6 nm	82.0 nm	15.0 µSec	0.23	0.00 %
122.0 nm	107.9 nm	92.7 nm	15.0 µSec	2.28	0.00 %
121.3 nm	103.2 nm	84.5 nm	15.0 µSec	0.46	0.01 %
121.5 nm	104. 7 nm	87.1 nm	15.0 µSec	1.90	0.00 %
121.3 nm	101.6 nm	81.7 nm	15.0 µSec	0.44	0.05 %
121.6 nm	102.2 nm	82.4 nm	15.0 µSec	1.30	0.00 %
121.7 nm	102.1 nm	82.1 nm	15.0 µSec	0.57	0.00 %
121.9 nm	102.9 nm	83.5 nm	15.0 µSec	0.93	0.00 %
122.1 nm	106.8 nm	90.5 nm	15.0 µSec	1.65	0.00 %

Table 9.10: PCS measurements of 100 nm liposomes, prepared with 10 mM $NaNO_3$ and sucrose equivalent of 90 mM $NaNO_3$, 1 hour after dilution with 10 mM $NaNO_3$

Intensity weighting	Volume weighting	Number weighting	Channel width	Chi squared	Baseline adjust
118.7 nm	118.9 nm	95.8 nm	13.0 µSec	**3.34**	0.00 %
118.2 nm	118.3 nm	95.7 nm	13.0 µSec	0.51	0.00 %
118.1 nm	118.3 nm	90.3 nm	13.0 µSec	0.20	0.00 %
118.4 nm	118.5 nm	98.1 nm	13.0 µSec	0.54	0.00 %
117.8 nm	117.8 nm	94.5 nm	13.0 µSec	0.30	0.05 %
118.7 nm	118.9 nm	92.3 nm	13.0 µSec	0.60	0.00 %
119.0 nm	119.1 nm	97.6 nm	13.0 µSec	1.74	0.00 %
118.7 nm	118.7 nm	98.1 nm	13.0 µSec	0.54	0.00 %
118.6 nm	118.7 nm	95.0 nm	13.0 µSec	0.68	0.00 %
118.5 nm	118.7 nm	92.8 nm	13.0 µSec	0.36	0.00 %

Table 9.11 PCS measurements of 100 nm liposomes, prepared with 10 mM $NaNO_3$ and sucrose equivalent of 90 mM $NaNO_3$, 24 hours after dilution with 10 mM $NaNO_3$

Intensity weighting	Volume weighting	Number weighting	Channel width	Chi squared	Baseline adjust
118.1 nm	118.2 nm	92.1 nm	12.0 µSec	0.37	0.00 %
118.0 nm	118.2 nm	91.9 nm	12.0 µSec	0.72	0.00 %
118.3 nm	118.4 nm	96.2 nm	12.0 µSec	0.75	0.00 %
118.8 nm	118.9 nm	97.1 nm	12.0 µSec	2.97	0.00 %
118.0 nm	118.1 nm	92.9 nm	12.0 µSec	0.57	0.00 %
118.3 nm	118.5 nm	93.9 nm	12.0 µSec	1.14	0.00 %
118.5 nm	118.6 nm	96.9 nm	12.0 µSec	2.17	0.00 %
118.1 nm	118.2 nm	97.7 nm	12.0 µSec	0.44	**0.07 %**
118.3 nm	118.5 nm	90.8 nm	12.0 µSec	0.35	0.00 %
118.5 nm	118.6 nm	95.2 nm	12.0 µSec	0.34	0.00 %

Table 9.12: PCS measurements of 100 nm liposomes, prepared with 10 mM $NaNO_3$ and sucrose equivalent of 90 mM $NaNO_3$, 48 hours after dilution with 10 mM $NaNO_3$

Intensity weighting	Volume weighting	Number weighting	Channel width	Chi squared	Baseline adjust
117.9 nm	118.0 nm	94.1 nm	13.0 µSec	1.08	0.00 %
118.4 nm	118.4 nm	98.0 nm	13.0 µSec	1.26	0.00 %
117.6 nm	117.7 nm	92.3 nm	13.0 µSec	0.25	**0.07 %**
118.5 nm	118.5 nm	96.7 nm	13.0 µSec	2.43	0.00 %
118.0 nm	118.0 nm	94.4 nm	13.0 µSec	0.45	0.05 %
118.9 nm	119.1 nm	95.5 nm	13.0 µSec	2.77	0.00 %
118.0 nm	118.2 nm	90.2 nm	13.0 µSec	0.26	0.00 %
118.7 nm	118.9 nm	95.9 nm	13.0 µSec	1.73	0.00 %
118.2 nm	118.4 nm	94.3 nm	13.0 µSec	0.32	0.00 %
118.6 nm	118.6 nm	97.0 nm	13.0 µSec	0.60	0.00 %

Table 9.13: Latex bead standards, 100 nm, diluted with 10 mM $NaNO_3$, PCS mean sizes calculated on the basis of viscosity and refractive index values of water

Intensity weighting	Volume weighting	Number weighting	Channel width	Chi squared	Baseline adjust
105.4 nm	100.4 nm	94.9 nm	12.0 µSec	0.44	0.01 %
105.7 nm	104.6 nm	103.3 nm	12.0 µSec	0.41	0.00 %
105.6 nm	104.5 nm	103.2 nm	12.0 µSec	1.06	0.00 %
105.7 nm	104.4 nm	102.8 nm	12.0 µSec	0.26	0.02 %
105. 6 nm	104.6 nm	103.3 nm	12.0 µSec	0.49	0.05 %
105.3 nm	105.3 nm	105.3 nm	12.0 µSec	0.38	**0.07 %**
105.6 nm	103.4 nm	100.8 nm	12.0 µSec	0.81	0.00 %
105.9 nm	104.3 nm	102.4 nm	12.0 µSec	0.58	0.00 %
105.3 nm	102.3 nm	98.9 nm	12.0 µSec	0.36	0.01 %
105.3 nm	104.7 nm	104.0 nm	12.0 µSec	0.39	0.00 %

Table 9.14: Latex bead standards, 100 nm, diluted with 10 mM $NaNO_3$ and sucrose equivalent to 90 mM $NaNO_3$. PCS mean sizes calculated on the basis of the viscosity and refractive index values of water

Intensity weighting	Volume weighting	Number weighting	Channel width	Chi squared	Baseline adjust
117.7 nm	116.9 nm	115.9 nm	13.0 µSec	0.40	0.02 %
117.5 nm	115.9 nm	114.0 nm	13.0 µSec	0.26	0.00 %
117.8 nm	116.3 nm	114.5 nm	13.0 µSec	0.74	0.00 %
117.6 nm	117.6 nm	117.6 nm	13.0 µSec	0.56	0.00 %
117.7 nm	117.2 nm	116.5 nm	13.0 µSec	0.31	0.02 %
117.6 nm	117.4 nm	117.1 nm	13.0 µSec	0.42	0.05 %
118.7 nm	116.4 nm	113.6 nm	13.0 µSec	2.01	0.00 %
117.9 nm	117.5 nm	116.8 nm	13.0 µSec	0.87	0.00 %
117.8 nm	115.9 nm	113.6 nm	13.0 µSec	0.42	**0.07 %**
117.9 nm	115.1 nm	111.7 nm	13.0 µSec	0.31	0.02 %

Table 9.15: Latex bead standards, 100 nm, diluted with 10 mM $NaNO_3$ and glucose equivalent of 90 mM $NaNO_3$. PCS mean sizes calculated on the basis of viscosity and refractive index values of water

Intensity weighting	Volume weighting	Number weighting	Channel width	Chi squared	Baseline adjust
112.9 nm	111.3 nm	109.5 nm	13.0 µSec	0.57	0.04 %
113.0 nm	110.9 nm	108.4 nm	13.0 µSec	0.50	0.00 %
113.4 nm	109.5 nm	105.0 nm	13.0 µSec	0.40	**0.13 %**
113.7 nm	112.1 nm	110.1 nm	13.0 µSec	0.34	0.04 %
113.8 nm	111.0 nm	107.8 nm	13.0 µSec	0.80	0.00 %
113.3 nm	111.8 nm	110.0 nm	13.0 µSec	0.39	0.00 %
113.3 nm	111.1 nm	108.5 nm	13.0 µSec	0.67	0.00 %
114.1 nm	106.2 nm	97.4 nm	13.0 µSec	0.33	0.03 %
113.5 nm	111.5 nm	109.1 nm	13.0 µSec	0.38	0.00 %
112.8 nm	109.7 nm	106.1 nm	13.0 µSec	0.30	**0.10 %**

Table 9.16: Latex bead standards, 100 nm, diluted with 10 mM $NaNO_3$ and sucrose equivalent of 90 mM $NaNO_3$. PCS mean sizes calculated on the basis of measured viscosity and refractive index values

Intensity weighting	Volume weighting	Number weighting	Channel width	Chi squared	Baseline adjust
104.5 nm	104.2 nm	103.8 nm	13.0 µSec	0.41	0.02 %
104.3 nm	102.7 nm	100.7 nm	13.0 µSec	0.26	0.00 %
104.6 nm	103.3 nm	101.8 nm	13.0 µSec	0.73	0.00 %
104.4 nm	104.4 nm	104.4 nm	13.0 µSec	0.56	0.00 %
104.6 nm	104.6 nm	104.6 nm	13.0 µSec	0.31	0.03 %
104.4 nm	104.1 nm	103.8 nm	13.0 µSec	0.41	0.05 %
105.4 nm	103.4 nm	101.1 nm	13.0 µSec	2.01	0.00 %
104.7 nm	103.7 nm	102.4 nm	13.0 µSec	0.78	0.00 %
104.6 nm	102.0 nm	99.1 nm	13.0 µSec	0.43	**0.07 %**
104.7 nm	102.1 nm	99.2 nm	13.0 µSec	0.31	0.02 %

Table 9.17: Latex bead standards, 100 nm, diluted with 10 mM $NaNO_3$ and glucose equivalent of 90 mM $NaNO_3$. PCS mean sizes calculated on the basis of measured viscosity and refractive index values

Intensity weighting	Volume weighting	Number weighting	Channel width	Chi squared	Baseline adjust
105.7 nm	104.1 nm	102.2 nm	13.0 µSec	0.55	0.04 %
105.8 nm	104.1 nm	102.2 nm	13.0 µSec	0.50	0.00 %
106.1 nm	102.4 nm	98.2 nm	13.0 µSec	0.40	**0.13 %**
106.5 nm	105.2 nm	103.8 nm	13.0 µSec	0.34	0.04 %
106.5 nm	103.8 nm	100.6 nm	13.0 µSec	0.80	0.00 %
106.1 nm	104.5 nm	102.7 nm	13.0 µSec	0.40	0.00 %
106.0 nm	103.6 nm	100.9 nm	13.0 µSec	0.68	0.00 %
106.9 nm	99.5 nm	91.5 nm	13.0 µSec	0.33	0.03 %
106.2 nm	104.3 nm	102.0 nm	13.0 µSec	0.37	0.00 %
105.6 nm	103.2 nm	100.5 nm	13.0 µSec	0.28	**0.10 %**

Table 9.18: Liposomes 100 nm, freeze-thawed (3 cycles) before extrusion. Frozen in -80 °C freezer, thawed on a 50°C water bath

Intensity weighting	Volume weighting	Number weighting	Channel width	Chi squared	Baseline adjust
116.5 nm	116.4 nm	90.7 nm	14.0 µSec	0.31	0.05 %
116.8 nm	116.8 nm	92.1 nm	14.0 µSec	**4.06**	0.00 %
116.6 nm	116.5 nm	94.5 nm	14.0 µSec	2.67	0.00 %
116.2 nm	116.1 nm	89.9 nm	14.0 µSec	0.53	0.00 %
116.0 nm	115.9 nm	88.7 nm	14.0 µSec	0.49	0.00 %
116.3 nm	116.2 nm	90.9 nm	14.0 µSec	0.31	0.05 %
116.7 nm	116.8 nm	86.4 nm	14.0 µSec	0.36	0.03 %
117.1 nm	117.0 nm	92.6 nm	14.0 µSec	0.55	0.00 %
116.8 nm	116.9 nm	85.5 nm	14.0 µSec	0.62	0.00 %
116.9 nm	116.9 nm	90.1 nm	14.0 µSec	0.55	0.00 %

Table 9.19: PCS measurements of 100 nm liposomes, freeze-thawed (3 cycles) during extrusion, after 400 nm filter, before 200 nm filter. Frozen in -80 °C freezer, thawed on a 50°C water bath

Intensity weighting	Volume weighting	Number weighting	Channel width	Chi squared	Baseline adjust
114.4 nm	114.0 nm	92.9 nm	12.0 µSec	0.90	0.00 %
114.8 nm	114.4 nm	95.0 nm	12.0 µSec	1.81	0.00 %
114.8 nm	114.5 nm	92.6 nm	12.0 µSec	1.35	0.00 %
114.3 nm	113.8 nm	89.3 nm	12.0 µSec	0.30	0.00 %
114.2 nm	113.8 nm	88.9 nm	12.0 µSec	1.22	0.00 %
114.4 nm	114.0 nm	89.4 nm	12.0 µSec	0.61	0.00 %
114.0 nm	113.6 nm	92.6 nm	12.0 µSec	0.27	**0.07 %**
114.9 nm	114.5 nm	94.7 nm	12.0 µSec	2.42	0.00 %
114.4 nm	114.0 nm	91.6 nm	12.0 µSec	0.94	0.00 %
114.4 nm	114.1 nm	87.4 nm	12.0 µSec	0.32	0.03 %

Table 9.20: PCS measurements of 100 nm liposomes, freeze-thawed (3 cycles) before extrusion. Frozen in liquid nitrogen (LN_2), thawed on a 50°C water bath

Intensity weighting	Volume weighting	Number weighting	Channel width	Chi squared	Baseline adjust
112.5 nm	111.8 nm	89.0 nm	13.0 µSec	1.26	0.00 %
112.2 nm	111.5 nm	84.4 nm	13.0 µSec	2.72	0.00 %
112.2 nm	111.5 nm	85.1 nm	13.0 µSec	0.73	0.00 %
112.3 nm	111.6 nm	83.8 nm	13.0 µSec	0.36	0.04 %
112.8 nm	112.2 nm	87.1 nm	13.0 µSec	2.72	0.00 %
112.3 nm	111.6 nm	85.0 nm	13.0 µSec	0.38	0.00 %
112.2 nm	111.5 nm	83.1 nm	13.0 µSec	0.30	0.01 %
112.4 nm	111.8 nm	89.3 nm	13.0 µSec	**4.61**	0.00 %
111.7 nm	110.9 nm	86.9 nm	13.0 µSec	0.58	0.01 %
113.1 nm	112.6 nm	87.7 nm	13.0 µSec	2.22	0.00 %

Table 9.21: Distribution width from PCS measurements of 100 nm liposomes, freeze-thawed (3 cycles) before extrusion. Frozen in -80 °C freezer, thawed on a 50°C water bath

Intensity weighting	Volume weighting	Number weighting
31.6 nm	31.6 nm	24.6 nm
31.0 nm	30.9 nm	24.4 nm
29.2 nm	29.1 nm	23.6 nm
31.8 nm	31.8 nm	24.6 nm
32.5 nm	32.5 nm	24.8 nm
34.4 nm	34.4 nm	25.5 nm
30.8 nm	30.8 nm	24.4 nm
35.2 nm	35.2 nm	25.7 nm
32.3 nm	32.3 nm	24.9 nm
31.3 nm	31.3 nm	24.4 nm

Table 9.22: Distribution width from PCS measurements of 100 nm liposomes, freeze-thawed (3 cycles) during extrusion, after 400 nm filter, before 200 nm filter. Frozen in -80 °C freezer, thawed on a 50°C water bath

Intensity weighting	Volume weighting	Number weighting
28.4 nm	28.3 nm	23.0 nm
27.2 nm	27.1 nm	22.5 nm
28.9 nm	28.8 nm	23.3 nm
30.6 nm	30.5 nm	23.9 nm
30.8 nm	30.7 nm	24.0 nm
30.7 nm	30.6 nm	24.0 nm
28.2 nm	28.0 nm	22.9 nm
27.6 nm	27.5 nm	22.7 nm
29.3 nm	29.2 nm	23.4 nm
32.0 nm	31.9 nm	24.5 nm

Table 9.23: Distribution width from PCS measurement of 100 nm liposomes, freeze-thawed (3 cycles) before extrusion. Frozen in liquid nitrogen (LN_2), thawed on a 50°C water bath

Intensity weighting	Volume weighting	Number weighting
29.4 nm	29.2 nm	23.2 nm
32.1 nm	31.9 nm	24.1 nm
31.6 nm	31.4 nm	24.0 nm
32.6 nm	32.4 nm	24.3 nm
30.9 nm	30.7 nm	23.9 nm
31.8 nm	31.6 nm	24.1 nm
32.9 nm	32.7 nm	24.3 nm
29.1 nm	28.9 nm	23.1 nm
30.0 nm	29.8 nm	23.4 nm
30.8 nm	30.6 nm	23.8 nm

Table 9.24: A summary of all the results presented in the tables above. Mean diameters and standard deviations for all the valid results. The results that had a too high value for chi squared or baseline adjust are not included.

Sample	Intensity weighting	Volume weighting	Number weighting
From table 9.1, liposomes prepared with 10 mM $NaNO_3$	119.7 nm ± 0.73 nm	120.4 nm ± 0.91 nm	86.8 nm ± 1.77 nm
From table 9.2, liposomes 1 hour after dilution with 10 mM $NaNO_3$ and glucose	110. 8 nm ± 0.93 nm	93.5 nm ± 2.02 nm	76.4 nm ± 3.11 nm
From table 9.3, liposomes 24 hours after dilution with 10 mM $NaNO_3$ and glucose	113.9 nm ± 0.44 nm	96.3 nm ± 2.36 nm	78.8 nm ± 4.32 nm
From table 9.4, liposomes 48 hours after dilution with 10 mM $NaNO_3$ and glucose	113.8 nm ± 0.35 nm	95.7 nm ± 0.96 nm	77.7 nm ± 1.60 nm
From table 9.5, liposomes prepared with 10 mM $NaNO_3$	118.3 nm ± 0.61 nm	118.6 nm ± 0.67 nm	90.5 nm ±3.34 nm
From table 9.6, liposomes 1 hour after dilution with 10 mM $NaNO_3$ and sucrose	114.3 nm ± 0.29	93.7 nm ± 1.71	73.8 nm ± 2.73
From table 9.7, liposomes 24 hours after dilution with 10 mM $NaNO_3$ and sucrose	116.5 nm ± 0.46 nm	97.0 nm ± 3.04 nm	77.8 nm ± 4.97 nm

From table 9.8, liposomes 48 hours after dilution with 10 mM $NaNO_3$ and sucrose	116.6 nm ± 0.29 nm	95.1 nm ± 2.10 nm	74.4 nm ± 3.54 nm
From table 9.9, liposomes prepared with 10 mM $NaNO_3$ and sucrose equivalent to 90 mM $NaNO_3$	121.6 nm ± 0.36 nm	103.8 nm ± 2.20 nm	85.4 nm ± 3.86 nm
From table 9.10, liposomes 1 hour after dilution 10 mM $NaNO_3$	118.4 nm ± 0.36 nm	118.5 nm ± 0.40 nm	96.1 nm ± 4.49 nm
From table 9.11, liposomes 24 hours after dilution with 10 mM $NaNO_3$	118.3 nm ± 0.26 nm	118.4 nm ± 0.25 nm	94.1 nm ± 2.34 nm
From table 9.12, liposomes 48 hours after dilution with 10 mM $NaNO_3$	118.4 nm ± 0.35 nm	118.5 nm ± 0.37 nm	95.1 nm ± 2.28 nm
From table 9.13, Duke size standards diluted with 10 mM $NaNO_3$	105.6 nm ± 0.21 nm	103.6 nm ± 1.52 nm	101.3 nm ± 1.97 nm
From table 9.14, Duke size standards diluted with 10 mM $NaNO_3$ and sucrose	117.9 nm ± 0.39 nm	116.6 nm ± 0.86 nm	115.1 nm ± 1.97 nm
From table 9.15, Duke size standards diluted with 10 mM $NaNO_3$ and glucose	113.5 nm ± 0.41 nm	110.7 nm ± 1.88 nm	107.6 nm ± 4.20 nm

From table 9.16, Duke size standards diluted with 10 mM $NaNO_3$ and sucrose	104.6 nm ± 0.34 nm	103.8 nm ± 0.64 nm	102.8 nm ± 1.52 nm
From table 9.17, Duke size standards diluted with 10 mM $NaNO_3$ and glucose	106.2 nm ± 0.40 nm	103.6 nm ± 1.74 nm	100.7 nm ± 3.86 nm
From table 9.18, liposomes frozen in -80°C freezer and thawed before extrusion	116.6 nm ± 0.35 nm	116.5 nm ± 0.40 nm	89.9 nm ± 2.81 nm
From table 9.19, liposomes frozen in -80°C freezer and thawed during extrusion	114.5 nm ± 0.25 nm	114.1 nm ± 0.28 nm	91.3 nm ± 2.70 nm
From table 10.20, liposomes frozen in liquid nitrogen and thawed before extrusion	112.4 nm ± 0.38 nm	111.7 nm ± 0.45 nm	86.1 nm ± 2.17 nm

Table 9.25: Mean distribution width and standard deviations for all the valid results. The results that had a too high value for chi squared or baseline adjust are not included.

Sample	Intensity weighting	Volume weighting	Number weighting
From table 9.21, liposomes frozen in -80 °C freezer and thawed before extrusion	32.1 nm ± 1.81 nm	32.1 nm ± 1.83 nm	24.7 nm ± 0.62 nm
From table 9.22, liposomes frozen in -80°C freezer and thawed during extrusion	29.5 nm ± 1.62 nm	29.4 nm ± 1.62 nm	23.5 nm ± 0.67 nm
From table 9.23, liposomes frozen in liquid nitrogen and thawed before extrusion	31.3 nm ± 1.17 nm	31.1 nm ± 1.17 nm	23.9 nm ± 0.38 nm

Table 9.26: The different liposome sizes (radius) gained from the AF4

Sample	R_n (nm)	R_w (nm)	R_z (nm)
1. Liposomes prepared in 10 mM sodium nitrate and diluted in 10 mM sodium nitrate and sucrose equivalent of 90 mM sodium nitrate	47.6 (1 %)	52.2 (0.8 %)	55.8 (0.8 %)
	46.7 (0.6 %)	51.7 (0.5 %)	55.3 (0.5 %)
	46.6 (0.7 %)	51.7 (0.6 %)	55.5 (0.6 %)
	46.7 (0.7 %)	51.7 (0.6 %)	55.5 (0.5 %)
	46.3 (0.8 %)	51.5 (0.6 %)	55.2 (0.6 %)
2. Liposomes prepared in 10 mM sodium nitrate and diluted in 10 mM sodium nitrate	53.6 (0.6 %)	57.1 (0.5 %)	59.3 (0.5%)
	53.0 (0.5 %)	56.9 (0.5 %)	59.7 (0.5 %)
	52.9 (0.6 %)	57.0 (0.5 %)	59.9 (0.5 %)
	52.9 (0.7%)	57.1 (0.7 %)	60.1 (0.7 %)
	52.9 (0.6 %)	57.0 (0.6 %)	60.0 (0.5 %)
3. Liposomes prepared in 10 mM sodium nitrate and sucrose equivalent of 90 mM sodium nitrate, diluted in 10 mM sodium nitrate and sucrose equivalent of 90 mM sodium nitrate	44.1 (1 %)	48.8 (0.7 %)	52.0 (0.6 %)
	44.3 (2 %)	48.3 (1 %)	51.2 (1 %)
	44.2 (2 %)	48.0 (2 %)	50.7 (2%)
	43.9 (3%)	47.6 (3 %)	50.3 (2 %)
	44.1 (4 %)	47.8 (3 %)	50.4 (3 %)
4. Liposomes prepared in 10 mM sodium nitrate and sucrose equivalent of 90 mM sodium nitrate, diluted in 10 mM sodium nitrate	45.7 (0.6 %)	50.0 (0.5 %)	52.9 (0.5 %)
	45.7 (0.6 %)	50.0 (0.5 %)	53.0 (0.5 %)
	45.9 (0.8 %)	50.2 (0.7 %)	53.3 (0.7 %)
	45.7 (0.7 %)	50.1 (0.6 %)	53.2 (0.6 %)
	45.8 (0.7 %)	50.2 (0.6 %)	53.3 (0.6 %)

Table 9.27: Mean radii and standard deviations for all samples in table 9.26

Sample	R_n (nm)	R_w (nm)	R_z (nm)
1.from table 9.26	46.8 nm ± 0.49 nm	51.8 nm ± 0.26 nm	55.5 nm ± 0.23 nm
2. from table 9.26	53.1 nm ± 0.35 nm	57.0 nm ± 0.08 nm	59.8 nm ± 0.32 nm
3. from table 9.26	44.1 nm ± 0.15 nm	48.1 nm ± 0.47 nm	50.9 nm ± 0.70 nm
4. from table 9.26	45.8 nm ± 0.09 nm	50.1 nm ± 0.10 nm	53.1 nm ± 0.18 nm

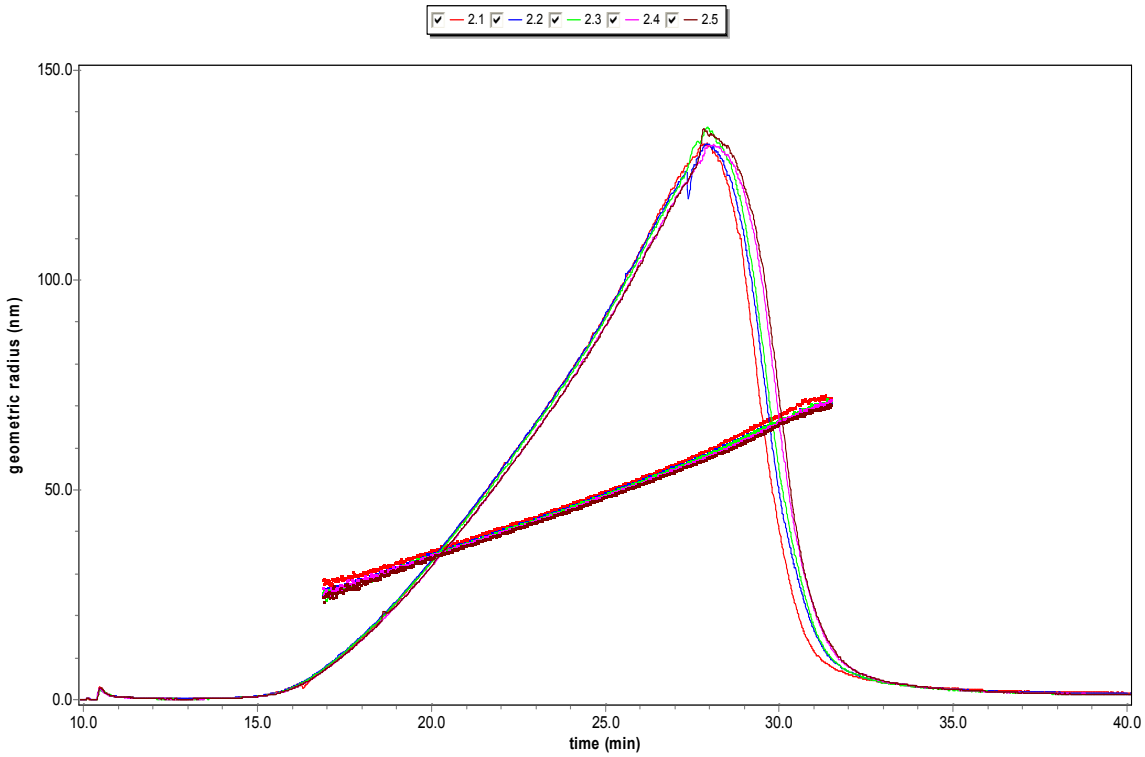

Figure 9.1: The five parallels of liposomes produced in 10 mM sodium nitrate, diluted 1:10 in 10 mM sodium nitrate and sucrose equivalent of 90 mM sodium nitrate. 10 mM sodium nitrate and sucrose equivalent of 90 mM sodium nitrate as mobile phase

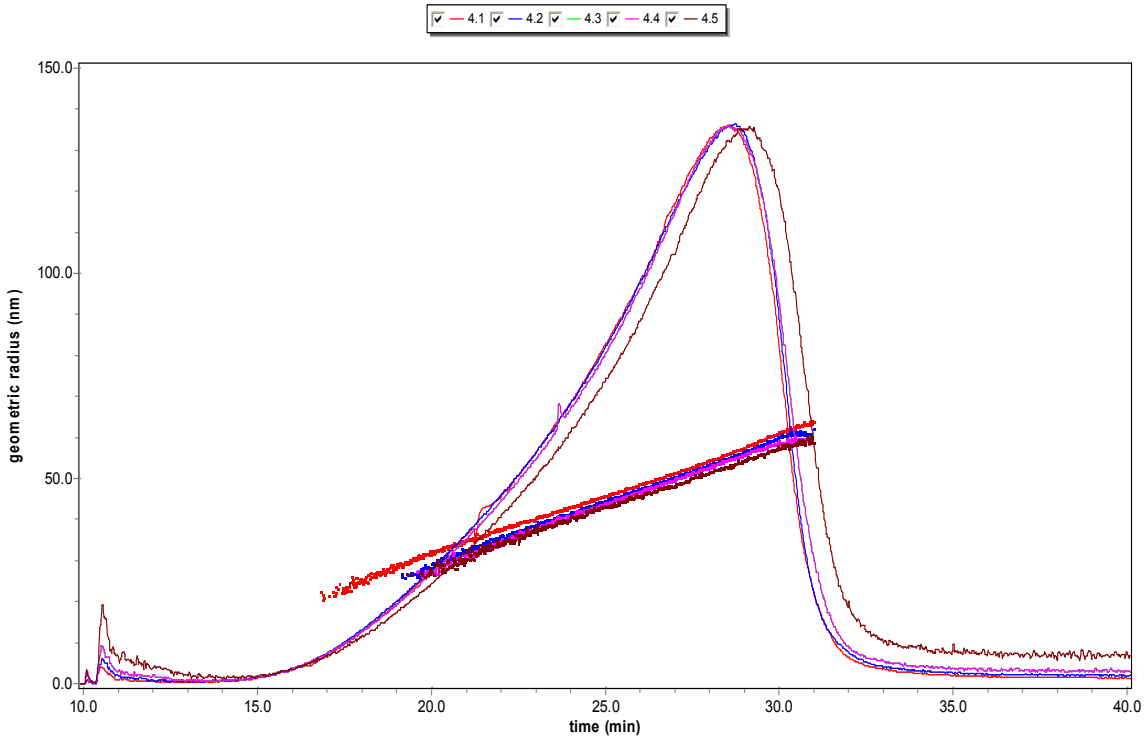

Figure 9.2: The five parallels of liposomes produced in 10 mM sodium nitrate and sucrose equivalent of 90 mM sodium nitrate, diluted 1:10 in 10 mM sodium nitrate and sucrose equivalent of 90 mM sodium nitrate. 10 mM sodium nitrate and sucrose equivalent of 90 mM sodium nitrate as mobile phase

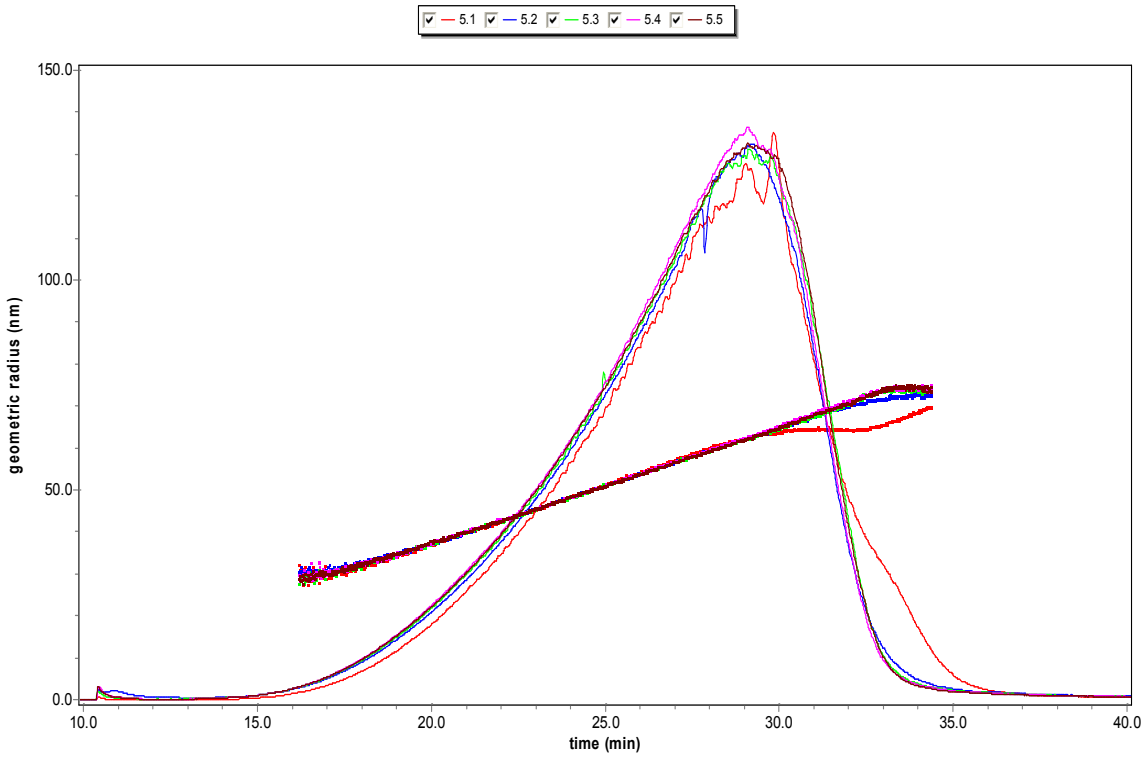

Figure 9.3: The five parallels of liposomes produced in 10 mM sodium nitrate, diluted 1:10 in 10 mM sodium nitrate. 10 mM sodium nitrate as mobile phase

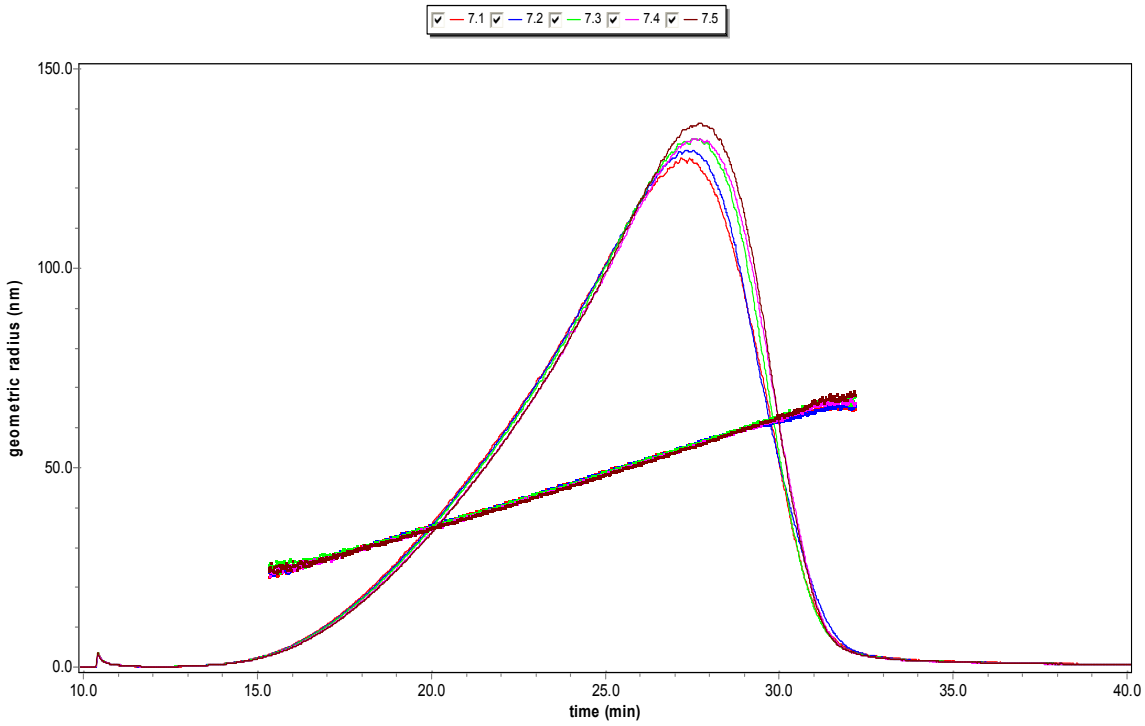

Figure 9.4: The five parallels of liposomes produced in 10 mM sodium nitrate and sucrose equivalent of 90 mM sodium nitrate, diluted 1:10 in 10 mM sodium nitrate. 10 mM sodium nitrate as mobile phase

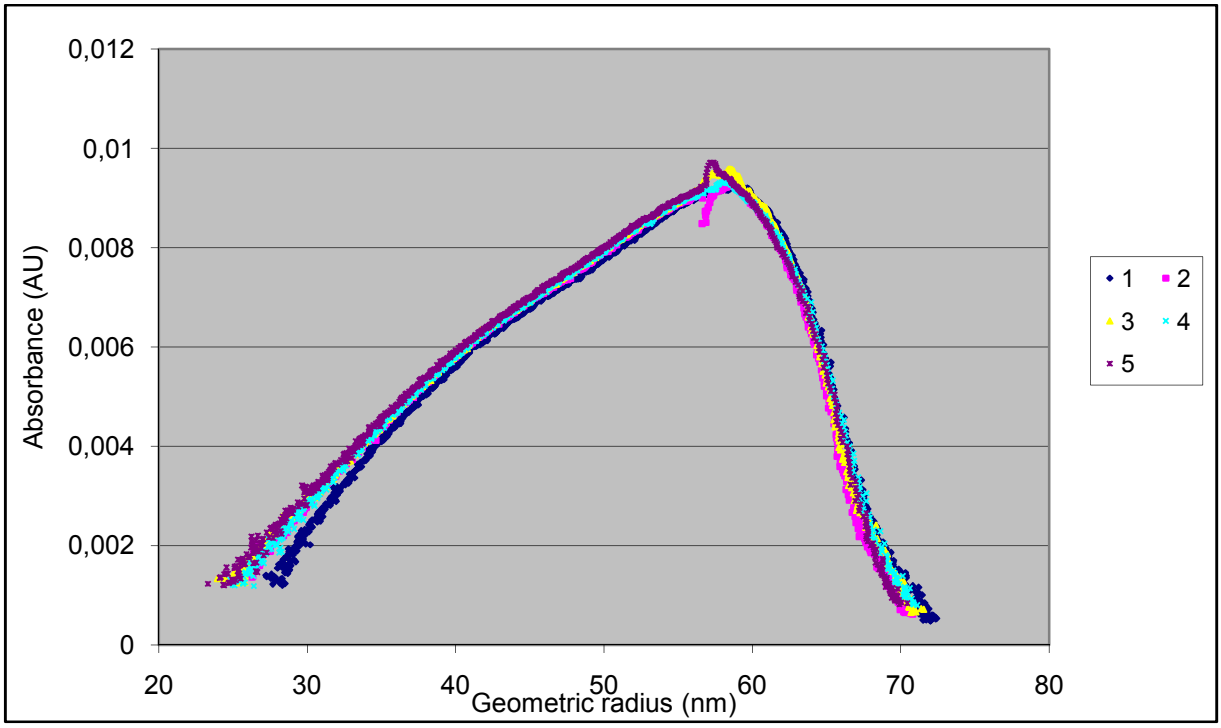

Figure 9.5: Parametric plot of the liposome sample prepared in 10 mM sodium nitrate solution, 10 mM sodium nitrate and sucrose equivalent of 90 mM sodium nitrate solution used as dilution medium and as mobile phase (five parallels)

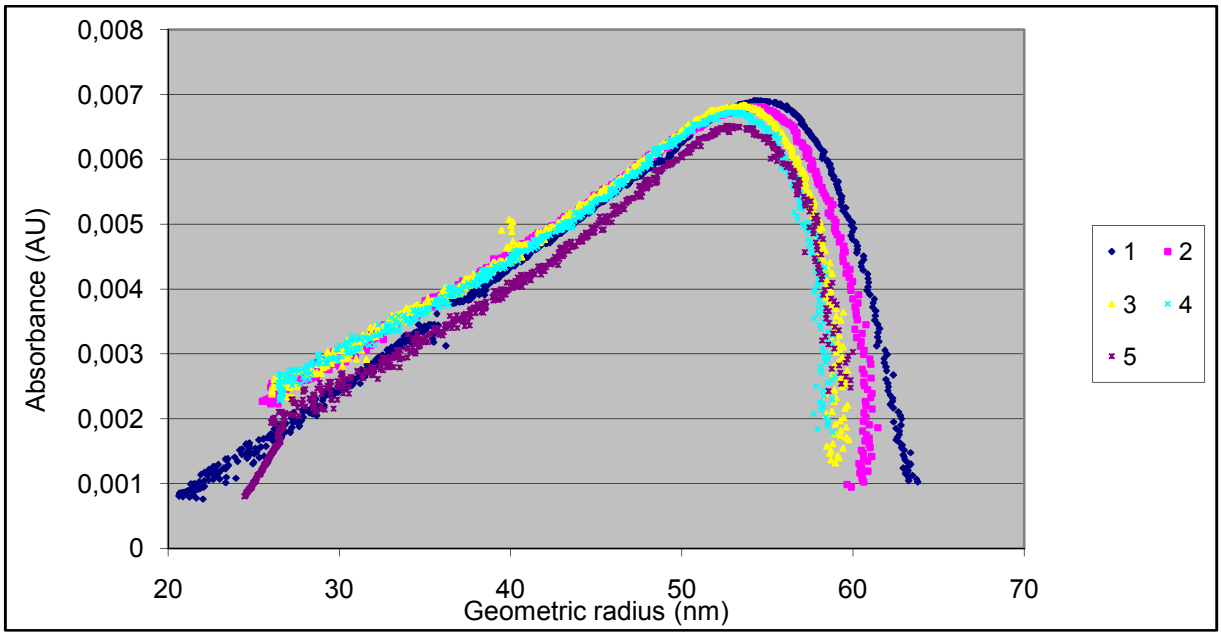

Figure 9.6: Parametric plot of the liposome sample prepared in 10 mM sodium nitrate and sucrose equivalent of 90 mM sodium nitrate solution, 10 mM sodium nitrate and sucrose equivalent of 90 mM sodium nitrate solution used as dilution medium and as mobile phase (five parallels)

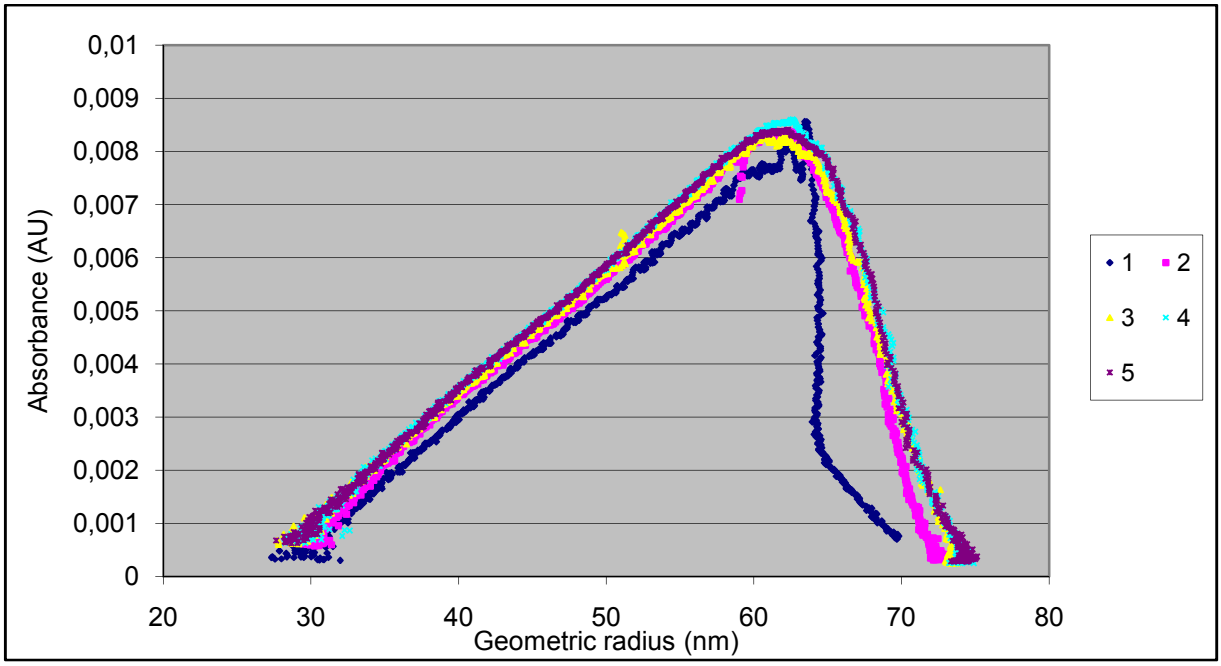

Figure 9.7: Parametric plot of the liposome sample prepared in 10 mM sodium nitrate solution, 10 mM sodium nitrate solution used as dilution medium and as mobile phase (five parallels)

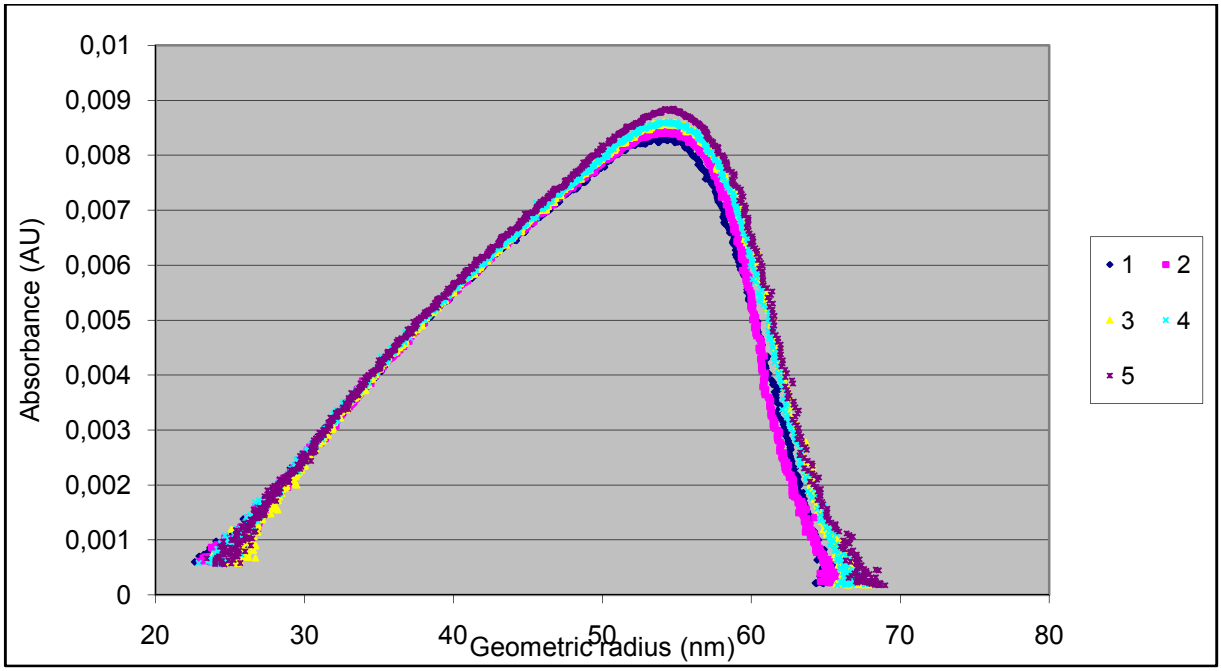

Figure 9.8: The five parallels of the liposome sample prepared in 10 mM sodium nitrate and sucrose equivalent of 90 mM sodium nitrate solution, 10 mM sodium nitrate

Appendix 4

The liposome samples which also were analyzed by AF4, but not were included in the thesis.

Table 9.28: Summary of the liposome samples which were analyzed by AF4, but not included in the thesis

Liposome dispersion medium	Dilution medium	Mobile phase
10 mM sodium nitrate	10 mM sodium nitrate	10 mM sodium nitrate and sucrose equivalent to 90 mM sodium nitrate
10 mM sodium nitrate	10 mM sodium nitrate and sucrose equivalent to 90 mM sodium nitrate	10 mM sodium nitrate
10 mM sodium nitrate	10 mM sodium nitrate	100 mM sodium nitrate
10 mM sodium nitrate	10 mM sodium nitrate and sucrose equivalent to 90 mM sodium nitrate	100 mM sodium nitrate
10 mM sodium nitrate and sucrose equivalent to 90 mM sodium nitrate	10 mM sodium nitrate	10 mM sodium nitrate and sucrose equivalent to 90 mM sodium nitrate
10 mM sodium nitrate and sucrose equivalent to 90 mM sodium nitrate	10 mM sodium nitrate	10 mM sodium nitrate
10 mM sodium nitrate and sucrose equivalent to 90 mM sodium nitrate	10 mM sodium nitrate	100 mM sodium nitrate
10 mM sodium nitrate and sucrose equivalent to 90 mM sodium nitrate	10 mM sodium nitrate and sucrose equivalent to 90 mM sodium nitrate	100 mM sodium nitrate

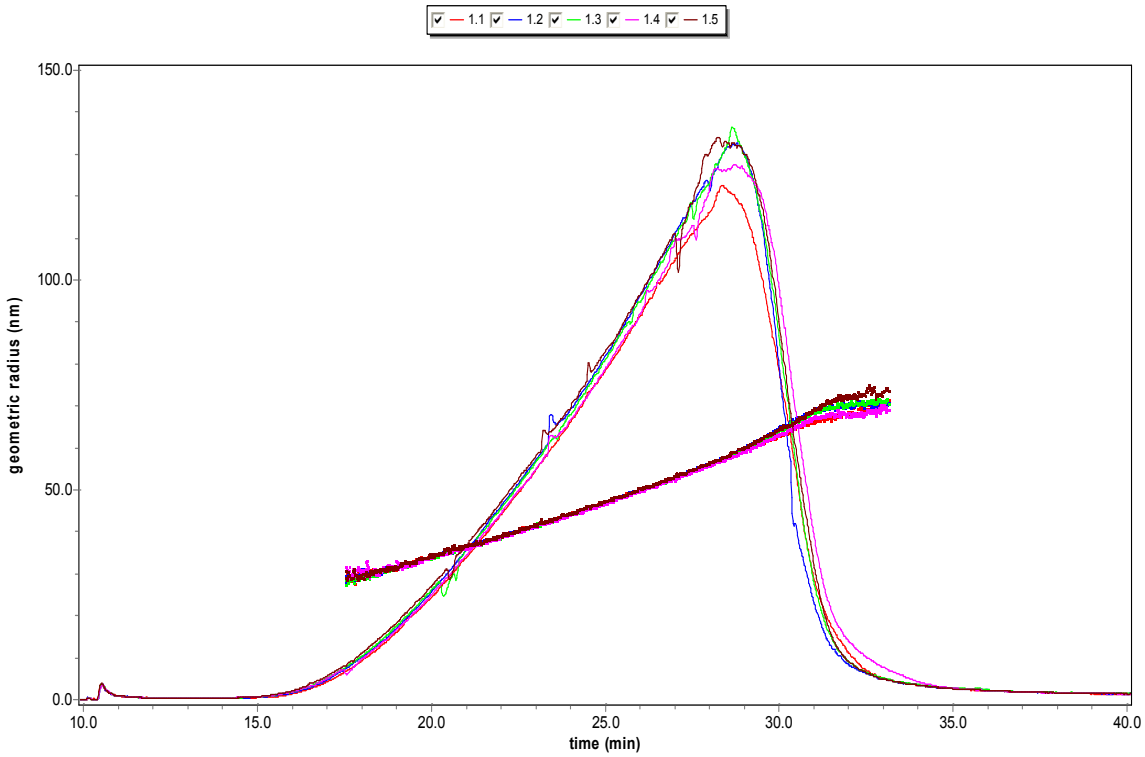

Figure 9.9: The five parallels of liposomes produced in 10 mM sodium nitrate, diluted 1:10 in 10 mM sodium nitrate. 10 mM sodium nitrate and sucrose equivalent of 90 mM sodium nitrate as mobile phase

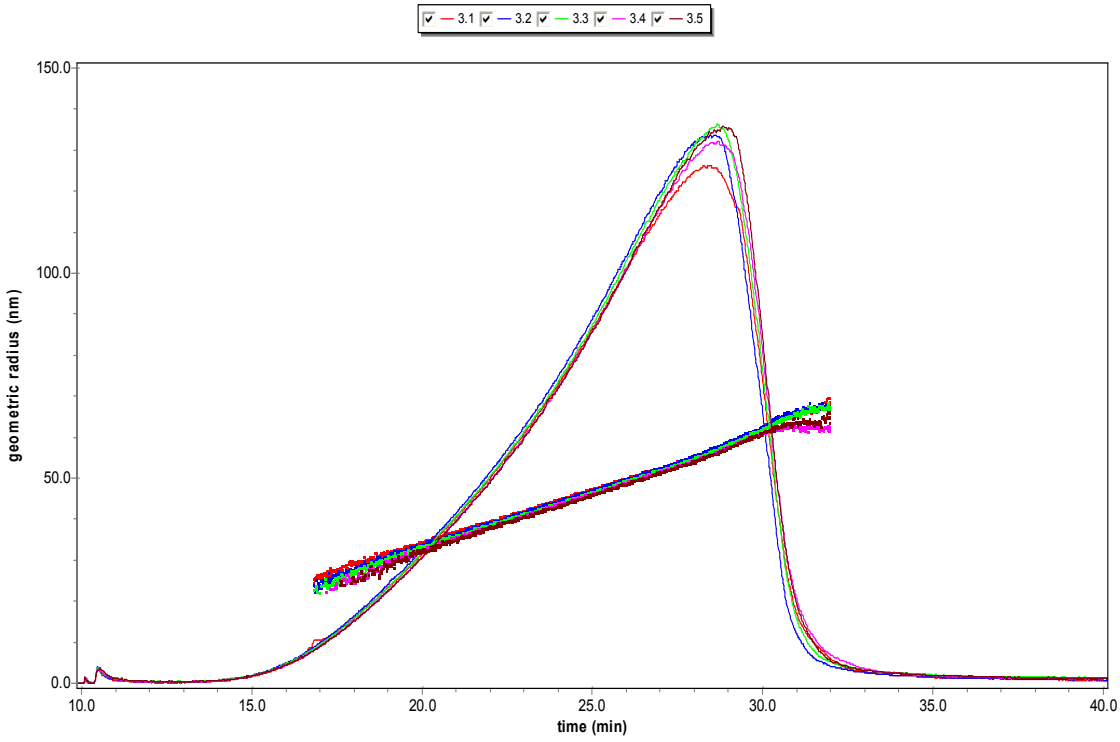

Figure 9.10: The five parallels of liposomes produced in 10 mM sodium nitrate and sucrose equivalent of 90 mM sodium nitrate, diluted 1:10 in 10 mM sodium nitrate. 10 mM sodium nitrate and sucrose equivalent of 90 mM sodium nitrate as mobile phase

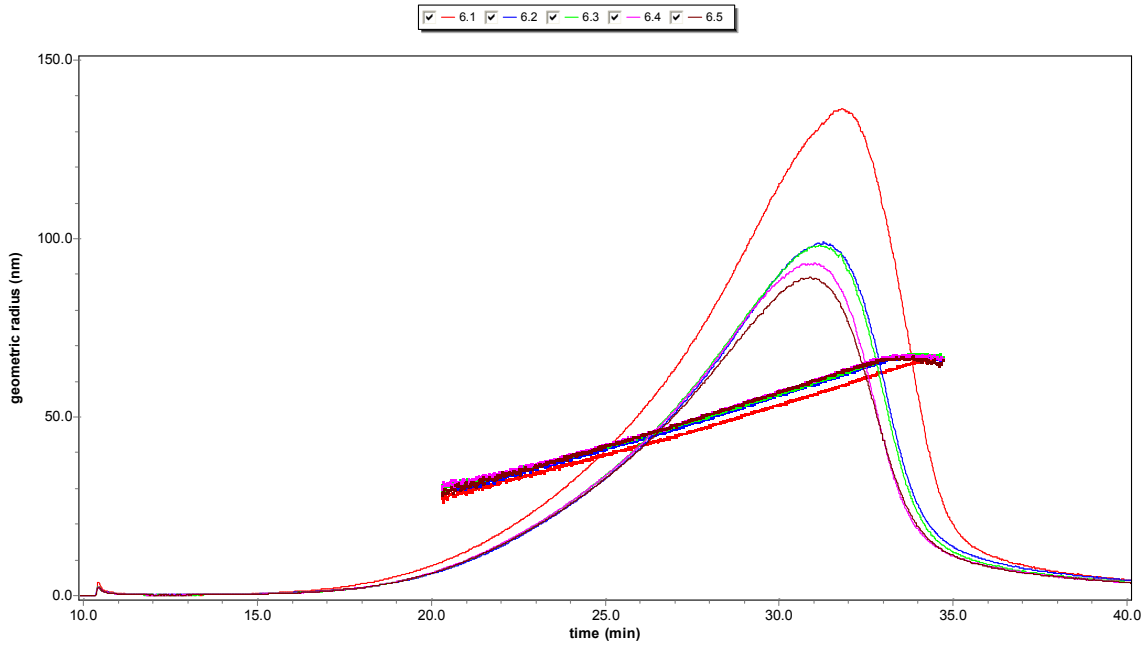

Figure 9.11: The five parallels of liposomes produced in 10 mM sodium nitrate, diluted 1:10 in 10 mM sodium nitrate and sucrose equivalent of 90 mM sodium nitrate. 10 mM sodium nitrate as mobile phase

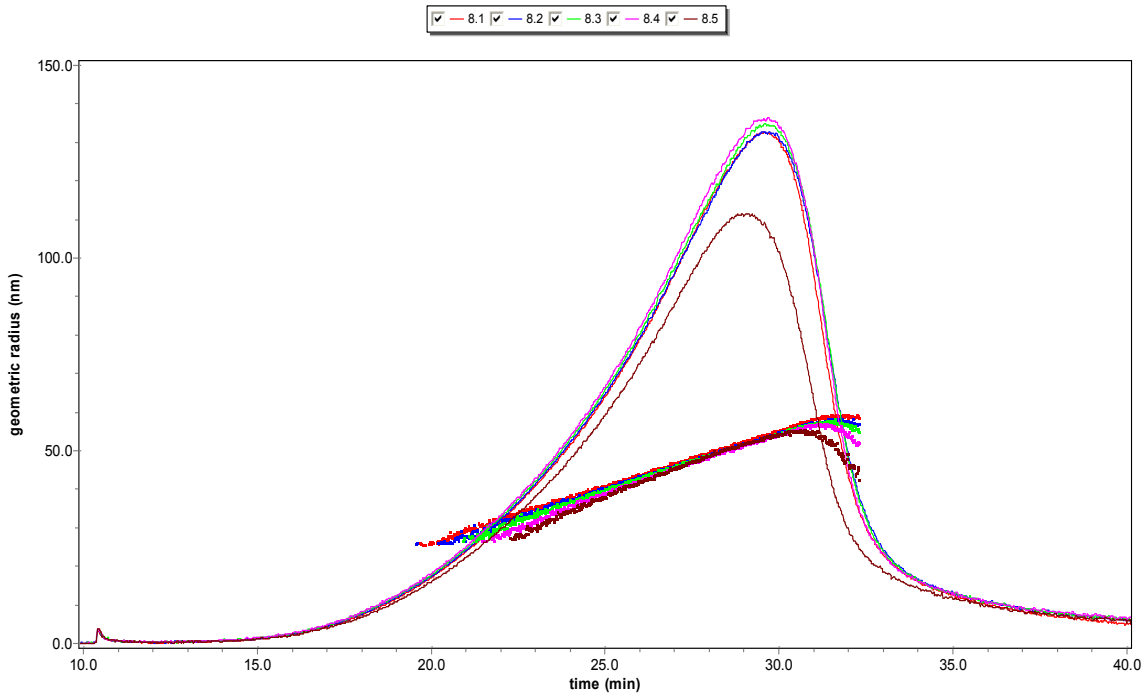

Figure 9.12: The five parallels of liposomes produced in 10 mM sodium nitrate and sucrose equivalent of 90 mM sodium nitrate, diluted 1:10 in 10 mM sodium nitrate and sucrose equivalent of 90 mM sodium nitrate. 10 mM sodium nitrate as mobile phase

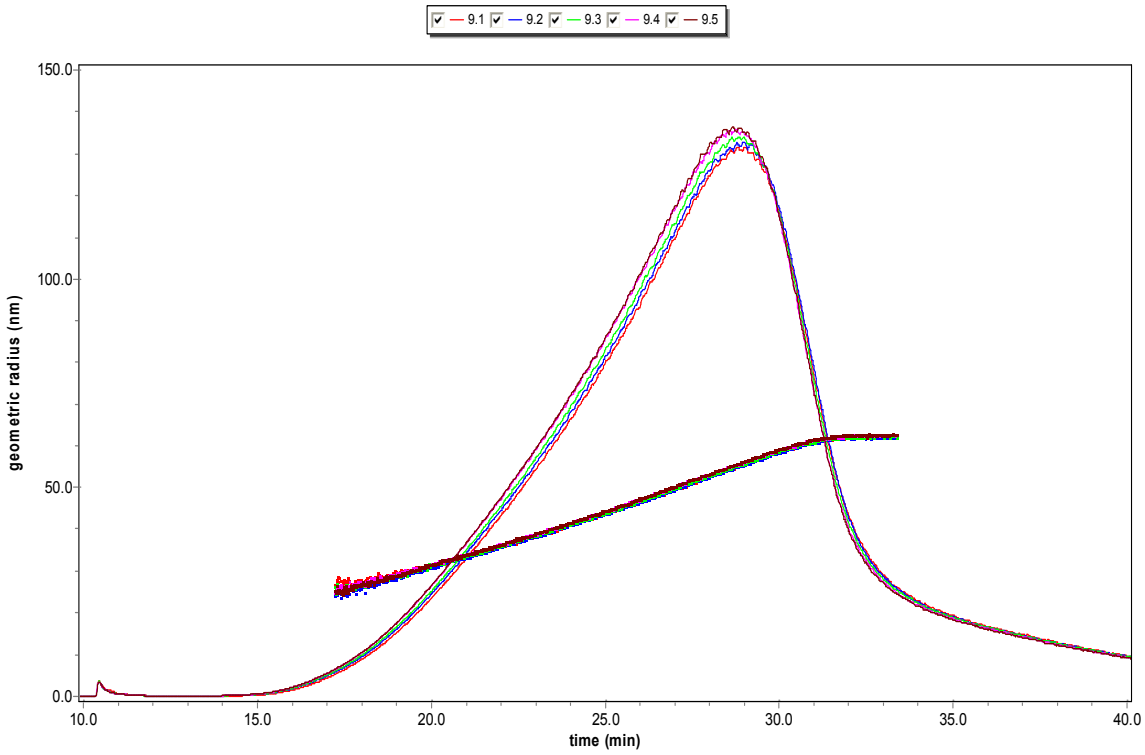

Figure 9.13: The five parallels of liposomes produced in 10 mM sodium nitrate, diluted 1:10 in 10 mM sodium nitrate. 100 mM sodium nitrate as mobile phase

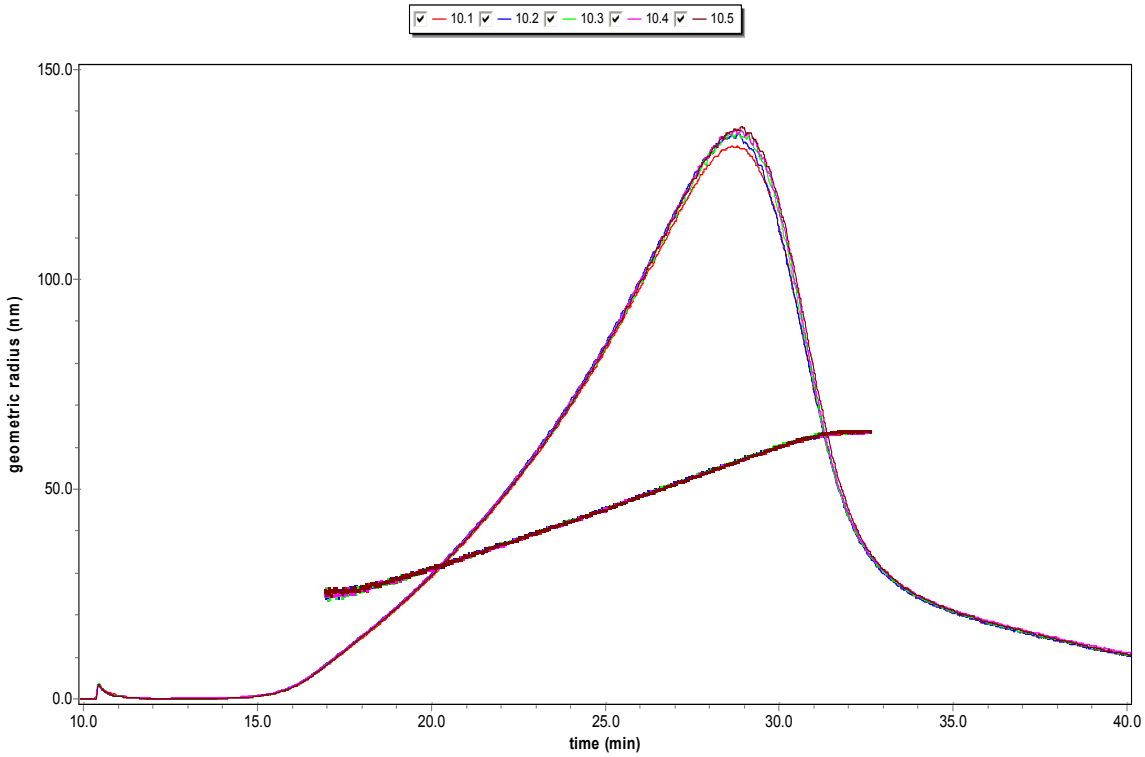

Figure 9.14: The five parallels of liposomes produced in 10 mM sodium nitrate, diluted 1:10 in 10 mM sodium nitrate and sucrose equivalent of 90 mM sodium nitrate. 100 mM sodium nitrate as mobile phase

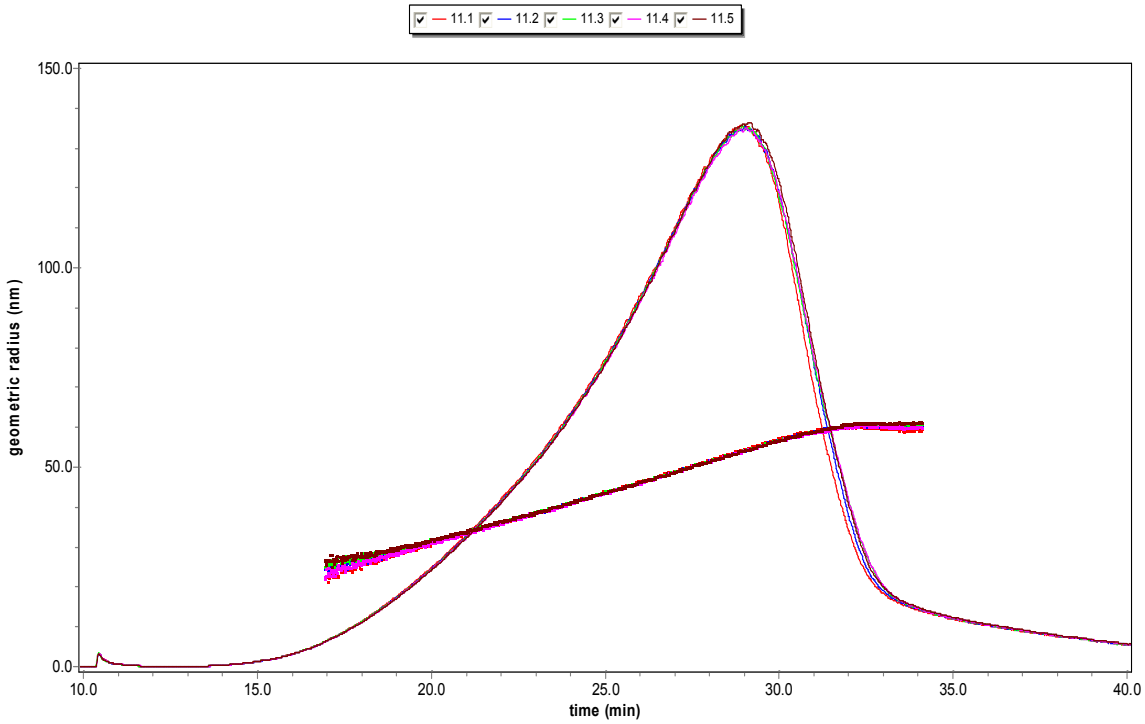

Figure 9.15: The five parallels of liposomes produced in 10 mM sodium nitrate and sucrose equivalent of 90 mM sodium nitrate, diluted 1:10 in 10 mM sodium nitrate. 100 mM sodium nitrate as mobile phase

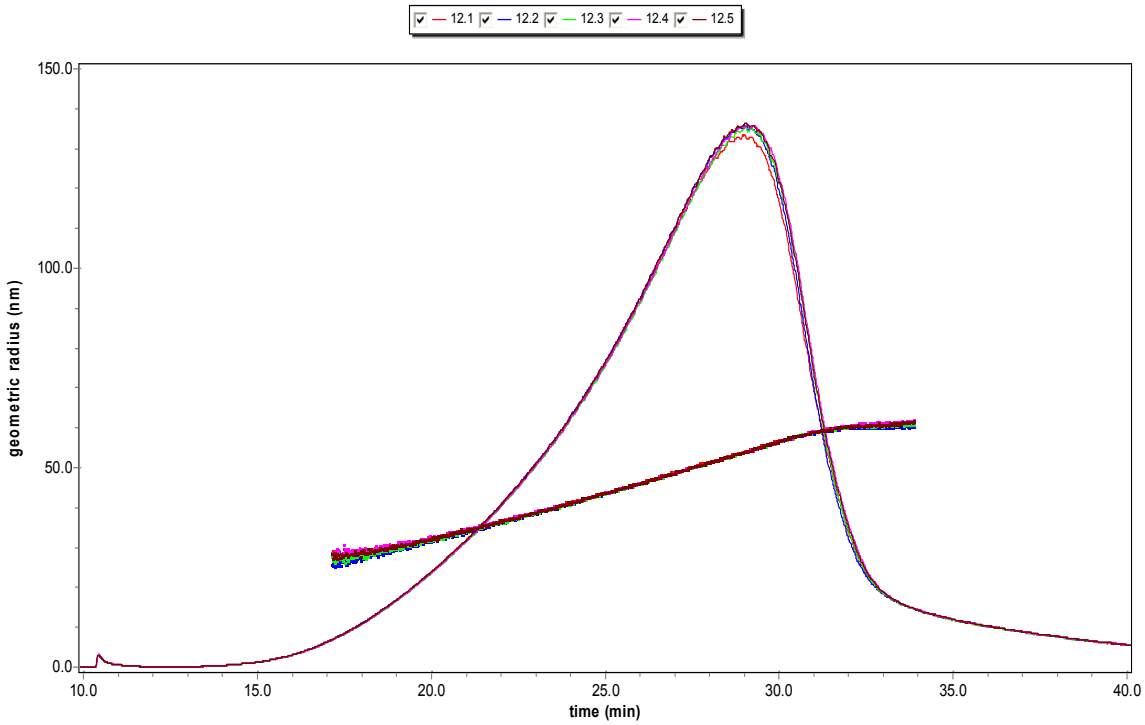

Figure 9.16: The five parallels of liposomes produced in 10 mM sodium nitrate and sucrose equivalent of 90 mM sodium nitrate, diluted 1:10 in 10 mM sodium nitrate and sucrose equivalent of 90 mM sodium nitrate. 10 mM sodium nitrate as mobile phase

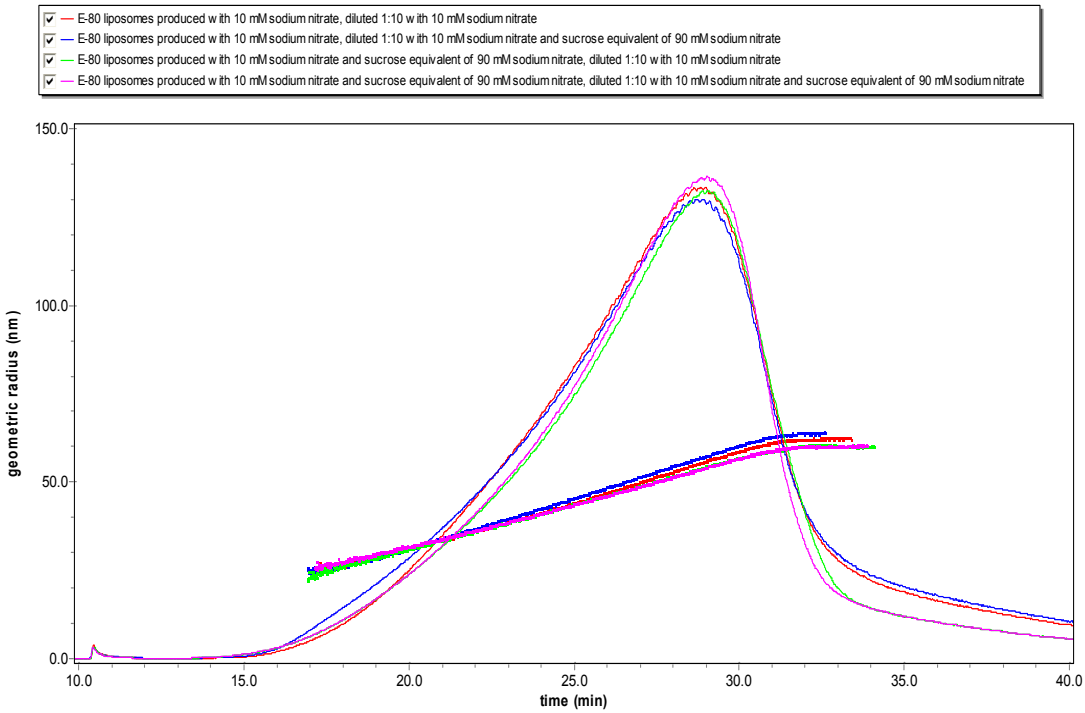

Figure 9.17: All the four liposome preparations with 100 mM sodium nitrate as mobile phase. Only one parallel of each sample shown

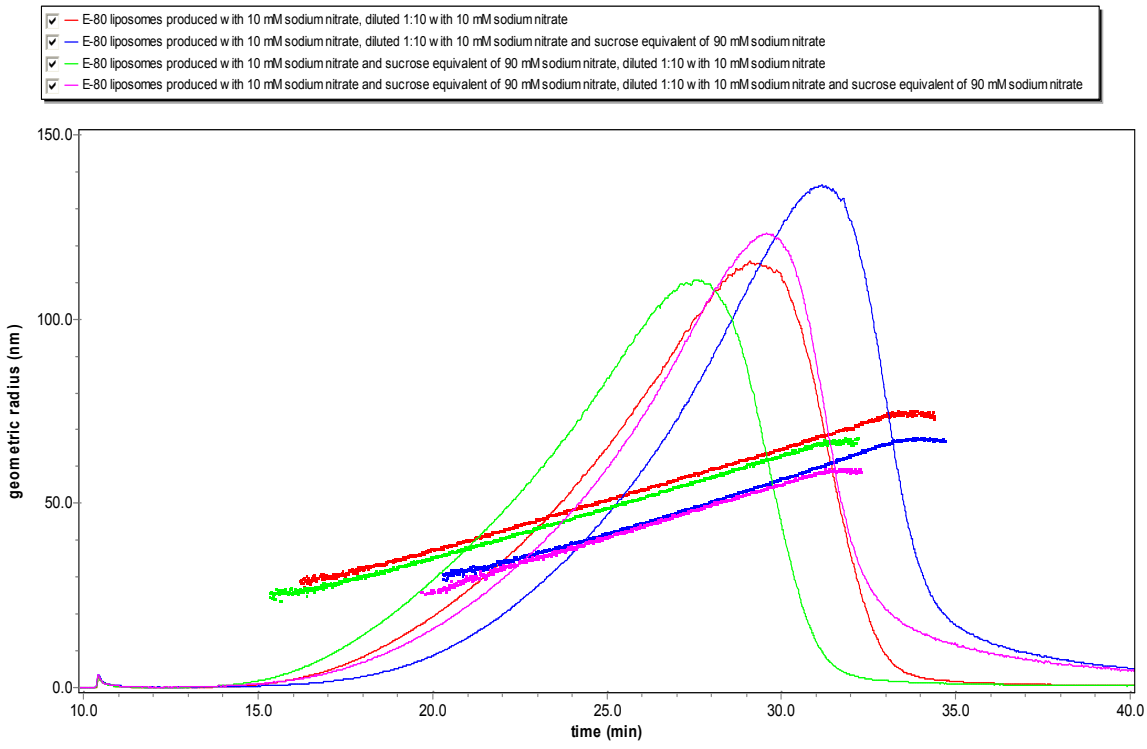

Figure 9.18: All the four liposome preparations with 10 mM sodium nitrate as mobile phase. Only one parallel of each sample shown

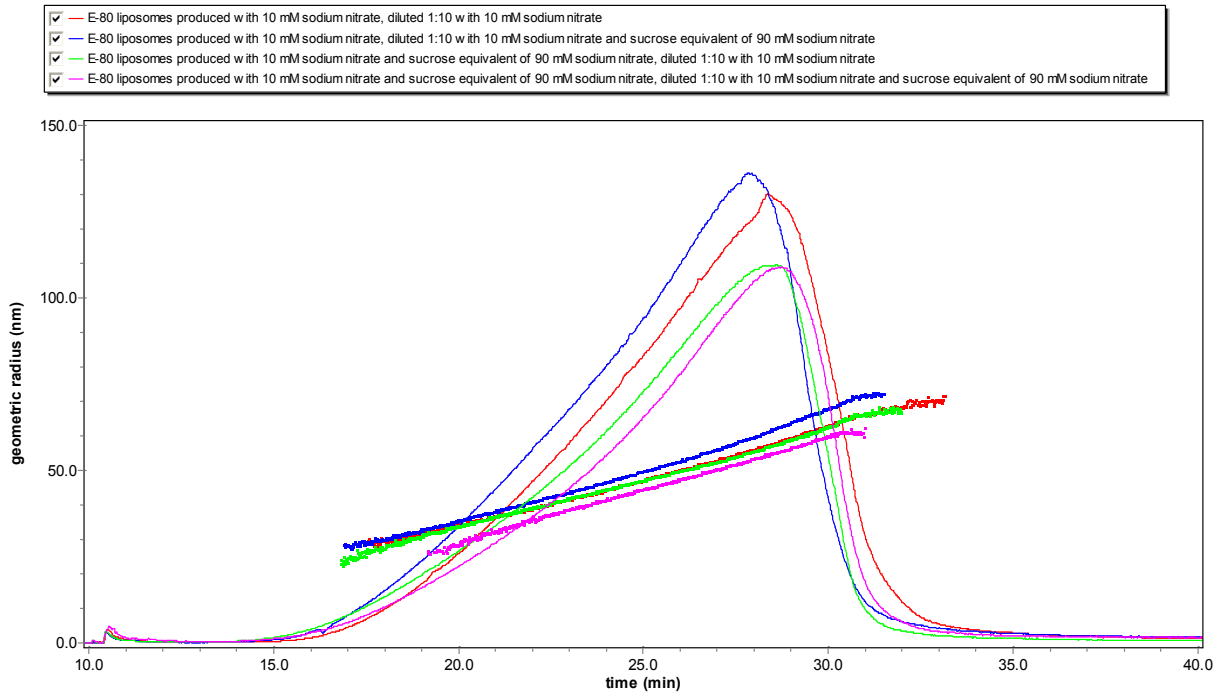

Figure 9.19: All the four liposome preparations with 10 mM sodium nitrate and sucrose equivalent to 90 mM sodium nitrate as mobile phase. Only one parallel of each sample shown

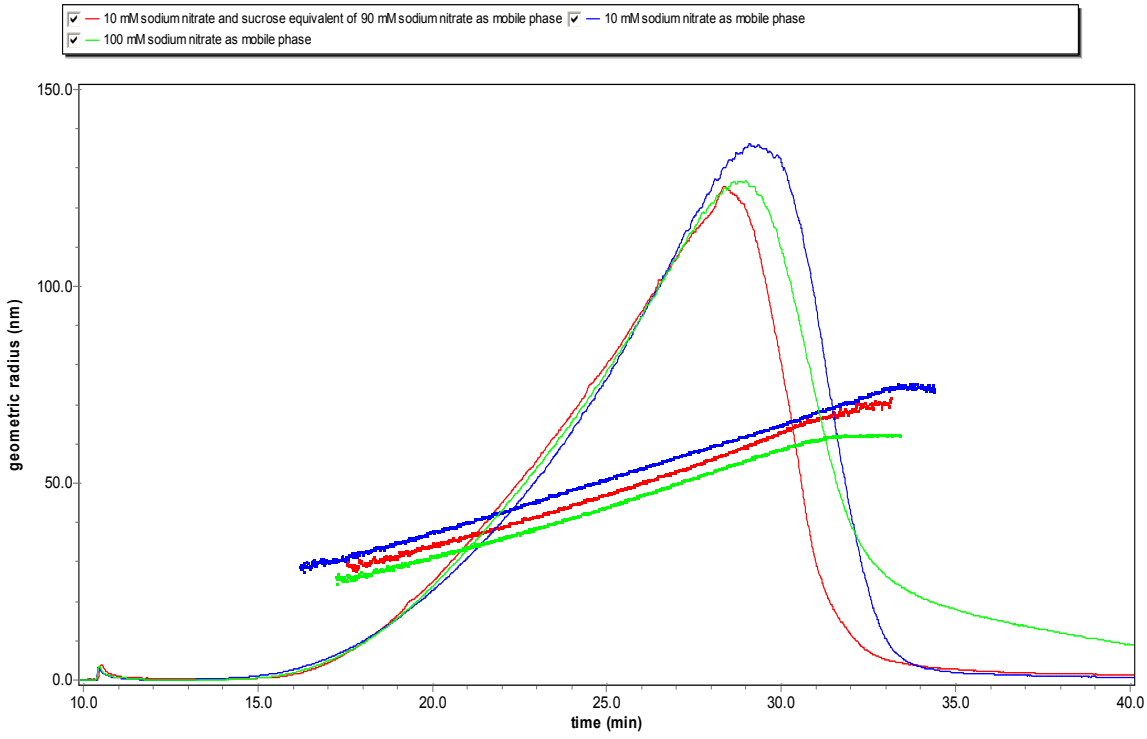

Figure 9.20: All the liposome samples prepared in 10 mM sodium nitrate and diluted 1:10 with 10 mM sodium nitrate. Only one parallel of each sample shown

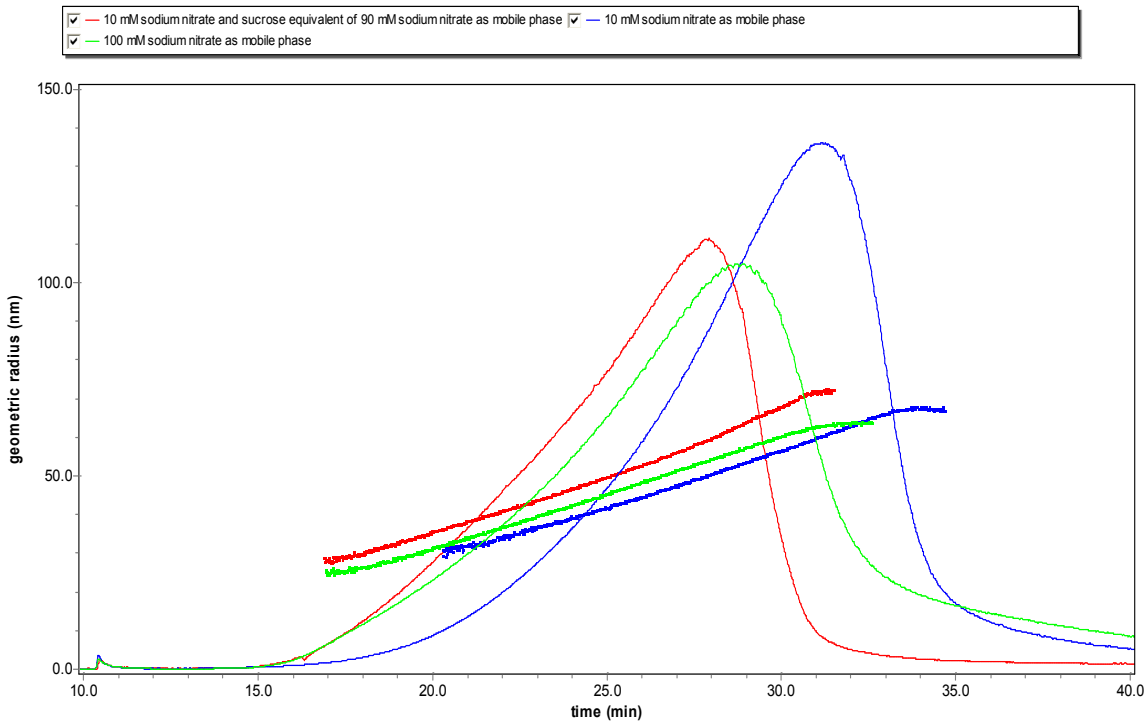

Figure 9.21: All the liposome samples prepared in 10 mM sodium nitrate and diluted 1:10 with 10 mM sodium nitrate and sucrose equivalent to 90 mM sodium nitrate. Only one parallel of each sample shown

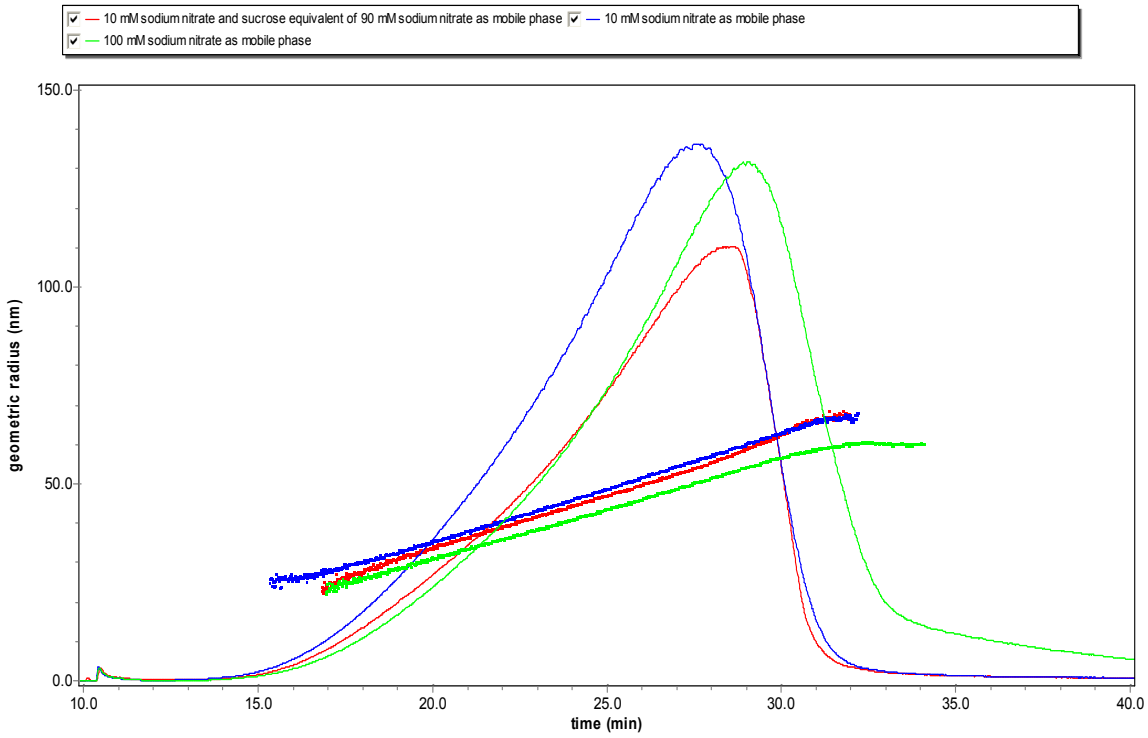

Figure 9.22: All the liposome samples prepared in 10 mM sodium nitrate and sucrose equivalent to 90 mM sodium nitrate, diluted 1:10 with 10 mM sodium nitrate. Only one parallel of each sample shown

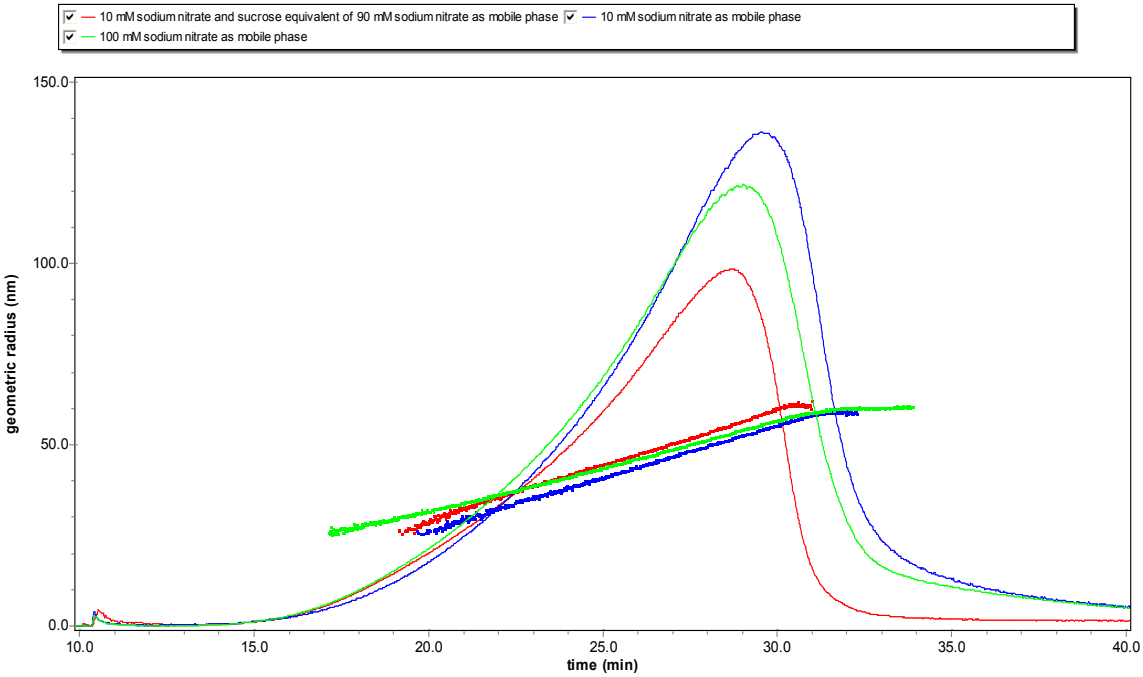

Figure 9.23: All the liposome samples prepared in 10 mM sodium nitrate and sucrose equivalent to 90 mM sodium nitrate, diluted 1:10 with 10 mM sodium nitrate and sucrose equivalent of 90 mM sodium nitrate. Only one parallel of each sample shown